National Library of Canada
Canadian Theses Service
Ottawa, Canada
K1A 0N4

Bibliothèque nationale du Canada
Service des thèses canadiennes

NOTICE

The quality of this microform is heavily dependent upon the quality of the original thesis submitted for microfilming. Every effort has been made to ensure the highest quality of reproduction possible.

If pages are missing, contact the university which granted the degree.

Some pages may have indistinct print especially if the original pages were typed with a poor typewriter ribbon or if the university sent us an inferior photocopy.

Reproduction in full or in part of this microform is governed by the Canadian Copyright Act, R.S.C. 1970, c. C-30, and subsequent amendments.

AVIS

La qualité de cette microforme dépend grandement de la qualité de la thèse soumise au microfilmage. Nous avons tout fait pour assurer une qualité supérieure de reproduction.

S'il manque des pages, veuillez communiquer avec l'université qui a conféré le grade.

La qualité d'impression de certaines pages peut laisser à désirer, surtout si les pages originales ont été dactylographiées à l'aide d'un ruban usé ou si l'université nous a fait parvenir une photocopie de qualité inférieure.

La reproduction, même partielle, de cette microforme est soumise à la Loi canadienne sur le droit d'auteur, SRC 1970, c. C-30, et ses amendements subséquents.

NL-339 (r. 88/04) c

Canada

National Library of Canada
Bibliothèque nationale du Canada

Canadian Theses Service
Service des thèses canadiennes

Ottawa Canada
K1A 0N4

The author has granted an irrevocable non-exclusive licence allowing the National Library of Canada to reproduce, loan, distribute or sell copies of his/her thesis by any means and in any form or format, making this thesis available to interested persons.

L'auteur a accordé une licence irrévocable et non exclusive permettant à la Bibliothèque nationale du Canada de reproduire, prêter, distribuer ou vendre des copies de sa thèse de quelque manière et sous quelque forme que ce soit pour mettre des exemplaires de cette thèse à la disposition des personnes intéressées.

The author retains ownership of the copyright in his/her thesis. Neither the thesis nor substantial extracts from it may be printed or otherwise reproduced without his/her permission.

L'auteur conserve la propriété du droit d'auteur qui protège sa thèse. Ni la thèse ni des extraits substantiels de celle-ci ne doivent être imprimés ou autrement reproduits sans son autorisation.

ISBN 0-315-55317-0

Canada

THE UNIVERSITY OF ALBERTA

LABORATORY MODELING OF BEACH PROFILES IN TAILINGS DISPOSAL

BY

XIAOSHENG FAN

A THESIS

SUBMITTED TO THE FACULTY OF GRADUATE STUDIES AND RESEARCH

IN PARTIAL FULFILLMENT OF THE REQUIREMENTS FOR THE DEGREE

OF MASTER OF SCIENCE

DEPARTMENT OF CHEMICAL ENGINEERING

EDMONTON, ALBERTA

FALL 1989

THE UNIVERSITY OF ALBERTA

RELEASE FORM

NAME OF AUTHOR:	Xiaosheng Fan
TITLE OF THESIS:	Laboratory Modeling of Beach Profiles in Tailings Disposal
DEGREE:	Master of Science
YEAR THIS DEGREE GRANTED:	1989

Permission is hereby granted to THE UNIVERSITY OF ALBERTA LIBRARY to reproduce single copies of this thesis and to lend or sell such copies for private, scholarly or scientific research purposes only.

The author reserves other publication rights, and neither the thesis nor extensive extracts from it may be printed or otherwise reproduced without the author's written permission.

(signed) Fan Xiaosheng

PERMANENT ADDRESS:

Date: Sept. 29, 1989

THE UNIVERSITY OF ALBERTA

FACULTY OF GRADUATE STUDIES AND RESEARCH

The undersigned certify that they have read, and recommend to the Faculty of Graduate Studies and Research for acceptance, a thesis entitled **Laboratory Modeling of Beach Profiles in Tailings Disposal** submitted by Xiaosheng Fan in partial fulfillment of the requirements for the degree of Master of Science.

J.H. Masliyah, Supervisor

P.J. Crickmore

N. Rajaratnam

Date: September 13, 1989

To my wife and parents

ABSTRACT

Transient beach profiles in tailings disposal were investigated both experimentally and theoretically. The effects of feed sediment concentration and total slurry discharge on beach profiles were examined using a flume 4.87 m long, 0.31 m wide, and 0.46 m deep.

A nonlinear parabolic mathematic model was developed to predict beach profiles using a modified form of Meyer–Peter and Muller sediment transport equation. Excellent agreement between the experimental data and the theoretical prediction was observed. It was found that the slope of the beach and the rising rate of the beach at the point of feed discharge to be much influenced by the feed sediment (solids) concentration. On the other hand, when the feed sediment concentration was kept constant and the total slurry discharge was allowed to vary, the slope of the beach did not change significantly.

A power expression, $Z/Z_0=(1-x/L)^m$, was used to correlate all the experimental data, where Z is the depth of deposition at location of x, Z_0 is the depth of deposition at $x = 0$, and L is the beach length. It was found that for $m = 2.16$, the power expression was capable of correlating all the experimental data. This is in agreement with published literature.

ACKNOWLEDGEMENT

My most sincere thanks go to Dr. J.H. Masliyah, my supervisor, for his guidance and ever–ready help throughout the course of this work and for his helpful suggestions in the preparation of this manuscript.

I would like to acknowledge the Chemical Engineering Workshop, Instrument Shop and the DACS center without whose expertise and ardent assistance this work would have not been possible.

Financial support from the University of Alberta is gratefully acknowledged.

TABLE OF CONTENTS

Chapter			Page
1.	INTRODUCTION		1
	1.1	Introductory Remarks	1
	1.2	Objectives of the Study	2
2.	LITERATURE REVIEW		4
	2.1	Beach Formation in Mining Engineering	4
		2.1.1 Tailings Disposal Operations	4
		2.1.2 Profiles of Hydraulic–Fill Tailings Beaches	7
	2.2	Aggradation of Alluvial Channel Beds in Hydraulic Engineering	8
		2.2.1 Theoretical Studies	9
		2.2.2 Experimental Studies	14
3.	EXPERIMENTAL STUDY		16
	3.1	General	16
	3.2	Experimental Set–Up	16
		3.2.1 Flume and Sand Feeder	16
		3.2.2 Beach Profiles Recording Instrument	18
	3.3	Experimental Procedure	18
	3.4	Qualitative Observations	22
	3.5	Experimental Data	26
		3.5.1 Properties of Sand	26
		3.5.2 Beach Profile Data	26
4.	THEORETICAL DERIVATIONS		31
	4.1	Governing Equations	31

4.2 Simplification of the Governing Equations 34
5. NUMERICAL SOLUTION 37
5.1 Finite Difference Formulations 37
5.2 Initial and Boundary Conditions 38
5.3 Stability Consideration 38
5.4 Computational Considerations and Procedure 39
5.4.1 Determination of the Length of Beach Profiles 39
5.4.2 Compensation of the Sediment Deposited Upstream Sediment Feed Point 39
5.4.3 Modification of the Meyer–Peter and Muller Equation 41
5.4.4 Computational Procedure 47
6. RESULTS AND DISCUSSIONS 48
6.1 Beach Profiles 48
6.1.1 Dimensional Form 48
6.1.2 Dimensionless Forms 60
6.1.2.1 Approach One 60
6.1.2.2 Approach Two 72
6.2 Maximum Depth of Deposition at x = 0 76
7. CONCLUSIONS 79
8. RECOMMENDATIONS 80

REFERENCES 81

APPENDIX A FORTRAN PROGRAM FOR BEACH PROFILE GENERATION 86
APPENDIX B NUMERICAL RESULTS FOR TESTS A AND B 90

LIST OF TABLES

Table	Description	Page
3.1	Beach Profile Data from Test A1	27
3.2	Beach Profile Data from Test A2	27
3.3	Beach Profile Data from Test A3	28
3.4	Beach Profile Data from Test A4	28
3.5	Beach Profile Data from Test B1	29
3.6	Beach Profile Data from Test B2	29
3.7	Beach Profile Data from Test B3	30
3.8	Beach Profile Data from Test B4	30
B.1	Numerical Results Modeling Test A1	90
B.2	Numerical Results Modeling Test A2	91
B.3	Numerical Results Modeling Test A3	92
B.4	Numerical Results Modeling Test A4	93
B.5	Numerical Results Modeling Test B1	94
B.6	Numerical Results Modeling Test B2	95
B.7	Numerical Results Modeling Test B3	96
B.8	Numerical Results Modeling Test B4	97

LIST OF FIGURES

Figure	Caption	Page
2.1	Tailings Dam Construction Methods	5
2.2	Definition Sketch for Eq. 2.1	8
3.1	Experimental Set–Up	17
3.2a	Arrangement for Sand and Water Feed	19
3.2b	Sand Distributor	20
3.3	Sediment Size Distribution	21
3.4	Typical Beach Profiles for Low Sand Feeding Rate	23
3.5	Typical Beach Profiles for High Sand Feeding Rate	24
3.6	A Typical Photograph from a Beach Profile	25
4.1	Definition Sketch of Deposition	33
5.1	Upstream Deposition of Sand	40
5.2a	Comparison between Experimental and Theoretical Beach Profiles with $A_k = 8.0$ for Test A1	42
5.2b	Comparison between Experimental and Theoretical Beach Profiles with $A_k = 8.0$ for Test A2	43
5.2c	Comparison between Experimental and Theoretical Beach Profiles with $A_k = 8.0$ for Test A3	44
5.2d	Comparison between Experimental and Theoretical Beach Profiles with $A_k = 8.0$ for Test A4	45
5.3	Variation of A_k with q_{stot}	46
6.1a	Beach Profiles of Test A1	49
6.1b	Beach Profiles of Test A2	50
6.1c	Beach Profiles of Test A3	51

6.1d Beach Profiles of Test A4 52

6.2 Effect of Feed Sediment Concentration on Beach Profiles 53

6.3a Beach Profiles of Test B1 55

6.3b Beach Profiles of Test B2 56

6.3c Beach Profiles of Test B3 57

6.3d Beach Profiles of Test B4 58

6.4 Effect of Total Slurry Discharge on Beach Profiles 59

6.5a Dimensionless Beach Profiles of Test A1 62

6.5b Dimensionless Beach Profiles of Test A2 63

6.5c Dimensionless Beach Profiles of Test A3 64

6.5d Dimensionless Beach Profiles of Test A4 65

6.6a Dimensionless Beach Profiles of Test B1 66

6.6b Dimensionless Beach Profiles of Test B2 67

6.6c Dimensionless Beach Profiles of Test B3 68

6.6d Dimensionless Beach Profiles of Test B4 69

6.7 Dimensionless Beach Profiles for All Group A Tests 70

6.8 Dimensionless Beach Profiles for All Group B Tests 71

6.9 Typical Dimensionless Beach Profiles for Group A Tests Modeled by Power Expression 73

6.10 Typical Dimensionless Beach Profiles for Group B Tests Modeled by Power Expression 74

6.11 Comparison of All the Beach Profile Data with the Curve Fitted by the Power Expression 75

6.12 Effect of Feed Sediment Concentration on the Maximum Depth of Deposition 77

6.13 Effect of Total Feed Slurry Discharge on the Maximum Depth of Deposition 78

NOMENCLATURE

a	dimensionless regressive coefficient in Eq. 2.2
A_k	dimensionless coefficient of the sediment transport equation, Eq. 4.7
b	dimensionless regressive coefficient in Eq. 2.2
c	celerity of a small disturbance at the bed, m/s
C	Chezy coefficient, $m^{0.5}/s$
C_{sv}	dimensionless volumetric sediment concentration in the slurry feed
d_{50}	median diameter of sand, m
D	typical grain size of sand mixture, $D = d_{50}$, m
E	specific energy, $E = u^2/2 + g\,h$, m^2/s^2
Fr	dimensionless Froude number defined as $Fr = u/(\sqrt{gh})$
g	gravitational acceleration, m/s^2
h	depth of water, m
k_s	height of the equivalent sand roughness, $k_s = d_{50}$, m
K	aggradation coefficient, m^2/s
L	length of the beach profile on top of the initial beach, m
L'	length of sediment deposition upstream of the feed point, m
m	dimensionless exponent of the master profile in Eq. 2.1
n	Manning's resistance coefficient, $m^{-1/3}s$
q_f	volumetric water discharge per unit width, m^3/s–m
q_s	volumetric sediment discharge per unit width, m^3/s–m
q_s^*	dimensionless sediment discharge defined by Eq. 2.26
q_{se}	initial equilibrium volumetric sediment discharge per unit width, m^3/s–m
q_{sf}	total feed slurry discharge per unit width, $q_{sf} = q_{stot} + q_f$, m^3/s–m
q_{s0}	volumetric sediment feed discharge per unit width traveling downstream of the feed point, m^3/s–m

q'_{s0} volumetric sediment feed discharge per unit width traveling upstream of the feed point, $m^3/s-m$

q_{stot} total volumetric sediment feed discharge per unit width, $m^3/s-m$

R hydraulic radius, R = area / wetted perimeter, m

S dimensionless beach slope

S_f dimensionless energy slope

S_0 dimensionless initial beach slope

t time, s

u average velocity of the the fluid, m/s

u_0 initial uniform velocity, m/s

x horizontal distance along the beach, m

Y dimensionless mobility number defined by Eq. 4.9

Y_{cr} dimensionless critical mobility number

z beach elevation with respect to a horizontal reference level, m

z_b initial beach elevation, m

Z depth of sediment deposition, m

Z_0 maximum depth of sediment deposition at x = 0, m

Greek Symbols

α dimensionless angle of the beach upstream the feed point

β ratio of grain volume to total volume in the beach, $\beta = 1 -$ bed porosity

η dimensionless variable defined as $\eta = x/(2\sqrt{Kt})$

ρ_f density of water, kg/m^3

ρ_s density of sand, kg/m^3

σ_g dimensionless geometric standard deviation of sand size defined as $\sigma_g = (d_{84}/d_{50} + d_{50}/d_{16})/2$

ϕ dimensionless sediment transport rate defined by Eq. 4.8

Subscripts and Superscripts

i	subscripts denoting space in x direction
n	superscripts denoting time

1. INTRODUCTION

1.1 Introductory Remarks

In many mining processes, large quantities of tailings are produced. Tailings disposal and the management of the tailings ponds formed from the disposal are indispensable. Disposal of oil sand tailings resulting from the hot water extraction of surface–mined Athabasca oil sands is a case in point. From the two bitumen producing plants, Suncor Inc. and Syncrude Canada Ltd., presently operating in the oil sands region of Northern Alberta, tailings are produced at an average rate of about 350,000 tons of solids per day and are transported to the disposal sites in hydraulic streams at about 40 to 45 percent solids by weight (Mittal, 1981).

At the disposal site, when the slurry is discharged into the tailings pond, the coarse sand settles out, forming a beach, while the water and the very fine solids including clays end up in the tailings pond. Some of the coarse sand is used for the construction of containment dykes while the remaining sand and the sludge are stored permanently in the pond.

The tailings containment dams are built of compacted tailings sand placed by the "hydraulic cell" method (see chapter 2). The compacted section is supported by the flat beach of sand tailings placed by hydraulic discharge.

The management of hydraulically deposited tailings is an important component of a mining operation. Failure to properly manage the tailings dykes often results in a potentially unsafe structure during both the mill operation and land reclamation stages. One component of tailings management is beach profile prediction. The ability of the impoundment manager to estimate the beach profile at any time can result in an improved means of monitoring the volume of tailings deposited, estimating the rate of rise of the crest, assessing the storm water storage

capacity on top of the dam and minimizing the need for moving drained tailings.

The fundamentals of beach formation occurring in the tailings disposal process are very much linked to the area of aggradation of bed material in river flow. It is interesting to note that the literature dealing strictly with bed formation in tailings disposal is not as mature as that of aggradation of bed material in river flow. A review of the open literature has shown that there were only a few attempts to predict the beach profiles in tailings disposal, and none of these studies dealt with transient beach profiles. On the other hand, a great deal of theoretical studies on the transient riverbed profiles due to overloading have been conducted. However, almost all the studies from river engineering point of view are only concerned with very dilute flow streams with considerable water depth, which is quite different from that encountered in tailings disposal.

1.2 Objectives of the Study

In this study, it was desired to:

1. conduct a series of experiments to model the transient beach profiles for two cases:
    a) a slurry having different sediment concentration with constant water flow rate and
    b) a slurry having different total flow rate with constant sediment concentration;
2. develop a nonlinear parabolic model to describe the transient sediment transport process and find out the appropriate initial and boundary conditions for the model;
3. solve the partial differential equation numerically to obtain beach profiles for the two experimental cases;

4. compare the numerical solution with the experimental data in both dimensional and nondimensional forms.
5. make recommendations based on the current study.

2. LITERATURE REVIEW

Beach formation in tailings disposal mainly involves two fields of study: mining engineering and hydraulic engineering. A brief literature review for both mining engineering and hydraulic engineering is given in the following sections.

2.1 Beach Formation in Mining Engineering

2.1.1 Tailings Disposal Operations

In the mining industry, tailings disposal is an integral part of the mining production. There are various methods available for tailings disposal. Dams, embankments, and related types of surface impoundments are by far the most common disposal methods and remain of primary importance in tailings disposal planning.

Brawner and Campbell (1973) have reviewed the three most commonly used tailings disposal methods which employ the tailings themselves as the construction material for the retaining dam. the methods are known as upstream method, downstream method and center line method as shown in Figs. 2.1.

With the upstream method shown in Fig. 2.1 (a), an initial starter dam is constructed at the downstream toe. Tailings are then discharged from the top of the starter dam using spigots or cyclones to develop a dyke composed of the coarser fraction. The center line of the top of the embankment is shifted towards the pond area as the height of the dam increases. In the downstream method delineated in Fig. 2.1 (b), the center line of the top of the dam shifts downstream as the dam rises. For the center line method depicted in Fig. 2.1 (c), the crest of the dam is essentially maintained at the same horizontal position as the height of the dam

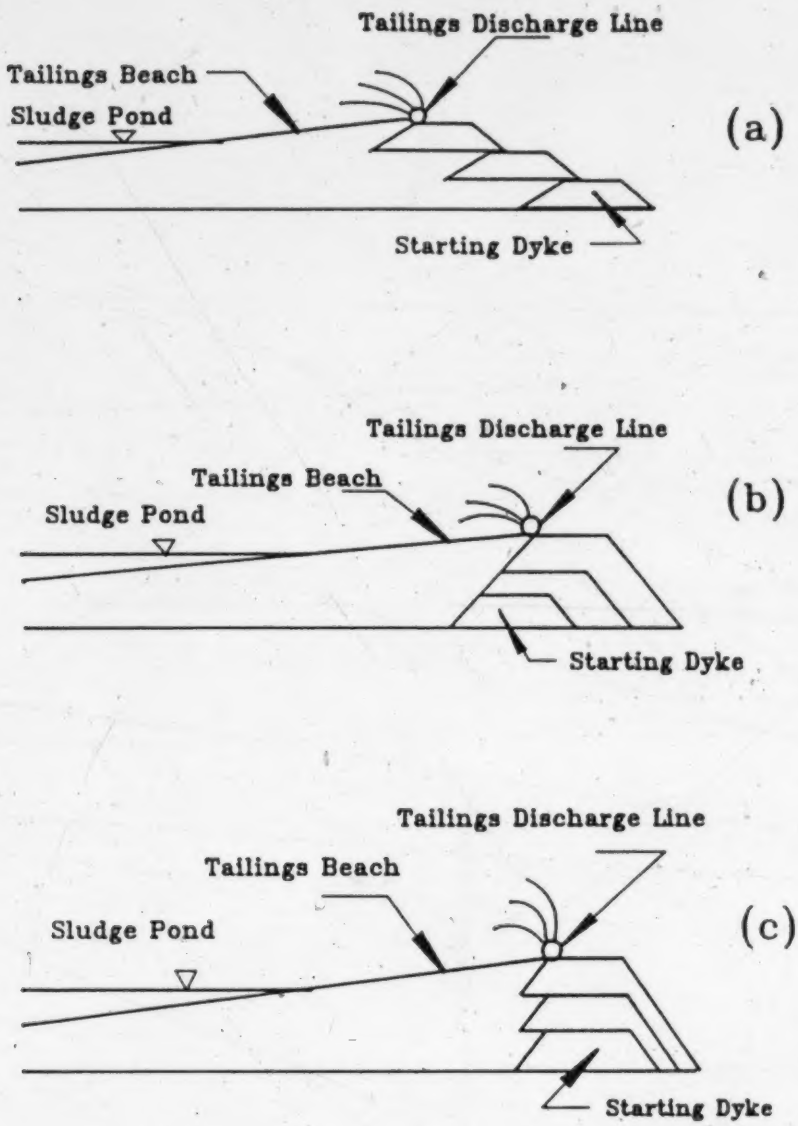

Fig. 2.1 Tailings Dam Construction Methods: a) Upstream Method; b) Downstream Method; c) Centerline Method

rises. Of the three methods shown in Figs. 2.1, the downstream method results in the most stable but most costly structure.

Robinsky (1975,1979) developed another approach to tailings disposal – thickened discharge method. In this method, the tailings are deposited in a cone–shaped hill which is one of the most stable structural shapes found in nature. Compared to the traditional approaches described above, this method is more stable and requires much lower dykes for equivalent storage capacity. However, it requires much higher solids–to–water ratio to make the tailing material accumulate at a steeper angle than possible by traditional methods. To achieve the required solid–to–water ratio (35 to 60 weight per cent), it is often necessary to install a thickener which may render this method uneconomical for large scale operations.

Mittal (1981) investigated the geotechnical aspects of the design, construction, and performance of the tar sand tailings dyke at the Suncor project. About 250,000 tons of tailings are handled daily including 100,000 tons of solids. The tailings disposal site, known as the Tar Island, has been created by diking off an oxbow in the valley of the Athabasca River. It provides a disposal area of about 3.1 km^2 with a height up to the level of the top of the valley wall of about 67 m. The Tar Island dyke has been built by the upstream method. The method employed in the dyke building operation is known as hydraulic cell method which involves sluicing of the tailings in "cells", usually oriented parallel to the longitudinal axis of the dyke. The cell being used is about 30 to 90 m wide and 300 to 450 m long, bounded by shallow sand dykes, 1.5 to 2.0 m high, pushed up by dozers. At the downstream end of the cell the stream containing the fine fraction in suspension in the oily water is collected into a spillway box from which it flows into the pond. The sand deposited in the cells is compacted by dozers to form the confinement dykes.

Nyren et al. (1979) studied the disposal of tar sand tailings at Syncrude Canada Ltd. The Syncrude plant has a production capacity of 129,000 barrels per

day of synthetic crude oil, generating about 250,000 tons of tailing solids. The Syncrude Mildred Lake Tailings pond covers an area of about 27 square km and requires about 23 km of continuous dykes. The dykes range in height from about 21 m to a maximum of about 84 m, with the majority of the dykes being of the order of 43 m high. The sand dykes are constructed by the "hydraulic cell" method in a manner essentially similar to that being used at the Suncor Tar Island tailings dyke as reported by Mittal and Hardy (1977).

2.1.2 Profiles of Hydraulic – Fill Tailings Beaches

When tailings are disposed using the hydraulic cell method, a beach is formed between the dyke and the sludge pond. Following Melent'ev et al. (1973), Blight and Bentel (1983) investigated six dam beaches of hydraulic – fill platinum tailings and showed that the beach profiles could be represented by a single dimensionless "master profile" given by

$$\frac{Z}{Z_0} = \left[1 - \frac{x}{L}\right]^m \tag{2.1}$$

where the variables L, x, Z, and Z_0 are defined in Fig. 2.2; m is a number between 1.4 and 4.0, depending on the tailings material.

Blight et al. (1985) conducted some experiments to model the tailings beaches with a short flume. They found that the profile of a full–scale hydraulic–fill tailings beach can be predicted fairly well using a small–scale laboratory model provided that the same material at a similar solid content is used.

Smith and Nelson (1986) conducted an empirical investigation to formulate design criteria for predicting the beach profiles of hydraulically deposited tailings. They collected field data from six types of tailings and found out that either a power

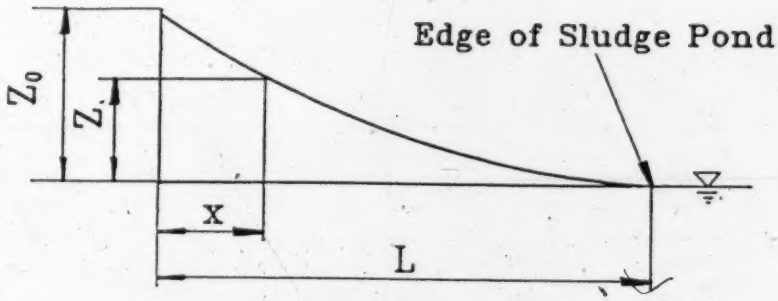

Fig. 2.2 Definition Sketch for Eq. 2.1

expression or an exponential expression could closely predict each beach slope. A general power expression as given by Eq. 2.1 and a general exponential expression were developed. The general exponential expression is given as follows:

$$\frac{Z}{Z_0} = a \cdot \exp\left(b \cdot \frac{x}{L}\right) \tag{2.2}$$

where a and b are regressive coefficients and the other variables are defined in Fig. 2.2.

2.2 Aggradation of Alluvial Channel Beds in Hydraulic Engineering

To some extent, the beach formation in tailings disposal is similar to the aggradation of a river reach due to overloading. Literature on the latter subject is voluminous. A complete list of literature, together with suitable editorial comments, is in itself a major undertaking. Therefore, no attempt will be made to review all literature in this area in detail.

2.2.1 Theoretical Studies

The theoretical foundation of aggradation and degradation of alluvial channel beds was laid by de Vries (1959,1965,1969,1973). In a series of papers, he showed in a rather general fashion that under the assumptions of steady and uniform flow along with some other suitable simplifications, the set of governing equations could be reduced to a linear parabolic partial differential equation. On the other hand, if the assumption of uniform flow was relaxed, then a hyperbolic partial differential equation was obtained. The following is the highlight of his theoretical derivations. For water, the equations of motion and continuity are, respectively:

$$\frac{\partial u}{\partial t} + u\frac{\partial u}{\partial x} + g\frac{\partial h}{\partial x} + g\frac{\partial z}{\partial x} = -g\frac{u|u|}{C^2R} \tag{2.3}$$

$$\frac{\partial h}{\partial t} + u\frac{\partial h}{\partial x} + h\frac{\partial u}{\partial x} = 0 \tag{2.4}$$

where C is Chezy coefficient; g is gravity acceleration constant; h is the depth of water; R is hydraulic radius; t is time; u is the flow velocity; x is the horizontal distance along the channel; z is the beach elevation with respect to a horizontal reference level.

For the sediment, the transport equation and the continuity equation are, respectively:

$$q_s = f\{u, \text{parameters}\} \tag{2.5}$$

$$\beta\frac{\partial z}{\partial t} + \frac{\partial q_s}{\partial x} = 0 \tag{2.6}$$

where, q_s is the volumetric solid transport per unit of width and time; β is the ratio of grain volume to total volume in the bed.

If the Froude number, defined as $Fr = u/\sqrt{gh}$, is not too close to unity ($Fr < 1$), then the terms $\frac{\partial u}{\partial t}$ and $\frac{\partial h}{\partial t}$ can be neglected with respect to other terms in the above equations. Therefore, the basic equations reduce to

$$u \frac{\partial u}{\partial x} + g \frac{\partial h}{\partial x} + g \frac{\partial z}{\partial x} = - g \frac{u|u|}{C^2 R} \tag{2.7}$$

$$u \cdot h = q_f(t) \tag{2.8}$$

$$q_s = f \{u, \text{parameters}\} \tag{2.9}$$

$$\beta \frac{\partial z}{\partial t} + \frac{\partial q_s}{\partial x} = 0 \tag{2.10}$$

where q_f is the water discharge per unit width.

These four equations can be combined into one differential equation to give:

$$\beta \frac{\partial z}{\partial t} + \left[\frac{g \, dq_s/du}{g \, q_f/u^2 - u} \right] \frac{\partial z}{\partial x} = - g \frac{u|u|}{C^2 R} \cdot \frac{dq_s/du}{g \, q_f/u^2 - u} \tag{2.11}$$

If the water movement is supposed to be steady and uniform during transient stages, the following equation is then obtained:

$$\frac{\partial z}{\partial t} = K \frac{\partial^2 z}{\partial x^2} \tag{2.12}$$

where

$$K = \frac{1}{3} \frac{C^2 \, q_f \, dq_s/du}{\beta \, u^2} \tag{2.13}$$

or after linearization,

$$K \approx \frac{1}{3} \frac{u_0 \, dq_s/du}{\beta \, S_0} \tag{2.14}$$

where u_0 refers to the initial uniform velocity and S_0 is the initial uniform bed slope. Setting $q_s = a \cdot u^b$ and linearizing, Eq. 2.14 becomes

$$K \approx \frac{1}{3} \frac{b}{\beta} \frac{q_s}{S_0} \tag{2.15}$$

Eqs. 2.12 and 2.15 form the linear parabolic model.

If the uniform flow condition is relaxed, the following hyperbolic model arises:

$$\frac{\partial z}{\partial t} = K \frac{\partial^2 z}{\partial x^2} + \frac{K}{c} \frac{\partial^2 z}{\partial x \partial t} \tag{2.16}$$

where c denotes the celerity of a small disturbance at the bed and K, when linearized, is the same as that given by Eq. 2.15.

The linear parabolic model was solved analytically by de Vries as follows. A new dependent variable, Z, is defined as.

$$Z(x,t) = z(x,t) - z_b(x) \tag{2.17}$$

where $z_b(x)$ is the initial beach elevation. Then the following boundary and initial conditions can be specified;

$$Z(x,0) = 0 \tag{2.18}$$

$$Z(0,t) = Z_0 \tag{2.19}$$

where Z_0 is the maximum change of the bed at $x = 0$. The solution is

$$Z/Z_0 = \text{erfc}(\eta) \tag{2.20}$$

where

$$\eta = x/(2\sqrt{Kt}) \tag{2.21}$$

$$\text{erfc}(\eta) = (2/\sqrt{\pi}) \cdot \int_{\eta}^{\infty} \exp(-y^2)dy \tag{2.22}$$

y is a dummy variable.

Soni et al. (1980) studied the aggradation problem both theoretically and experimentally. Following de Vries (1973), Soni et al. obtained the same analytical solution (Eq. 2.20) to the linear parabolic model (Eqs. 2.12 and 2.15). The comparison between the analytical solution and their experimental data showed poor agreement. The authors attributed the discrepancy to the linearization of the aggradation coefficient, K, and resorted to modifying it according to the excess rate of the sediment supply.

In a discussion on a paper by Soni et al. (1980), Jain (1980) pointed out an inappropriate boundary condition applied by Soni et al. (1980) when obtaining the analytical solution. The boundary condition for the aggradation problem studied experimentally by Soni et al. (1980) is that the rate of the increased sediment supply at $x = 0$ is a constant for $t > 0$, while the boundary condition used by Soni et al. (1980) in solving the parabolic partial differential equation (Eq. 2.12) is that

the bed elevation at $x = 0$ is a constant for $t > 0$. This incorrect boundary condition was also employed by de Vries (1973). With the correct boundary condition, Jain (1981) obtained the following analytical solution to the linear parabolic equation (Eq. 2.12):

$$Z/Z_0 = [\exp(-\eta^2) - \eta \sqrt{\pi}\ \mathrm{erfc}(\eta)] \tag{2.23}$$

This solution is in better agreement with the experimental data of Soni et al. (1980).

Garde et al. (1981) and Mehta et al. (1983) studied both the parabolic model and hyperbolic model derived by de Vries (1973). They gave the same solution as given by Jain (1981) for the parabolic model and a numerical solution for the hyperbolic model. By comparing the analytical and numerical solutions with their data and the data obtained by Soni et al. (1980), they concluded that the aggradation coefficient, K, used in the parabolic model needs to be modified according to the initial flow conditions and the excess rate of the sediment discharge and that the modified parabolic model gives better results than the hyperbolic model.

Jaramillo and Jain (1983) presented analytical solutions of the bed profile and the sediment transport rate of alluvial channels of finite length with the parabolic model proposed by de Vries (1973). The analytical solution for small time is identical to that for a semi–infinite reach. The experimental results agreed with the analytical solution for moderate values of sediment overloading.

Jaramillo and Jain (1984) developed the following nonlinear parabolic model for nonequilibrium processes in alluvial rivers:

$$\frac{\partial q_s^*}{\partial t} - K(q_s^*)\frac{\partial^2 q_s^*}{\partial x^2} = 0 \tag{2.24}$$

$$\frac{\partial Z}{\partial t} + \frac{\Delta q_{s0}}{\beta}\frac{\partial q_s^*}{\partial x} = 0 \tag{2.25}$$

where

$$q_s^* = \frac{q_s - q_{se}}{\Delta q_{s0}} \tag{2.26}$$

q_{se} is the initial equilibrium sediment transport rate; Δq_{s0} is the excess sediment transport rate at $x = 0$, $\Delta q_{s0} = q_{s0} - q_{se}$; q_{s0} is the sand feed rate traveling downstream of the feed point. They obtained the analytical solution for the above model by the method of weighted residuals. The agreement between the analytical solution and the available experimental data was good. Zhang and Kahawita (1987) pointed out an error in the derivation of the nonlinear parabolic model by Jaramillo and Jain (1984), but the correction worsened the agreement rather than improved it.

Zhang and Kahawita (1987) presented the following nonlinear parabolic model:

$$\frac{\partial q_s}{\partial t} = K(q_s)\,\frac{\partial^2 q_s}{\partial x^2} \tag{2.27}$$

$$\frac{\partial z}{\partial t} = K(q_s)\cdot\left[\frac{\partial^2 z}{\partial x^2} + \frac{1}{g}\frac{\partial^2 E}{\partial x^2}\right] \tag{2.28}$$

where $E = u^2/2 + g\,h$. They proposed an indirect method for evaluating the nonequilibrium sediment transport relation. The technique was illustrated by numerical experiment.

In a recent paper, Zhang and Kahawita (1988) developed a complicated one dimensional hyperbolic model describing the unsteady sediment transport rate in an alluvial channel. Asymptotic equations to predict the solutions at large time and with a constant overloading upstream have been provided.

Gill (1983) investigated the linear parabolic model developed by de Vries (1973) and obtained solutions in two forms: Fourier series and error function. With the perturbation method, Gill (1987) obtained an analytical solution for the following nonlinear parabolic model:

$$\frac{\partial z}{\partial t} = K(q_s)\cdot\frac{\partial^2 z}{\partial x^2} \tag{2.29}$$

Ribberink and Van der Sande (1985) showed that with various simplifications, the governing equations may be reduced to simple–wave model, linear parabolic model and hyperbolic model, with the latter two being similar to those developed by de Vries (1973). They presented the analytical solutions for the simple–wave model and the linear parabolic model. As for the more general hyperbolic model, they presented exact solutions for some specified distances and approximate solutions for small and large values of time. The general solution of the hyperbolic model was later obtained by Gill (1988) through Laplace transform.

Park and Jain (1986) provided a numerical solution for the coupled governing equations using the weighted implicit finite difference scheme. Numerical results showed that the sediment diffusion coefficient is a function of the rate of sediment overloading. The agreement between the numerical results and the available experimental data is satisfactory.

2.2.2 Experimental Studies

The pioneering experiments concerning aggradation due to overloading at the upstream end of a laboratory flume were carried out by Bhamidipathy and Shen (1971). They found that the bed profile of an aggrading channel in uniform bed material was straight and proposed a logarithmic relationship between the bed level and time.

The most frequently quoted experimental data were reported by Soni et al. (1977a, 1977b, 1980). The experiments were performed in a 0.20 m wide, 0.50 m deep and 30 m long recirculatory tilting flume using sediment of median size 0.32 mm and geometric standard deviation 1.30. Uniform flow condition was first established for a prescribed discharge and slope. The equilibrium concentration was then obtained. Then the rate of sediment supply was increased over and above the

equilibrium sediment transport rate, the additional sediment being fed manually at a constant rate at the upstream end of the flume. The additional sediment was deposited downstream in the flume. The bed and water surface profiles were recorded at regular time intervals and the run was continued until the aggradation front reached close to the end of the flume. The range of the sediment excess ratio, $\Delta q_s/q_{se}$, covered during the experiments was from 0.30 to 4.0. In a few ensuing papers, Soni (1981a,1981b,1981c) presented very detailed information on his experimental studies of aggradation in alluvial channels, giving error function solutions for the bed profile and the unsteady sediment load.

To study the relationship between the equilibrium bed profile and its influencing factors, Wang et al. (1983) conducted a series of experiments with a flume measured 40 m long, 0.60 m wide and 0.75 m deep using three different sands with median diameters being 0.20, 0.35 and 0.47 mm, respectively. They found that with fixed water and sediment discharges and other boundary conditions, as the delta extending downstream, the longitudinal bed profile rises in a roughly parallel fashion.

In summary, most of the theoretical studies are based on the work of de Vries (1973). The differences between the various models are due to different degrees of simplification to the governing equations. Most studies use the much simplified relation, $q_s = a \cdot u^b$, as the sediment discharge equation. Comparing to the large amount of theoretical work, very little experimental work was conducted. As for the widely quoted experimental studies by Soni et al. (1980), the sediment concentrations used are only up to a few times of the equilibrium concentrations. Such dilute concentrations are not suitable for studying the beach formation in tailings disposal.

3. EXPERIMENTAL STUDY

3.1 General

As mentioned earlier, in tailings disposal study, no transient beach profiles have ever been considered. On the other hand, in the hydraulic transport field, there are considerable number of theoretical studies on aggradation due to overloading. However, very few laboratory studies have ever been published to date. With the limited experimental works (Bhamidipathy and Shen, 1971, Garde et al., 1981, Mehta et al., 1983, Soni et al., 1977, Soni, 1981), the investigators were only interested in very dilute sediment concentrations which were not far from the equilibrium ones. Furthermore, the depth of water in those studies was also significantly larger than that in tailings disposal.

Consequently, a laboratory research was planned to model the beach profiles as a function of both time and distance along with other parameters during hydraulic deposition of tailings and to find out the effects of sediment concentration and slurry discharge on the transient beach profiles. The concentrations used were much higher than those in the published experimental studies.

3.2 Experimental Set–Up

3.2.1 Flume and Sand Feeder

The main experimental facility was a plexiglas flume measuring 4.87 m in length, 0.31 m in width, and 0.46 m in depth. Fig. 3.1 shows the flume and the auxiliary equipment of the set–up. The slope of the flume could be adjusted through a hydraulic jack. Tap water was fed into the system through a stainless steal box in

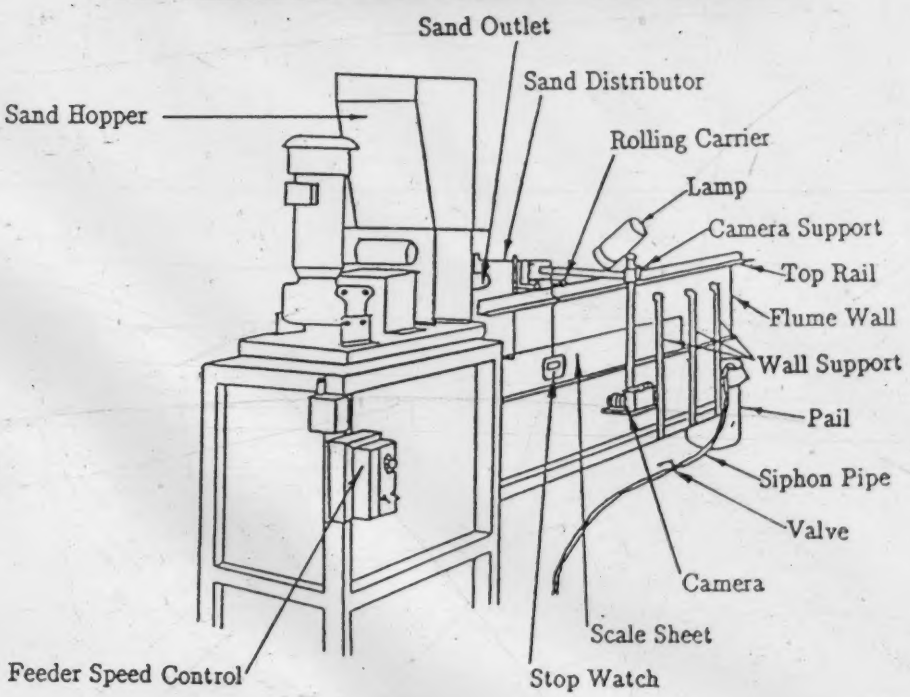

Fig. 3.1 Experimental Set–up

the upstream end of the flume, sluicing out uniformly across the width of the flume. The discharge of water was measured by a rotameter. Dry sand is fed steadily by a mechanically operated feeder onto a specially designed distributor (Figs. 3.2a, 3.2b), spreading evenly and forming a mixture with the oncoming water. The outflow of the flume was collected and decanted in a big plastic pail, with the water being dumped into the drainage system through a valve–controlled siphon pipe. The sand used in the study was Sil.2 purchased from Edmonton based Sil Silica, having a median diameter of 0.267 mm and a geometric standard deviation (Garde and Ranga Raju, 1985) of 1.30. A plot of the sieve–diameter distribution of the sand is shown in Fig. 3.3.

3.2.2 Beach Profile Recording Instrument

The beach profiles as a function of time and distance were recorded by taking photographs on one side of the bed through the transparent wall of the flume. Acetate sheets with both horizontal and vertical rulers generated by the MTS computing system at University of Alberta were taped on the front wall of the plexiglas flume, showing the vertical and horizontal readings of the beach profile. A camera support along with a rolling carriage on top of the flume allowed the camera to move in all three directions. A stopwatch attached to the camera support in front of the wall allowed the run number, date and time to be recorded in each photograph taken.

3.3 Experimental Procedure

Before starting an experimental run, the flume slope was adjusted to the desired value and the stopwatch along with the identification of the run number and

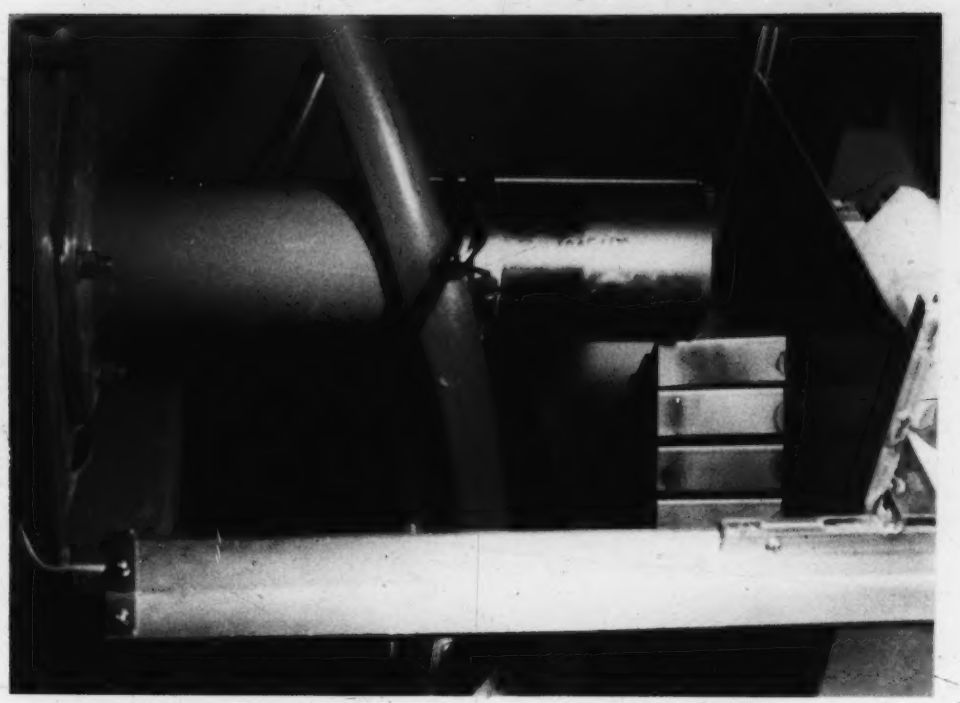

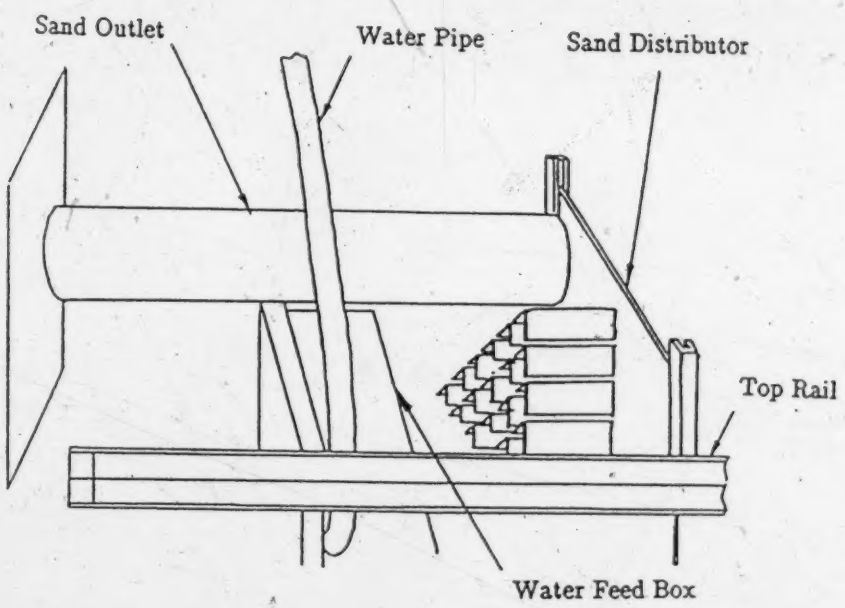

Fig. 3.2a Arrangement for Sand and Water Feed

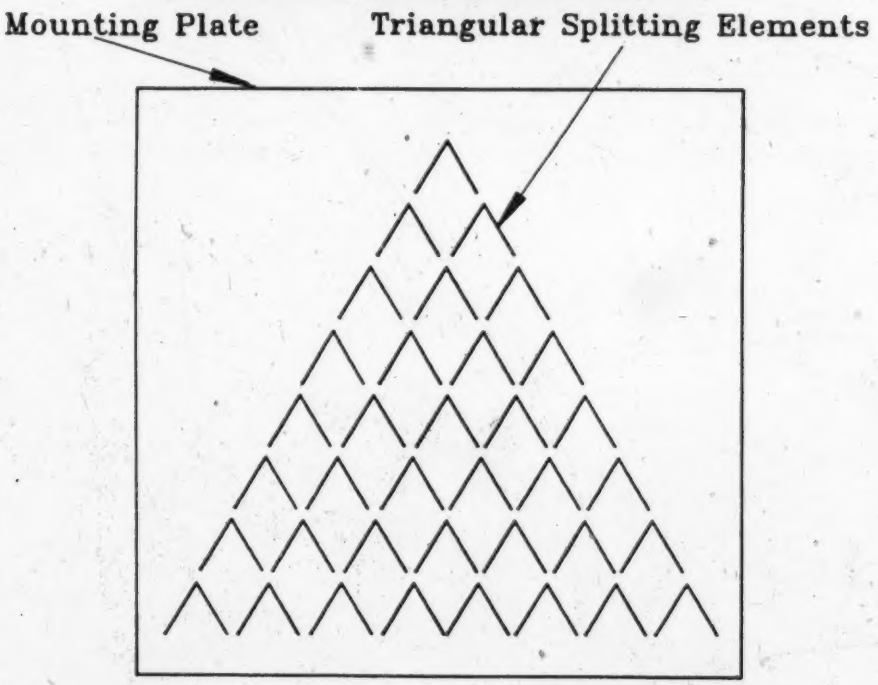

Fig. 3.2b Sand Distributor

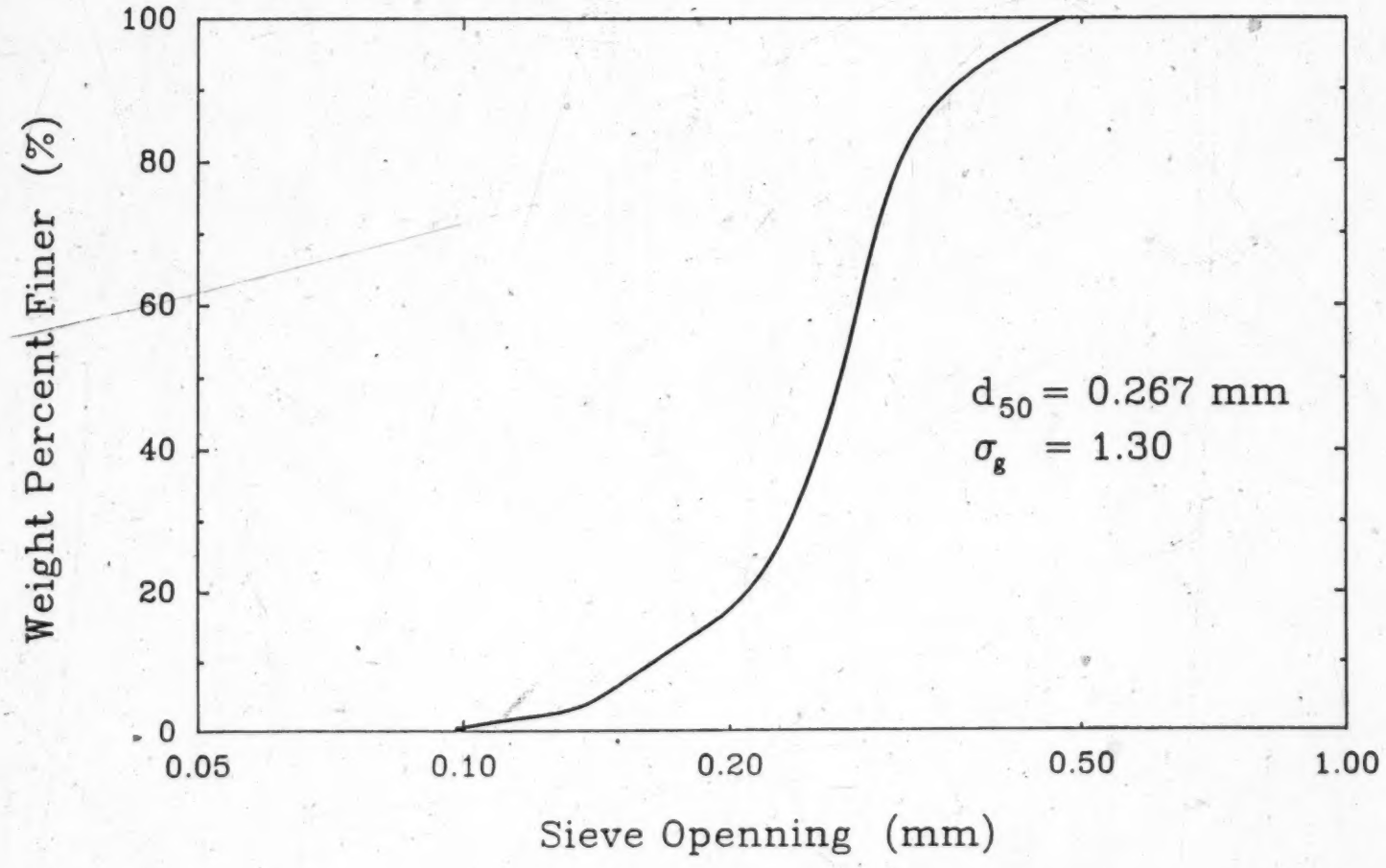

Fig. 3.3 Sediment Size Distribution

date was mounted on the camera support. The camera was then mounted to the camera support. Next, water was fed into the water feed box in the flume with a specified flow rate. When the water in the collecting pail reached a certain level, the discharging siphon pipe was set to operate. The sand feeder was then turned on at a pre–set sand feeding rate and the stop watch was started simultaneously. The beach profile was recorded by taking photographs at 5 minute interval. The number of photographs taken for each profile depended on the length of the beach. If more than one photograph was required, the operation had to be conducted as quickly as possible to minimize the time lag. Four beach profiles were recorded for a typical run which lasted about twenty minutes.

3.4 Qualitative Observations

As the sediment load was much higher than that the water could carry in suspension, it could be seen that most of the sand settled out very quickly after being fed into the flume. The sand was transported downstream mainly as bed load through saltation and rolling. The growth of the beach profile slowed down as time and the length of the beach increased. The largest slope of the beach occurred at the feeding section of the flume. The photographs of two typical runs are shown in Figs 3.4 and 3.5, one for a low sand feeding rate and the other for a high sand feeding rate. Each figure shows four beach profiles at t = 5, 10, 15 and 20 minutes respectively. A closer view of a typical individual photograph is presented as Fig. 3.6.

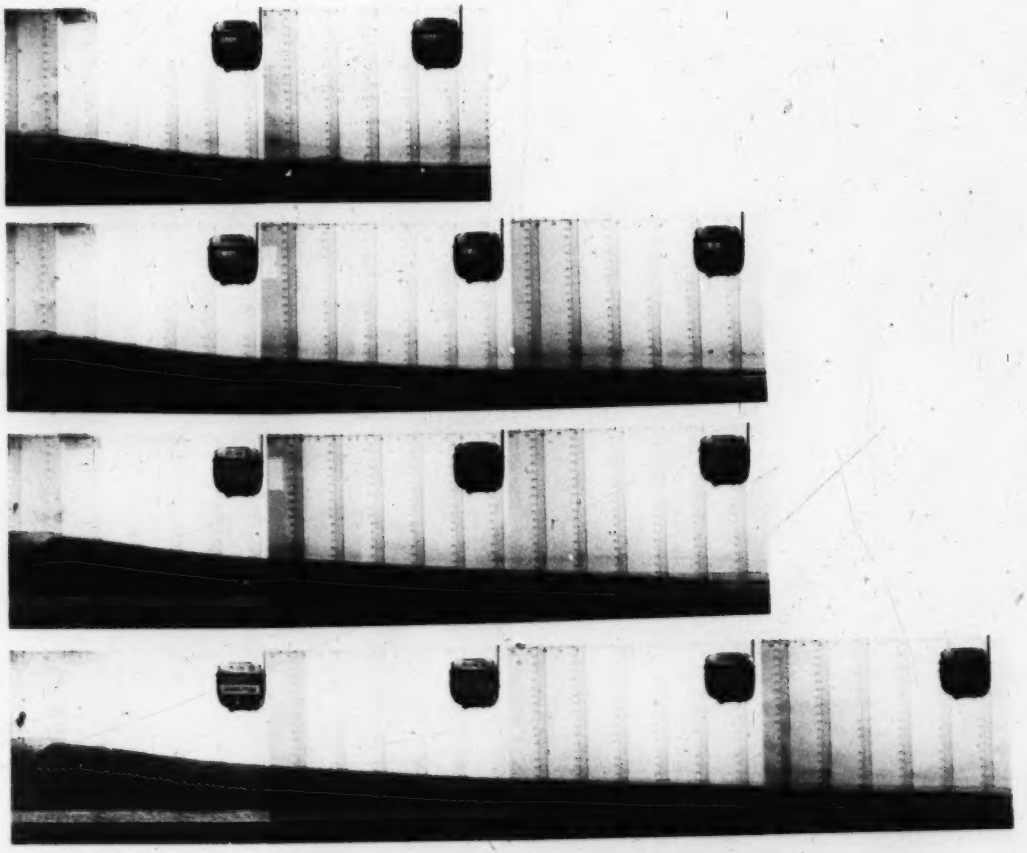

Fig. 3.4 Typical Beach Profiles for Low Sand Feeding Rate

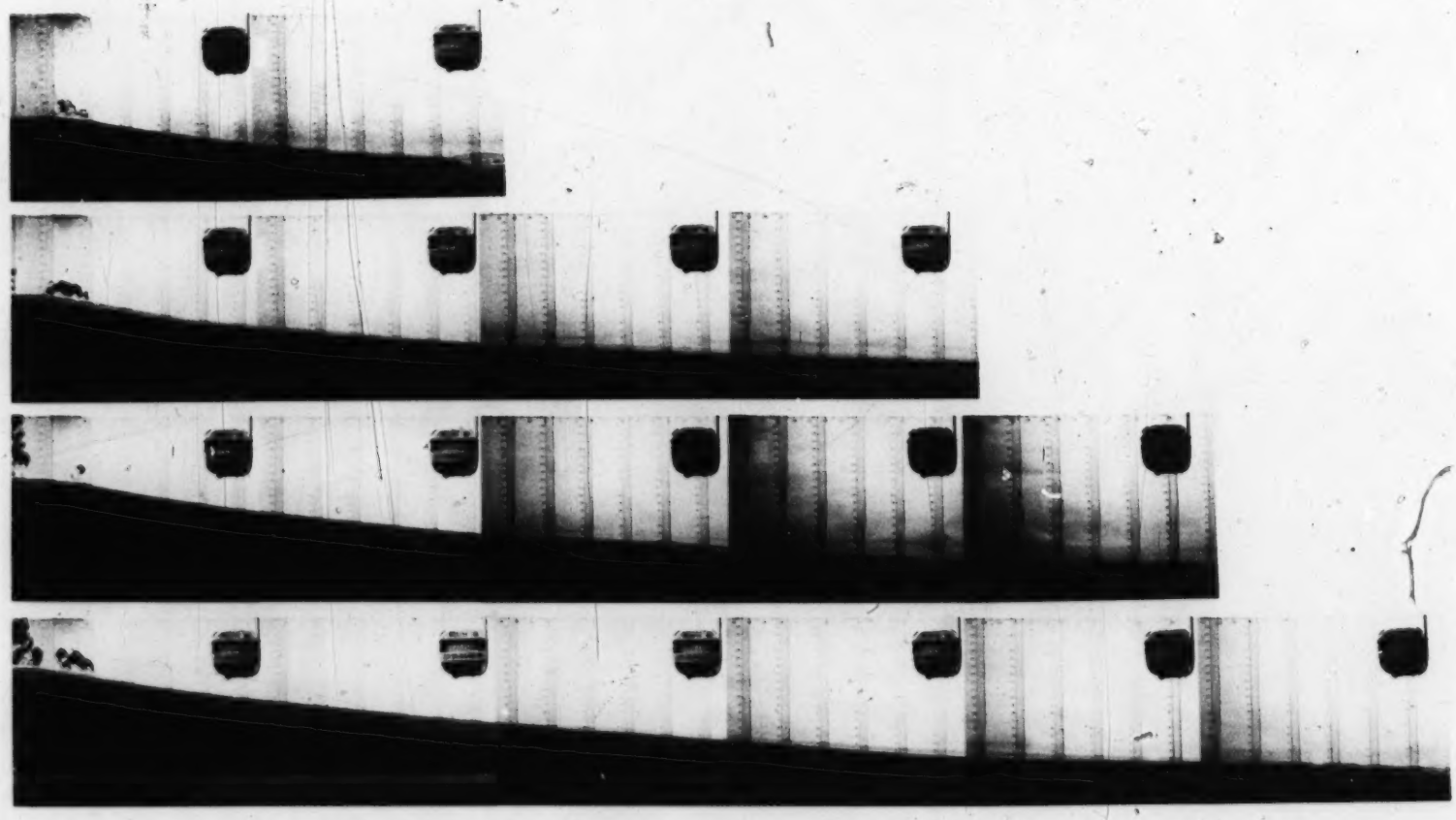

Fig. 3.5 Typical Beach Profiles for High Sand Feeding Rate

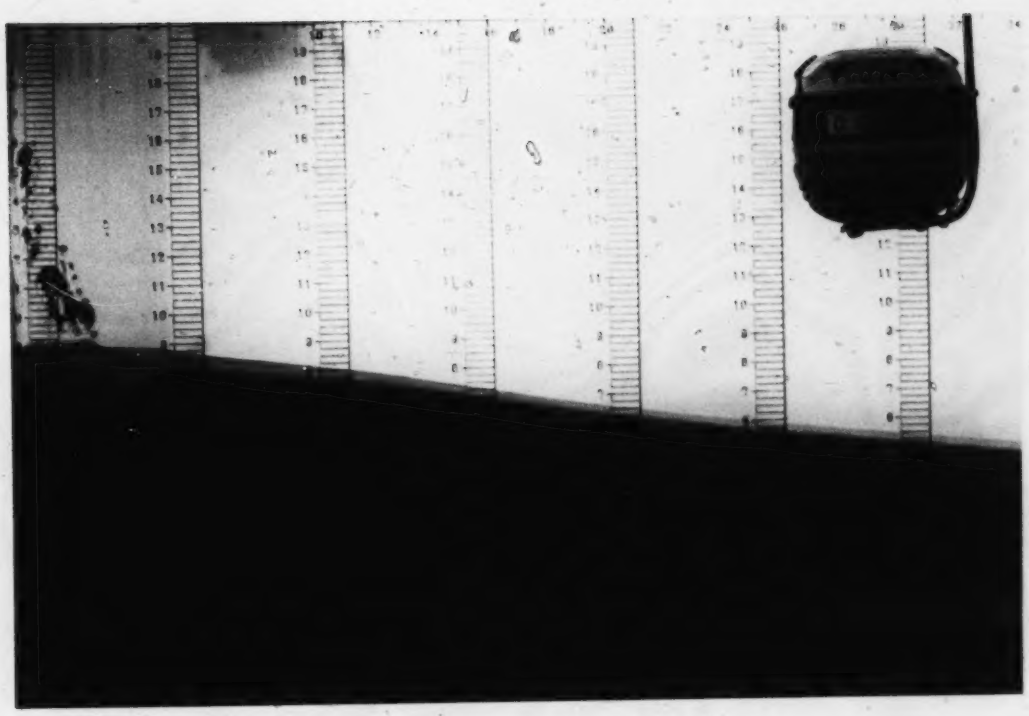

Fig. 3.6 A Typical Photograph from a Beach Profile

3.5 Experimental Data

3.5.1 Properties of Sand

The properties of sand used in the experiments are given below.

$d_{50} = 0.267 \times 10^{-3}$ m

$\rho_s = 2650$ kg/m^3

$\sigma_g = 1.30$

$\beta = 0.57$

where d_{50} is the median diameter of sand; ρ_s is the density of sand; σ_g is the geometric standard deviation of the sand size; and β is the ratio of solid volume to total volume in the beach.

3.5.2 Beach Profile Data

The experiments were arranged in two groups: (A) constant water discharge with different sediment concentration; (B) constant sediment concentration in the feed with different total slurry discharge. For the first group, four different solid concentrations were tested while for the second group four different total slurry discharge were examined. For convenience in referring the tests hereafter, the four tests in the first group are referred as A1 to A4 while the four tests in the second group are referred as B1 to B4. To ensure reliability of the beach profile data, for group A tests, each set of parameters (initial beach slope, water discharge, sediment feeding rate, etc.) was run at least three times. The average values of the three successful runs were taken to be plotted and analyzed. The beach profile data for all the eight different tests are presented in tables 3.1 through 3.8.

Table 3.1
Beach Profile Data from Test A1

$q_f = 7.67 \times 10^{-4} m^3/s-m$, $q_{stot} = 2.47 \times 10^{-5} m^3/s-m$, $S_0 = 0.00543$

x (cm)	Z,cm t=5 min	Z,cm t=10 min	Z,cm t=15 min	Z,cm t=20 min
0	4.2	6.2	7.6	8.8
5	4.0	5.8	7.2	8.3
15	2.7	4.6	5.9	7.0
25	1.7	3.5	4.9	5.9
35	1.25	2.8	4.1	5.2
45	0.73	2.1	3.4	4.5
55	0.55	1.5	2.7	3.7
65		1.3	2.2	3.2
75		1.1	1.9	2.7
85		0.8	1.4	2.1
95			1.2	1.8
105				1.3
115				1.0

Table 3.2
Beach Profile Data from Test A2

$q_f = 7.67 \times 10^{-4} m^3/s-m$, $q_{stot} = 3.07 \times 10^{-5} m^3/s-m$, $S_0 = 0.00543$

x (cm)	Z,cm t=5 min	Z,cm t=10 min	Z,cm t=15 min	Z,cm t=20 min
0	4.7	7.1	8.6	10.0
5	4.5	6.7	8.2	9.4
15	3.2	5.3	6.8	8.1
25	2.3	4.3	5.8	7.1
35	1.7	3.5	5.0	6.2
45	1.1	2.7	4.2	5.3
55	0.8	2.1	3.3	4.5
65		1.7	2.8	4.0
75		1.2	2.4	3.4
85		1.0	1.8	2.8
95			1.5	2.2
105			1.3	2.0
115			0.6	1.5
125				1.1

Table 3.3
Beach Profile Data from Test A3

$q_f = 7.67 \times 10^{-4} m^3/s-m$, $q_{stot} = 3.83 \times 10^{-5} m^3/s-m$, $S_0 = 0.00543$

x (cm)	Z,cm t=5 min	Z,cm t=10 min	Z,cm t=15 min	Z,cm t=20 min
0	5.6	8.1	10.0	11.5
5	5.4	7.6	9.5	11.0
15	3.9	6.2	8.0	9.6
25	2.9	5.1	6.9	8.4
35	2.3	4.3	6.0	7.3
45	1.7	3.5	5.1	6.3
55	1.2	2.8	4.3	5.5
65		2.3	3.7	5.0
75		1.9	3.2	4.4
85		1.3	2.6	3.8
95			2.1	3.3
105			1.6	2.7
115			1.1	2.2

Table 3.4
Beach Profile Data from Test A4

$q_f = 7.67 \times 10^{-4} m^3/s-m$, $q_{stot} = 4.77 \times 10^{-5} m^3/s-m$, $S_0 = 0.00543$

x (cm)	Z,cm t=5 min	Z,cm t=10 min	Z,cm t=15 min	Z,cm t=20 min
0	6.5	9.4	11.7	13.3
5	6.2	8.9	11.4	12.8
15	4.8	7.4	9.8	11.2
25	3.5	6.2	8.4	9.9
35	2.6	5.2	7.3	8.9
45	1.8	4.4	6.2	7.9
55	1.3	3.5	5.4	7.1
65	0.9	3.0	4.7	6.3
75	0.5	2.5	4.0	5.4
85		1.9	3.3	4.7
95		1.6	2.6	4.1
105		1.2	2.1	3.4
115			1.6	2.8
125			1.3	2.5
135				2.2
145				1.9

Table 3.5
Beach Profile Data from Test B1

$q_f = 3.49 \times 10^{-4} m^3/s-m$, $q_{stot} = 1.99 \times 10^{-5} m^3/s-m$, $S_0 = 0.00543$

x (cm)	Z,cm t=5 min	Z,cm t=10 min	Z,cm t=15 min	Z,cm t=20 min
0	4.05	7.25	8.2	9.05
5	3.3	6.0	7.5	8.25
15	2.3	4.2	5.9	6.5
25	1.25	2.85	4.5	5.25
35	0.75	1.85	3.5	
45		1.0	2.5	
55		0.5	1.75	
65			1.25	
75			0.7	
85			0.3	

Table 3.6
Beach Profile Data from Test B2

$q_f = 5.17 \times 10^{-4} m^3/s-m$, $q_{stot} = 2.94 \times 10^{-5} m^3/s-m$, $S_0 = 0.00543$

x (cm)	Z,cm t=5 min	Z,cm t=10 min	Z,cm t=15 min	Z,cm t=20 min
0	5.25	8.25	9.0	10.25
5	4.75	7.25	8.5	9.75
15	3.25	5.5	7.0	8.25
25	2.05	4.0	5.75	6.75
35	1.2	3.2	4.75	5.8
45	0.6	2.5	3.75	4.85
55		1.8	3.0	4.4
65		1.6	2.5	3.75
75		1.0	2.0	3.25
85		0.5	1.5	2.5
95			1.1	1.9
105			0.6	1.3
115				1.0
125				0.5

Table 3.7
Beach Profile Data from Test B3

$q_f = 6.88 \times 10^{-4} m^3/s-m$, $q_{stot} = 3.91 \times 10^{-5} m^3/s-m$, $S_0 = 0.00543$

x (cm)	Z,cm t=5 min	Z,cm t=10 min	Z,cm t=15 min	Z,cm t=20 min
0	5.75	8.4	10.8	12.0
5	5.4	7.8	10.4	11.3
15	3.95	6.35	8.6	9.9
25	2.6	5.0	7.2	8.5
35	2.0	4.0	6.1	7.5
45	1.3	3.5	5.2	6.5
55		2.55	4.3	5.3
65		1.75	3.5	
75			2.8	
85			2.0	

Table 3.8
Beach Profile Data from Test B4

$q_f = 8.54 \times 10^{-4} m^3/s-m$, $q_{stot} = 4.86 \times 10^{-5} m^3/s-m$, $S_0 = 0.00543$

x (cm)	Z,cm t=5 min	Z,cm t=10 min	Z,cm t=15 min	Z,cm t=20 min
0	6.45	9.5	11.5	
5	6.0	9.1	10.8	
15	4.5	7.5	9.3	
25	3.35	6.25	8.2	
35	2.75	5.25	7.3	
45	2.0	4.3	6.3	
55	1.7	3.7	5.4	
65	1.25	3.2	4.7	
75	1.0	2.7	4.0	
85	0.75	2.0	3.5	
95		1.4	3.0	
105		0.8	2.5	
115		0.7	2.2	
125			2.0	
135			1.5	

4. THEORETICAL DERIVATIONS

A nonlinear parabolic model for the beach profile was developed in this chapter. The model is different from those used by all the other investigators, notably by de Vries, mentioned in the previous chapter. The main differences are due to the adoption of two equations, Manning's equation as the fluid resistance relation and Meyer–Peter and Muller bed–load formula as the sediment transport relation. The former relates the average flow velocity directly to the energy slope and the depth of water while the latter is the widely used bed–load formula which takes the critical shear stress into consideration. The detailed derivation of the nonlinear parabolic model is given in the following sections.

4.1 Governing Equations

The basic equations governing the transient problems in alluvial streams can be written for one dimensional flow in the following manner (Gard and Ranga Raju, 1985; de Vries, 1973).

The continuity equations for water and sediment, respectively, are

$$\frac{\partial h}{\partial t} + u\frac{\partial h}{\partial x} + h\frac{\partial u}{\partial x} = 0 \tag{4.1}$$

$$\beta\frac{\partial z}{\partial t} + \frac{\partial q_s}{\partial x} = 0 \tag{4.2}$$

The momentum equation for the water in a channel of constant width can be written in the following form

$$\frac{\partial u}{\partial t} + u\frac{\partial u}{\partial x} + g\frac{\partial h}{\partial x} + g\frac{\partial z}{\partial x} + g\,S_f = 0 \tag{4.3}$$

as for the resistance relationship of the water, the Manning's equation in SI units gives

$$u = \frac{1}{n} h^{\frac{2}{3}} S_f^{\frac{1}{2}} \tag{4.4}$$

where n can be written as follows (Ranga Raju, 1981):

$$n = \frac{k_s^{\frac{1}{6}}}{8.16\sqrt{g}} \tag{4.5}$$

In the above equations, g is the gravitational acceleration; h is the average depth of water; k_s is the height of the equivalent sand roughness which in this case is the median diameter of sand; n is Manning's resistance coefficient; q_s is the volumetric sediment discharge per unit width; S_f is the energy slope; t is time; u is the average velocity of the water; x is the horizontal distance along the channel; z is the beach elevation with respect to a horizontal reference level; β is the ratio of solid volume to total volume in the beach ($\beta = 1 -$ porosity). Fig. 4.1 shows a sketch of the flow system.

For the sediment transport relation, there are numerous equations available (Anonymous, 1971; Yalin, 1977; Garde and Ranga Raju, 1985; Wiberg and Smith, 1989). The bed–load equation of Bagnold modified by Yalin (1977) was originally employed to compute the beach profiles. It was found that the coefficient of this equation was about four times too small to predict results matching the experimental data. When the bed–load formula of Meyer–Peter and Muller given by Yalin (1977) was tested, the computed results showed very good agreement with our experimental data. Therefore, in this work, the following bed–load formula of Meyer–Peter and Muller was adopted:

$$\phi = 0 \text{ , for } Y < Y_{cr} \tag{4.6}$$

$$\phi = A_k (Y - Y_{cr})^{1.5} \text{ , for } Y \geq Y_{cr} \tag{4.7}$$

where ϕ is dimensionless transport rate defined as

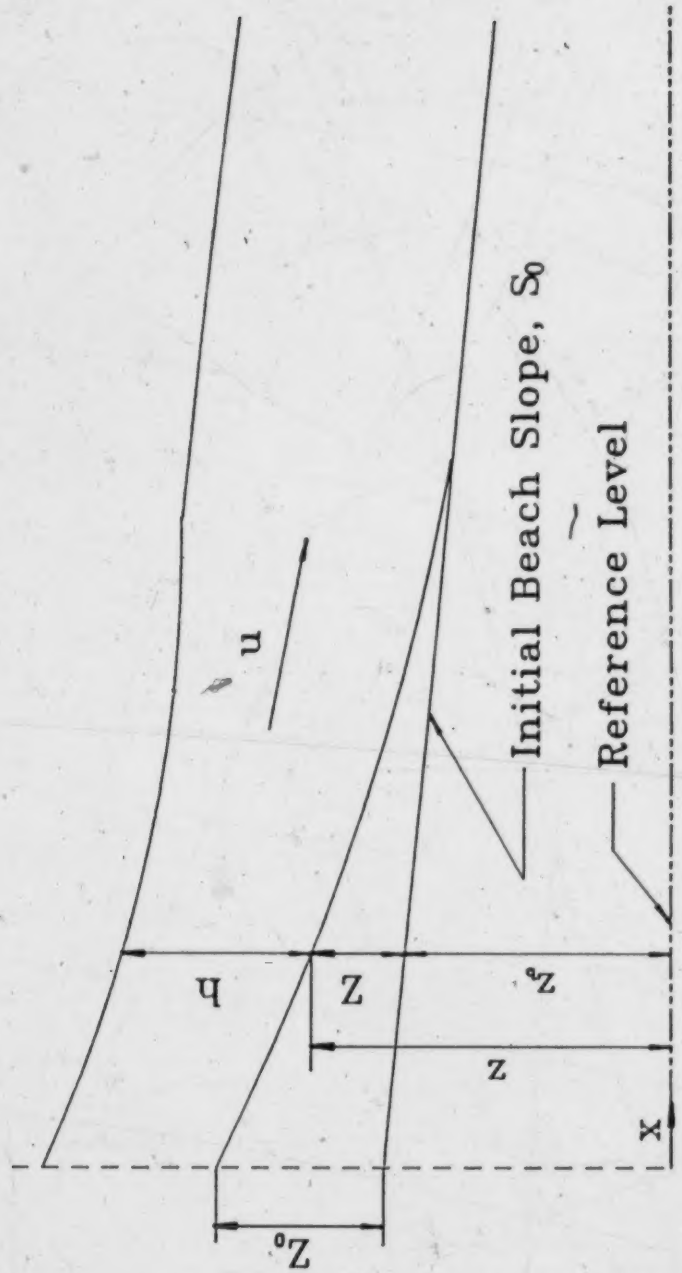

Fig. 4.1 Definition Sketch of Deposition

$$\phi = \frac{q_s \rho_f^{0.5}}{[(\rho_s - \rho_f) g D^3]^{0.5}} \tag{4.8}$$

Y is the mobility number defined as

$$Y = \frac{\rho_f S h}{(\rho_s - \rho_f) D} \tag{4.9}$$

Y_{cr} is the critical mobility number which is taken as a constant, $Y_{cr} = 0.047$; A_k is a coefficient originally specified as a constant, $A_k = 8$; ρ_s and ρ_f are the density of sand and water, respectively; D is the typical grain size of the sand, $D = d_{50}$; S is the beach slope.

According to Wiberg and Smith (1989), the coefficient of the Meyer–Peter and Muller equation, A_k, should be a variable between 5 and 15, depending on the excess of the shear stress. In this work, it will be shown that A_k slightly depends on the feed rate of the sediment.

4.2 Simplification of the Governing Equations

According to de Vries (1973), if the flow is supposed to be quasi–steady and uniform, i.e., $\partial u/\partial t \approx 0$, $\partial u/\partial x \approx 0$ and $\partial h/\partial x \approx 0$, then Eq. 4.3 reduces to

$$S_f = -\frac{\partial z}{\partial x} = S \tag{4.10}$$

and Eq. 4.1 becomes

$$q_f = u \cdot h = \text{constant} \tag{4.11}$$

where q_f is the volumetric flow rate of water per unit width.

Substituting Eq. 4.5 into Eq. 4.4 yields

$$u = 8.16\sqrt{g}\, h^{\frac{2}{3}} S_f^{\frac{1}{2}} k_s^{-\frac{1}{6}} \tag{4.12}$$

Combining Eqs. 4.10 with 4.12 results in

$$h = \left[\frac{q_f k_s^{\frac{1}{6}}}{8.16\sqrt{gS}} \right]^{\frac{3}{5}} \tag{4.13}$$

From Eqs. 4.8 and 4.9 one obtains

$$q_s = A_k \frac{\rho_f}{\rho_s - \rho_f} \sqrt{g} \left[S\, h - Y_{cr} \frac{\rho_s - \rho_f}{\rho_f} D \right]^{1.5} \tag{4.14}$$

Substitution of Eq. 4.13 into Eq. 4.14 yields

$$q_s = A_k \sqrt{g} \frac{\rho_f}{\rho_s - \rho_f} \left[8.16^{-0.6} g^{-0.3} k_s^{0.1} q_f^{0.6} S^{0.7} - Y_{cr} \frac{\rho_s - \rho_f}{\rho_f} D \right]^{1.5} \tag{4.15}$$

When Eq. 4.10 is substituted into Eq. 4.15, one obtains,

$$q_s = A_k \sqrt{g} \frac{\rho_f}{\rho_s - \rho_f} \left[8.16^{-0.6} g^{-0.3} k_s^{0.1} q_f^{0.6} \left(-\frac{\partial z}{\partial x}\right)^{0.7} - Y_{cr} \frac{\rho_s - \rho_f}{\rho_f} D \right]^{1.5} \tag{4.16}$$

From Eq. 4.2 and Eq. 4.16, it follows that

$$\frac{\partial z}{\partial t} = K \frac{\partial^2 z}{\partial x^2} \tag{4.17}$$

where

$$K = 0.298\, g^{0.2} A_k k_s^{0.1} q_f^{0.6} \beta^{-1} \frac{\rho_f}{\rho_s - \rho_f} \left(-\frac{\partial z}{\partial x}\right)^{-0.3}$$

$$\times \left[0.284\, g^{-0.3} k_s^{0.1} q_f^{0.6} \left(-\frac{\partial z}{\partial x}\right)^{0.7} - Y_{cr} \frac{\rho_s - \rho_f}{\rho_f} D \right]^{0.5} \tag{4.18}$$

To solve the nonlinear parabolic partial differential equation, Eq. 4.17, the following initial and boundary conditions are specified.

The initial condition is :

$$z(x,0) = z_b(x) \tag{4.19}$$

where $z_b(x)$ is the initial bed elevation at x. If at $t = 0$, the bed slope is uniform along the channel, then Eq. 4.19 is equivalent to

$$-\frac{\partial z}{\partial x}\bigg|_{t=0} = S_0 \tag{4.20}$$

where S_0 is the initial bed slope.

As for the boundary condition at $x = 0$ and $t > 0$, it is not possible to explicitly specify z. Instead, the only known quantity at $x = 0$ is q_{s0}, the feed flow rate of the sediment. Therefore, Eq. 4.2 can be employed for the first boundary

condition to advantage, i.e.,

$$\beta \left.\frac{\partial z}{\partial t}\right|_{x=0} = - \left.\frac{\partial q_s}{\partial x}\right|_{x=0} \tag{4.21}$$

The second boundary condition can be written as

$$z(\infty,t) \doteq z_b(\infty) \tag{4.22}$$

Eqs. 4.17 and 4.18 along with the initial and boundary conditions form the desired nonlinear parabolic model for computing the beach profiles.

5. NUMERICAL SOLUTION

For the non–linear parabolic model defined by Eqs 4.17 and 4.18, there is no analytical solution. Therefore, a numerical solution by finite difference method was employed.

5.1 Finite Difference Formulations

Since the length of the beach profile propagates downstream with time, for simplicity of computation, the explicit scheme was adopted to discretize Eq. 4.17 (Gerald and Wheatley, 1984). In this method, the time derivative is replaced by Newton forward difference while the spatial derivatives are discretized by the central difference schemes at the old time level. Hence, at any interior point i, Eq. 4.17 can be discretized as follows,

$$\frac{z_i^{n+1} - z_i^n}{\Delta t} = K_i^n \left[\frac{z_{i+1}^n - 2\, z_i^n + z_{i-1}^n}{(\Delta x)^2} \right] \tag{5.1}$$

or

$$z_i^{n+1} = z_i^n + K_i^n \frac{\Delta t}{(\Delta x)^2} \left[z_{i+1}^n - 2\, z_i^n + z_{i-1}^n \right] \tag{5.2}$$

where K_i^n can be approximated by

$$K_i^n = 0.298\, g^{0.2}\, A_k\, k_s^{0.1}\, q_f^{0.6}\, \beta^{-1} \frac{\rho_f}{\rho_s - \rho_f} \left[\frac{z_{i-1}^n - z_{i+1}^n}{2\ \Delta x} \right]^{-0.3}$$

$$\times \left[0.284\, g^{-0.3}\, k_s^{0.1}\, q_f^{0.6} \left[\frac{z_{i-1}^n - z_{i+1}^n}{2\ \Delta x} \right]^{0.7} - Y_{cr} \frac{\rho_s - \rho_f}{\rho_f} D \right]^{0.5} \tag{5.3}$$

In the above equations, n denotes the time level and i indicates the location in x direction.

5.2 Initial and Boundary Conditions

The initial condition of Eq. 4.17 is given in Eqs. 4.19 and 4.20. The first boundary condition of Eq. 4.17 at $x = 0$ for $t > 0$ is given in Eq. 4.21. If the first and second order forward difference formulas are used to approximate the time and space derivatives in Eq. 4.21, then the first boundary condition can be discretized as:

$$\frac{z_0^{n+1} - z_0^n}{\Delta t}\beta = \frac{3\ q_{s0}^n - 4\ q_{s1}^n + q_{s2}^n}{2\ \Delta x} \tag{5.4}$$

or

$$z_0^{n+1} = z_0^n + \frac{\Delta t}{2\ \Delta x\ \beta}(3\ q_{s0}^n - 4\ q_{s1}^n + q_{s2}^n) \tag{5.5}$$

where q_{s0}, is the feed flow rate of the sediment traveling downstream the sediment feed point; q_{s1} and q_{s2} are the local sediment transport rates at grid points Δx and $2 \cdot \Delta x$ from the feed point respectively. q_{s0} is known; q_{s1} and q_{s2} may be computed from Eq. 4.16.

The second boundary condition is given in Eq. 4.22. However, it is impractical from a computational point of view to impose the infinitive boundary condition. In fact, at $x = L$, the length of the beach profile, z remains the initial value. Hence the following boundary condition may be specified:

$$z(L,t) = z_b(L) \tag{5.6}$$

5.3 Stability Consideration

One disadvantage of the simple explicit scheme is that it may be unstable, i.e., an error made at one stage of the computations is magnified as the computation proceeds. To avoid the unstable condition, the following criterion must be met when choosing the time and space steps (Gerald and Wheatley, 1984).

$$K^n \frac{\Delta t}{(\Delta x)^2} < \frac{1}{2} \tag{5.7}$$

This condition can be easily met in this study.

5.4 Computational Considerations and Procedure

5.4.1 Determination of the Length of Beach Profiles

To implement the second boundary condition, Eq. 5.6, the length of the beach profile, L, must be defined. For each time step, L is defined such that when $x = L$, the increase of the beach elevation over the initial elevation at that point just drops to less than one diameter of the sand. Computations are carried out until $x = L$ for each time step.

5.4.2 Compensation of the Sediment Deposited Upstream Sediment Feed Point

In the experiments, there was a 5–cm distance between the water feed box and the sediment feed point. Therefore, there was always some sediment settling out upstream the sediment feed point. It was observed that the upstream portion of the sediment was significant, especially at the beginning of a run. Consequently, this effect should be taken into account in order to model the development of the beach profiles accurately.

Figs. 5.1a and 5.1b show two different cases during a run. It was observed that the beach profile rose in a roughly parallel fashion both upstream and downstream of the sediment feed point.

From the geometric relationship shown in Figs. 5.1a and 5.1b, it is seen that

$$q_{s0} = \frac{dz}{dt} L \tag{5.8}$$

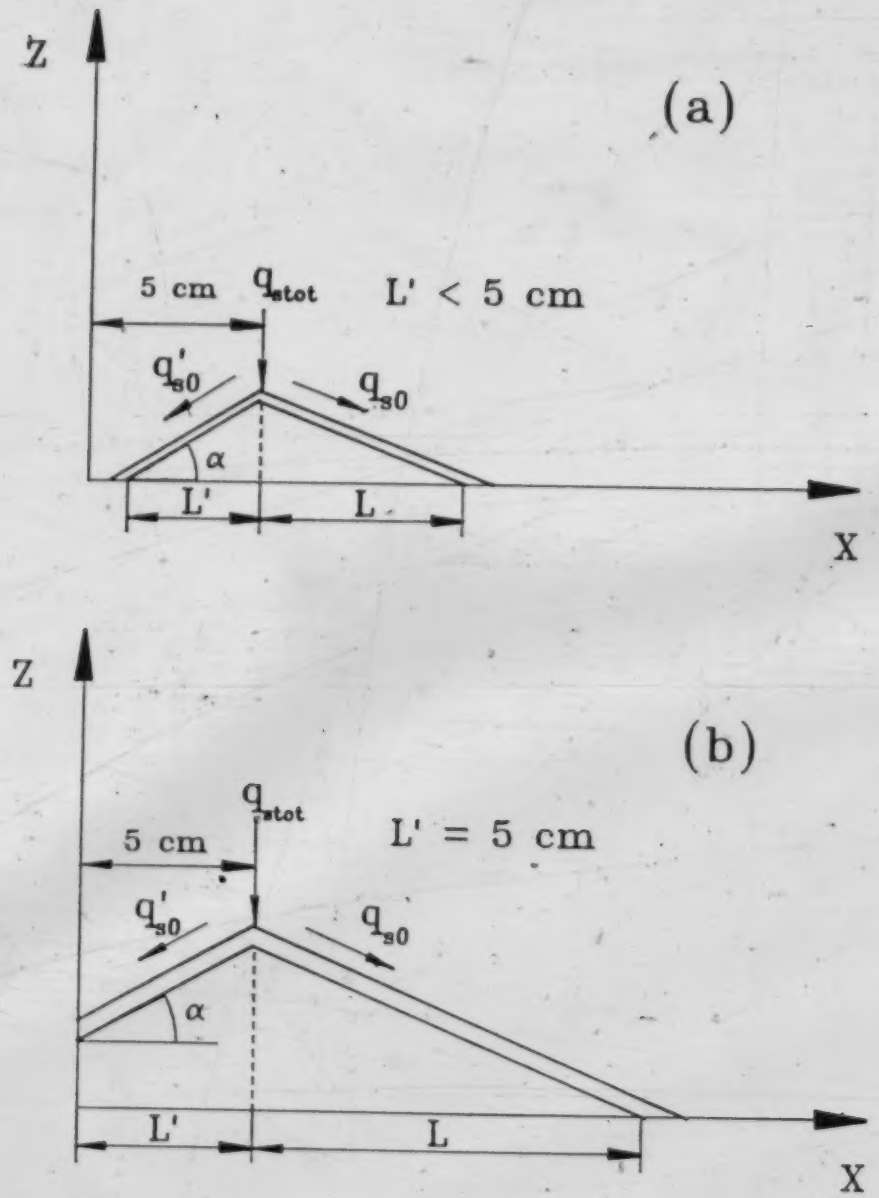

Fig. 5.1 Upstream Deposition of Sand

(a) L' < 5 cm ; (b) L' = 5 cm

$$q'_{s0} = \frac{dz}{dt} L' \tag{5.9}$$

$$q_{stot} = q_{s0} + q'_{s0} \tag{5.10}$$

Hence,

$$q_{s0} = \frac{L}{L + L'} q_{stot} \tag{5.11}$$

Through measurement, it was found that the slope of the upstream portion of the beach profile, α, is roughly a constant and

$$\tan(\alpha) = 2.9/5.0 \tag{5.12}$$

5.4.3 Modification of the Meyer–Peter and Muller Equation

The sediment transport formula of Meyer–Peter and Muller is given as Eqs. 4.6 to 4.9 in this study. Wiberg and Smith (1989) have pointed out that the coefficient of the sediment transport equation, A_k, is a variable between 5 and 15 rather than a constant, 8, as given in the original equation. Preliminary computation of this work lent further support to their conclusion. Figs. 5.2a to 5.2d show the comparison between the experimental and computed beach profiles with $A_k = 8$ for group A tests. It can be seen that not all the tests show good agreement. For the same four tests, in order to match the experimental results, the coefficient of the sediment transport equation, A_k, varies from 6.0 to 8.2, depending on the feed sediment discharge. The relation between the coefficient and the feed sediment discharge was fitted and is given in Eq. 5.13.

$$A_k = 4.05 + 8.69 \times 10^4 \, q_{stot} \tag{5.13}$$

The plot of A_k versus q_{stot} is presented in Fig. 5.3. With variable A_k, the computed beach profiles show very good agreement with the experimental ones for almost all the tests. Detailed comparison and analysis will be given in chapter 6.

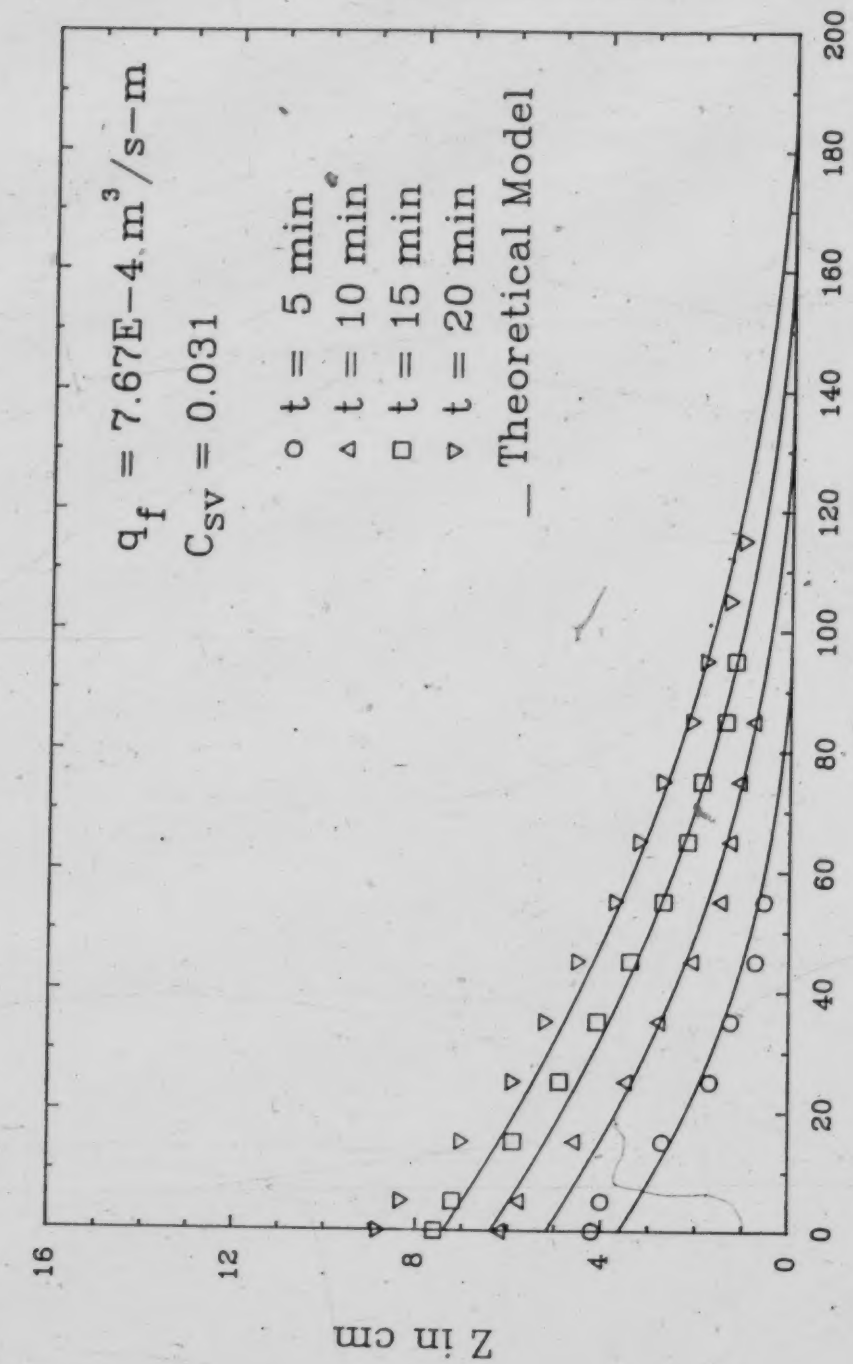

Fig. 5.2a Comparison between Experimental and Theoretical Beach Profiles with A_k = 8.0 for Test A1

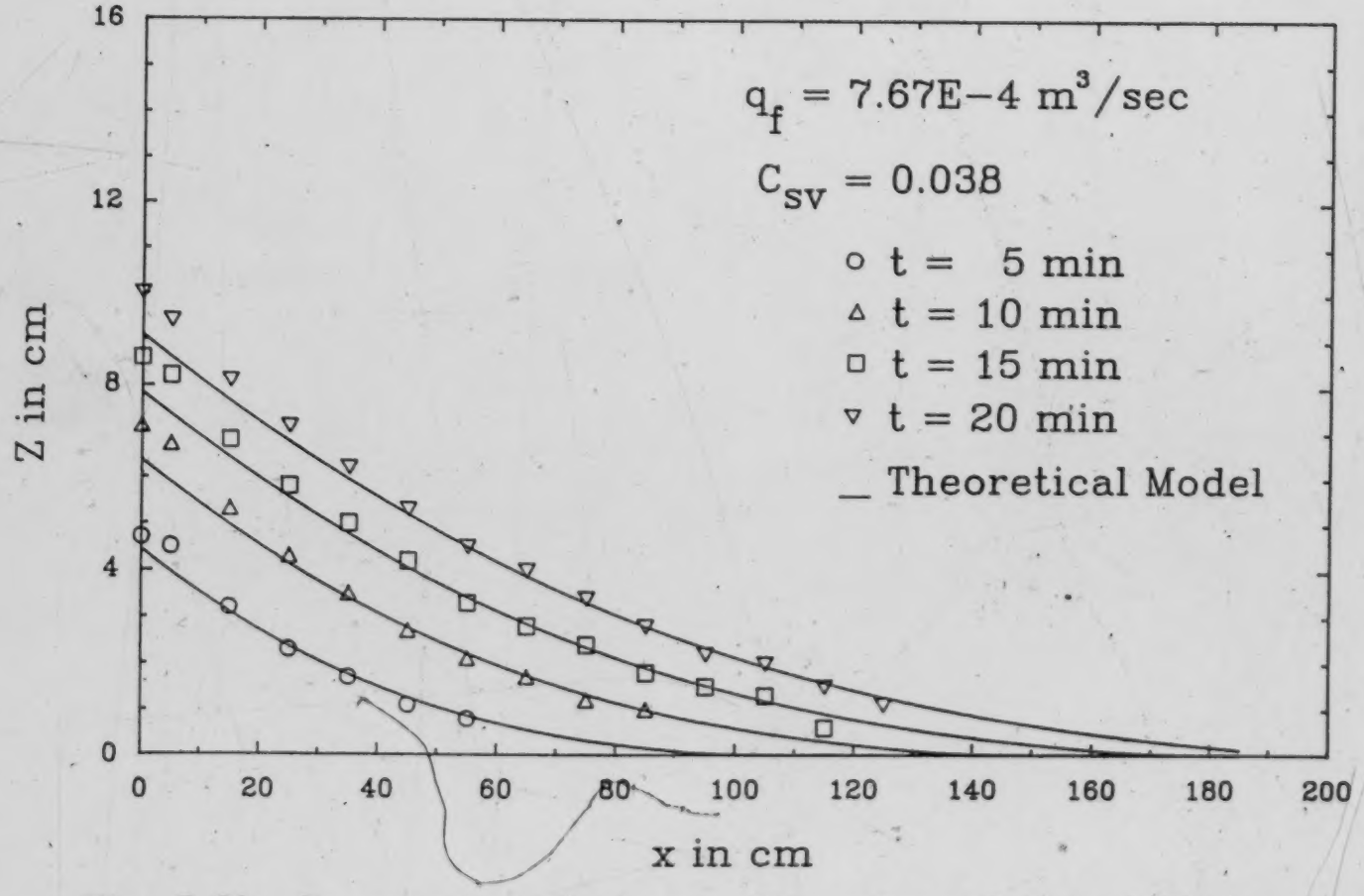

Fig. 5.2b Comparison between Experimental and Theoretical Beach Profiles with A_k = 8.0 for Test A2

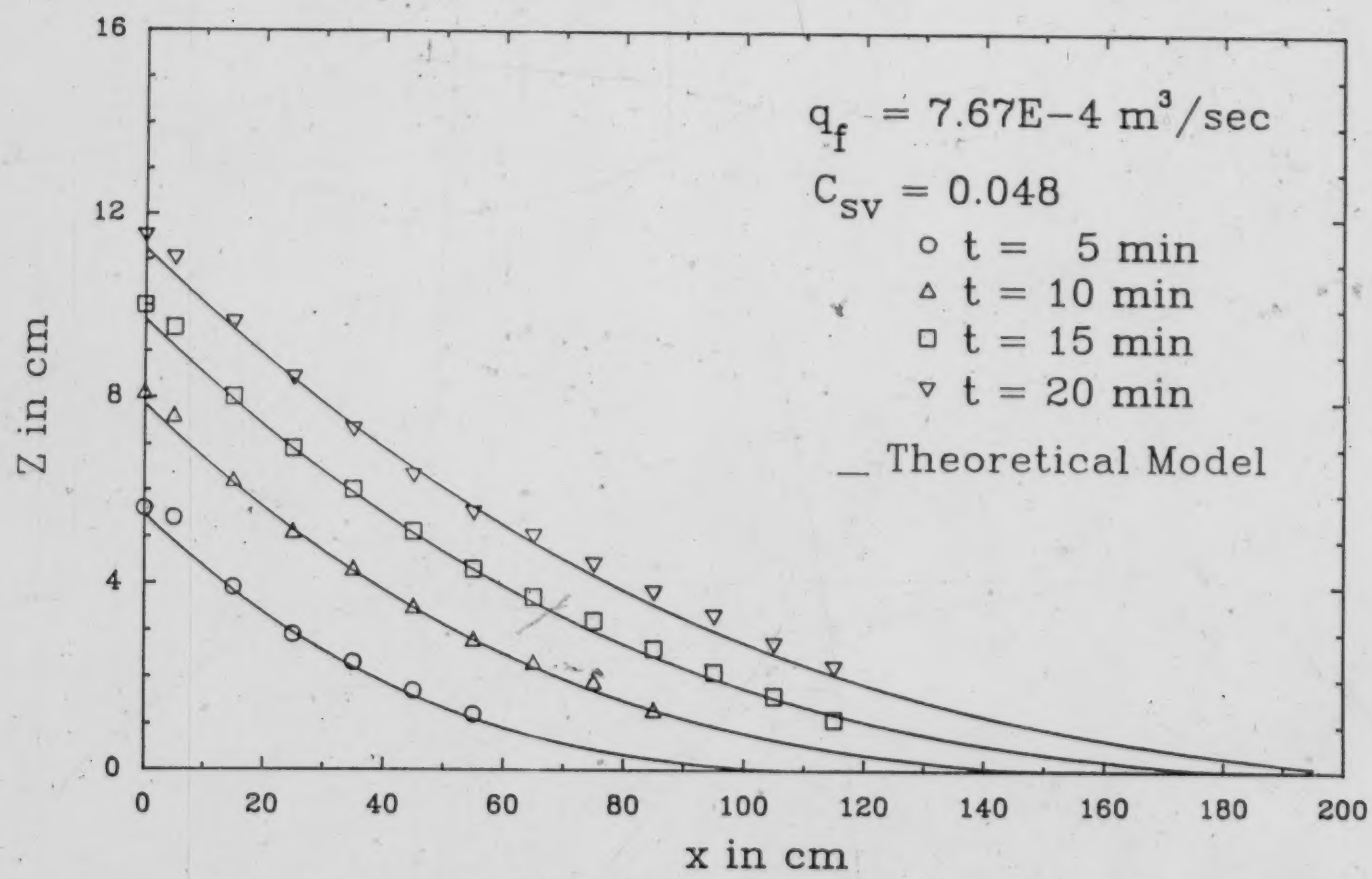

Fig. 5.2c Comparison between Experimental and Theoretical Beach Profiles with A_k = 8.0 for Test A3

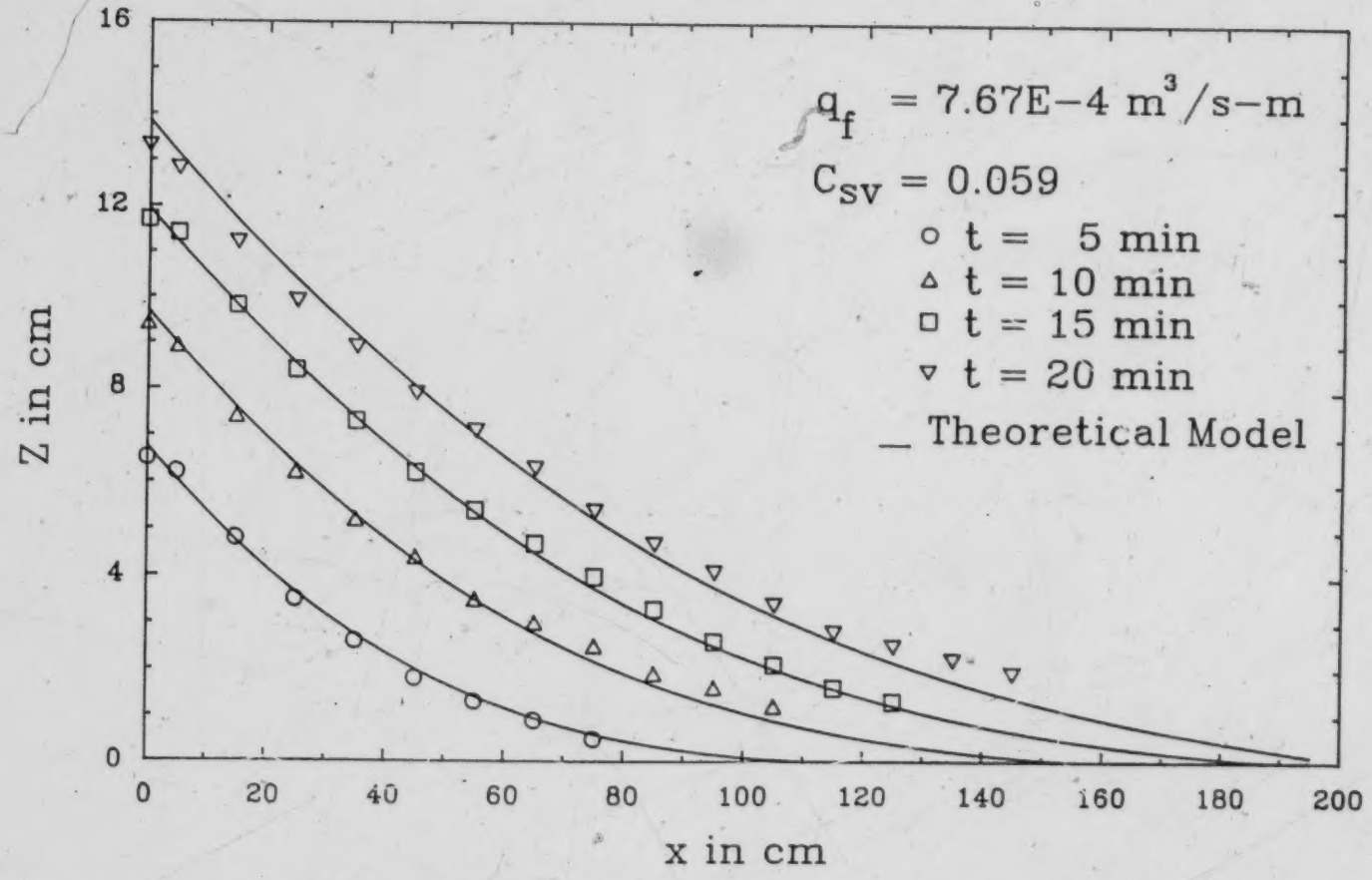

Fig. 5.2d Comparison between Experimental and Theoretical Beach Profiles with A_k = 8.0 for Test A4

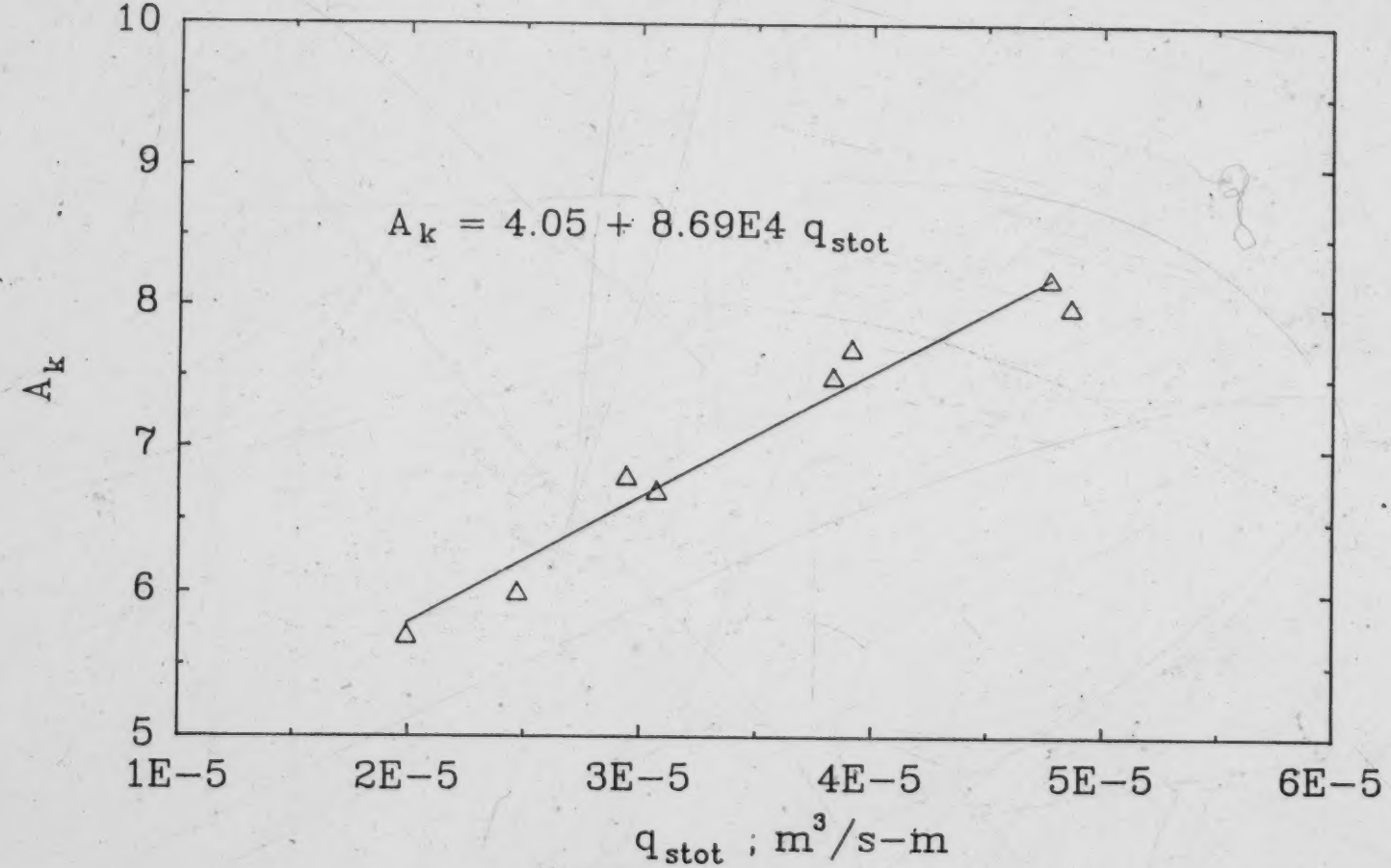

Fig. 5.3 Variation of A_k with q_{stot}

5.4.4 Computational Procedure

For each run, the water discharge, q_f, total sediment feed rate, q_{stot}, the initial beach slope, S_0, and the coefficient of the sediment transport relation, A_k, are fixed. At any time level, the following computational procedure is followed to compute the beach profile for the next time level.

1. Determining L and L' (L = length of the beach measured from the sediment feed point; L' = the length of the sediment deposition upstream the sediment feed point, L' $\leq$ 5 cm as shown in Figs. 5.1a and 5.1b);
2. Calculating q_{s0} from Eq. 5.11;
3. Calculating q_{s1} and q_{s2} from Eq. 4.16;
4. Calculating $z(x = 0, t)$ from Eq. 5.5;
5. Calculating $z(0 < x \leq L, t)$ from Eqs. 5.2 and 5.3.

6. RESULTS AND DISCUSSIONS

As mentioned in chapter 3, the experiments were conducted for two cases: constant water discharge with different feed sediment concentrations (group A tests) and constant feed sediment concentration with different total slurry discharge (group B tests). In this chapter, the beach profiles from numerical computations are compared with those from experimental data. The comparison is performed in both dimensional and dimensionless forms. The effect of feed sediment concentration at constant water discharge on the maximum depth of deposition is investigated. The effect of total feed slurry discharge at constant feed sediment concentration on the maximum depth of deposition is also studied.

6.1 Beach Profiles

6.1.1 Dimensional Form

To present the experimental beach profile in a convenient form, it is necessary to define a new variable, the depth of deposition, as follows

$$Z(x,t) = z(x,t) - z_b(x) \tag{6.1}$$

where $z(x,t)$ is the beach elevation at distance x and time t with respect to a horizontal reference datum ; $z_b(x)$ is the initial beach elevation at the same distance with respect to the same reference datum.

The dimensional transient beach profiles from experiments and numerical computations are compared in Figs 6.1 to 6.4. In these figures, the volumetric feed sediment concentration is defined as $C_{sv} = q_{stot} / (q_{stot} + q_f)$; the total slurry discharge is defined as $q_{sf} = q_{stot} + q_f$.

For group A tests, the beach profiles for the four different feed sediment

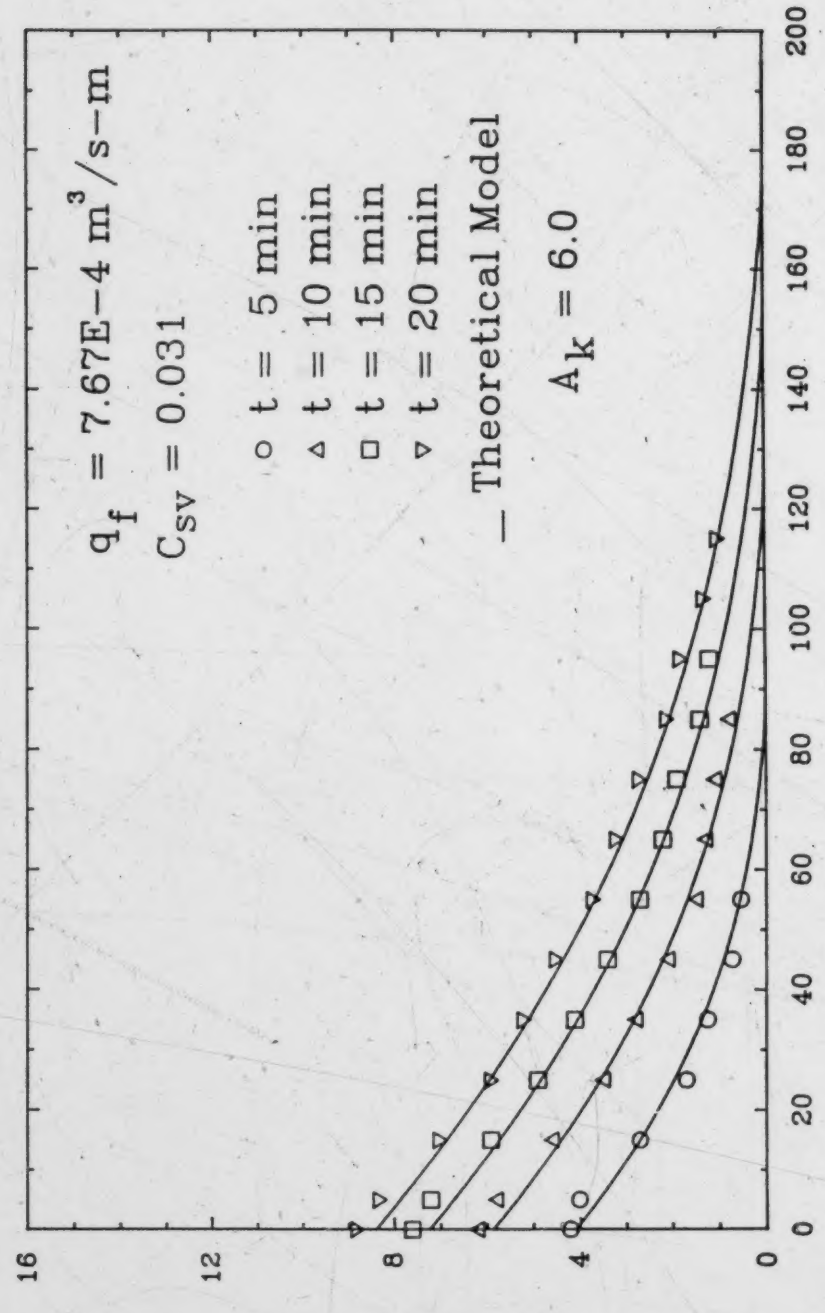

Fig. 6.1a Beach Profiles of Test A1

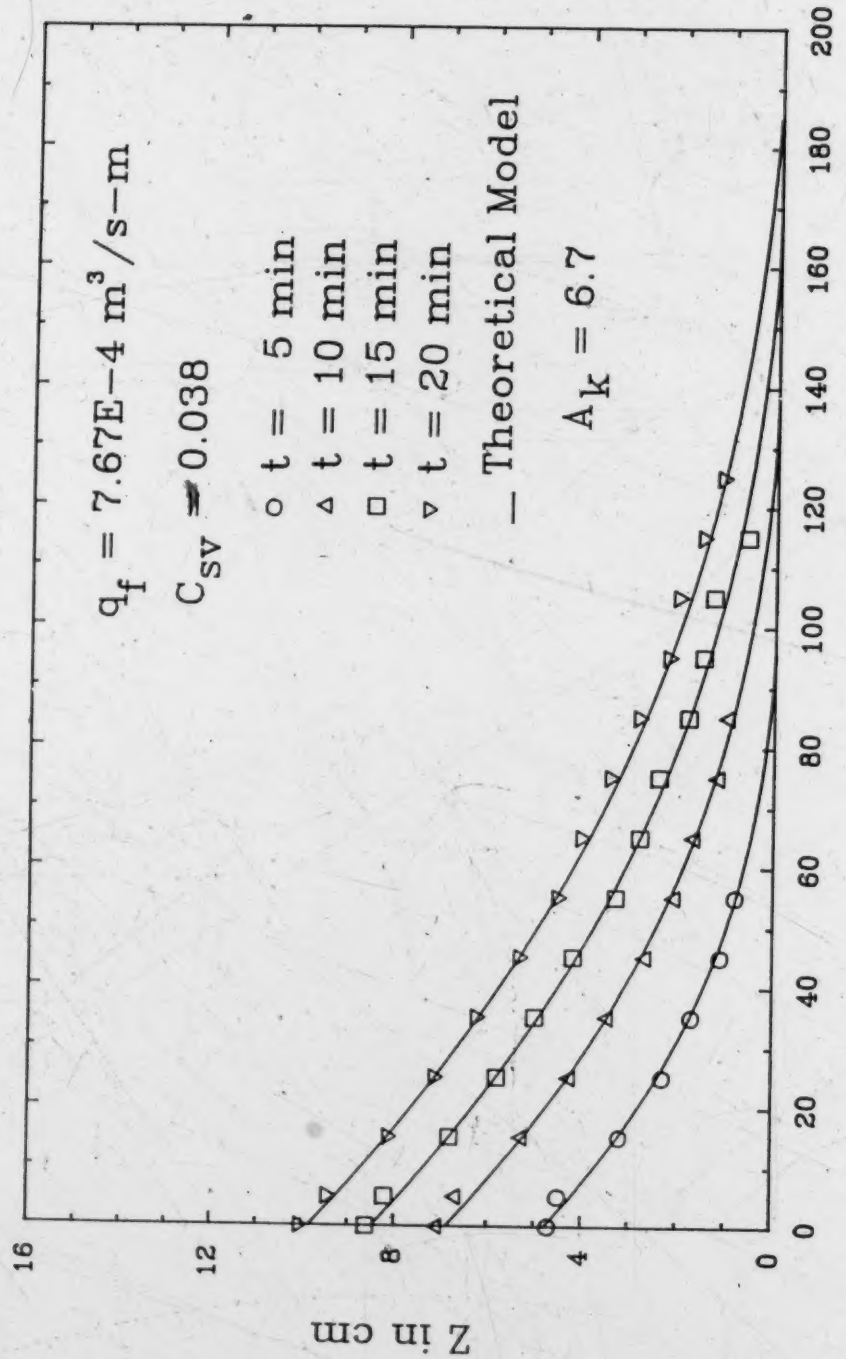

Fig. 6.1b Beach Profiles of Test A2

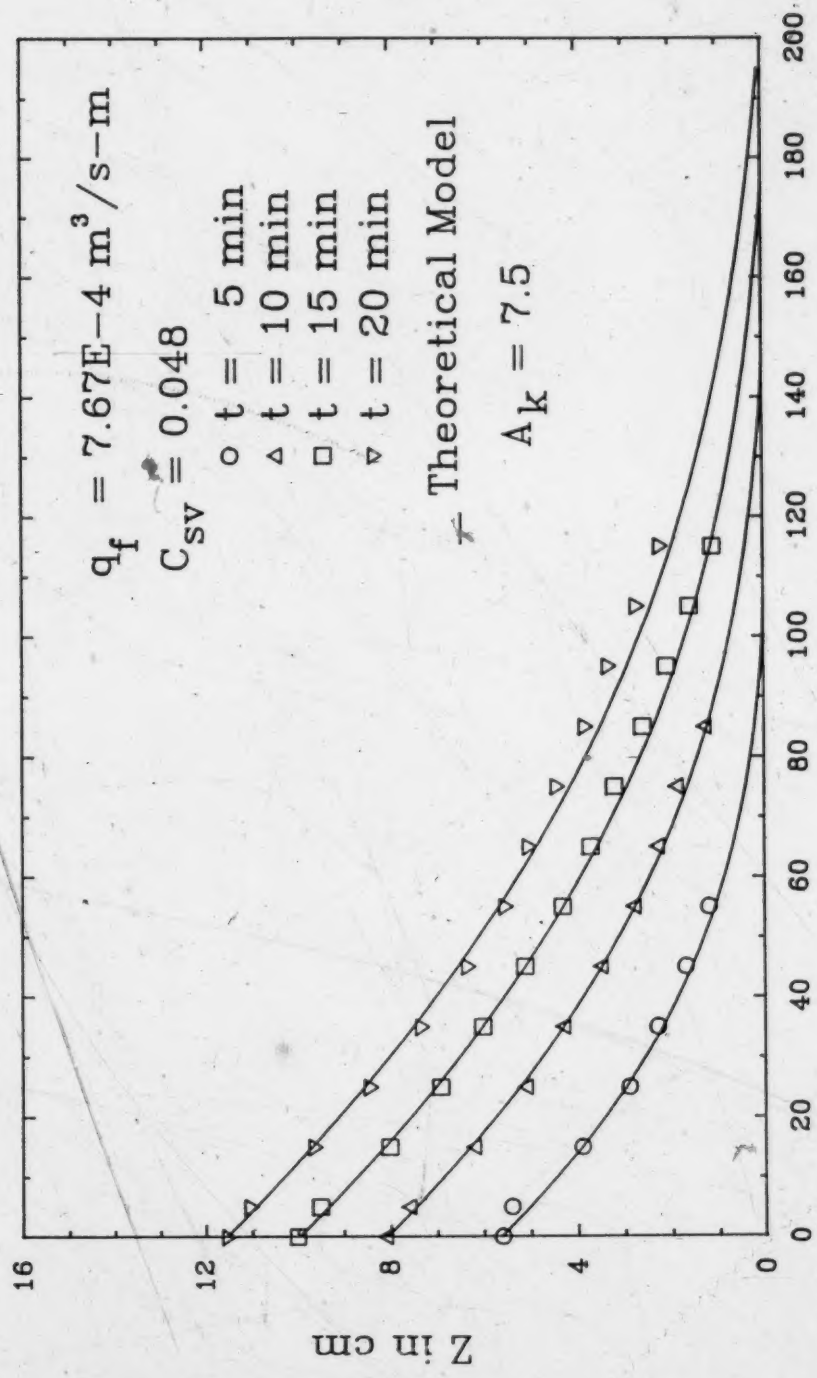

Fig. 6.1c Beach Profiles of Test A3

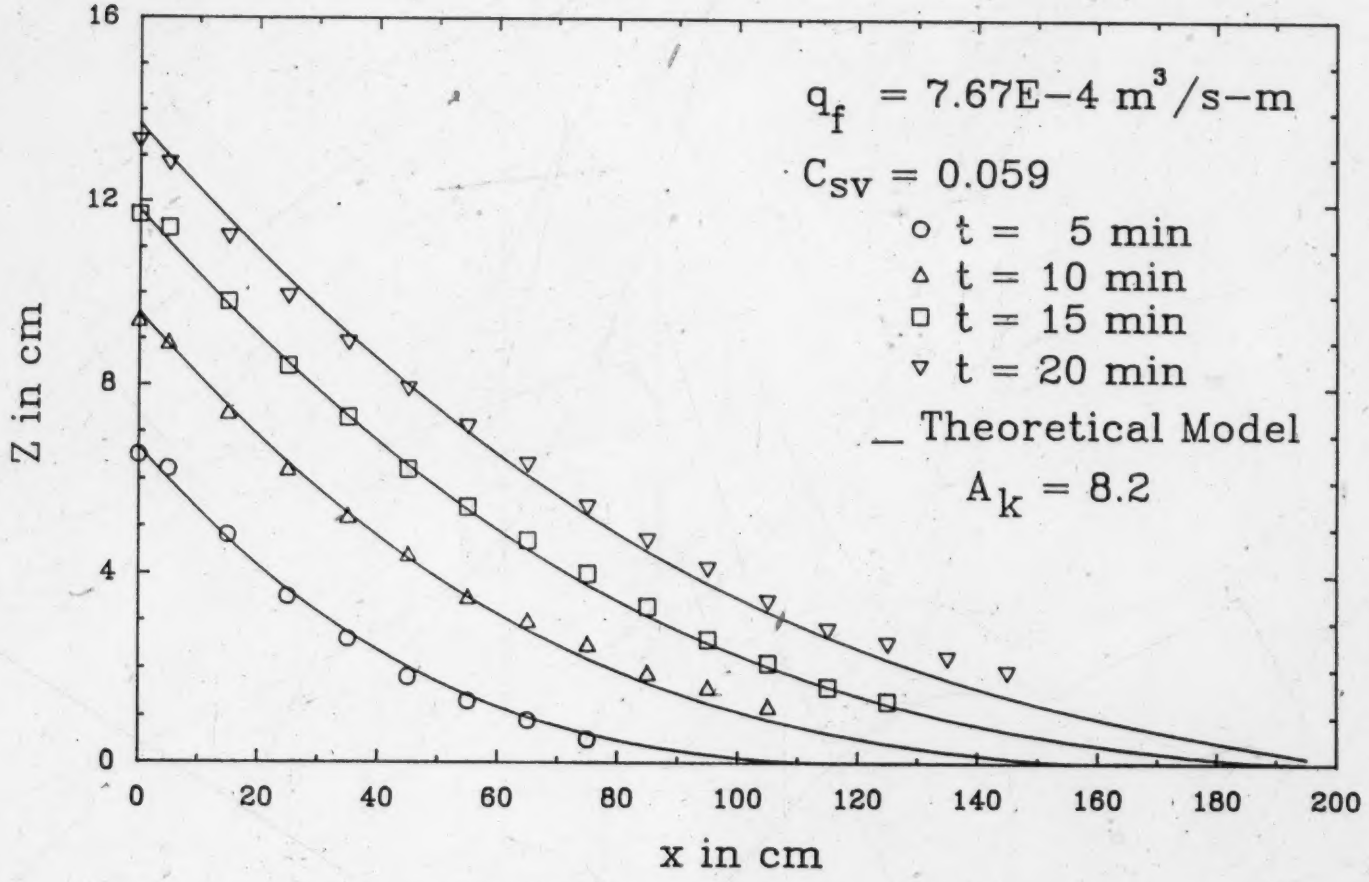

Fig. 6.1d Beach Profiles of Test A4

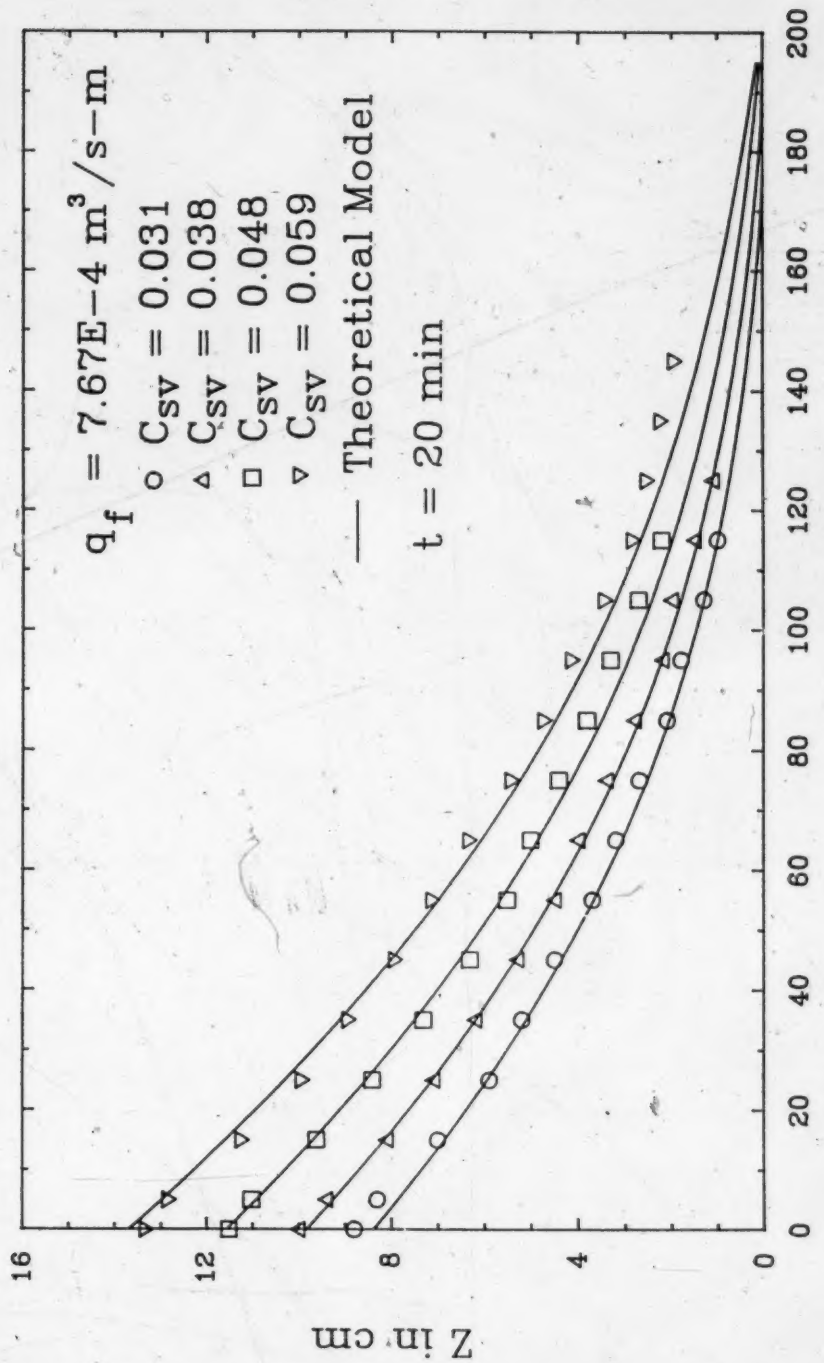

Fig. 6.2 Effect of Feed Sediment Concentration on Beach Profiles

concentrations are presented in Figs. 6.1a to 6.1d. Fig. 6.2 shows the effect of feed sediment concentration on the beach profiles. From Figs. 6.1a to 6.1d, it can be seen that the agreement between the experimental data and the computed results is almost perfect. The excellent agreement is present for all the four concentrations at all time levels. It is to be noted that when computing the numerical results, the modified coefficient of the sediment transport equation, A_k, was used. For the same sediment feed rate, the same A_k was employed to compute the beach profiles at all different times. From Fig. 6.2, one can see that under the same water discharge, with increasing feed sediment concentration, both the slope of and the rising rate of the beach increase accordingly.

For group B tests, the beach profiles for the four different total feed slurry flow rates are shown in Figs. 6.3a to 6.3d. The effect of the total feed slurry flow rate on the beach profiles can be seen in Fig. 6.4. From Figs. 6.3a to 6.3d, it can be seen that although generally the agreement between the computed beach profiles and the experimental ones is good, there are certain discrepancies. Since the beach profiles for Group B tests are not the averages of three runs for each set of parameters, more fluctuations can be observed. For the four cases, the largest discrepancy occurred in test B1 where the discharge of water was so small as to be less than the incipient water discharge at the initial slope of the beach. Under this circumstance, the sediment piled up until the slope of the beach was large enough to overcome the incipient state. During the piling–up process, the flow occurred through channeling. Therefore, the beach profiles could not be predicted with reasonable accuracy. From Figs. 6.3b to 6.3d, it is seen that with increasing total slurry discharge, the agreement between the predicted and the experimental beach profiles improves. From Fig. 6.4, it can be concluded that under the same feed sediment concentration, the increase of the total slurry discharge results in an increase of the rising rate of the beach profile. However, the slope of the beach

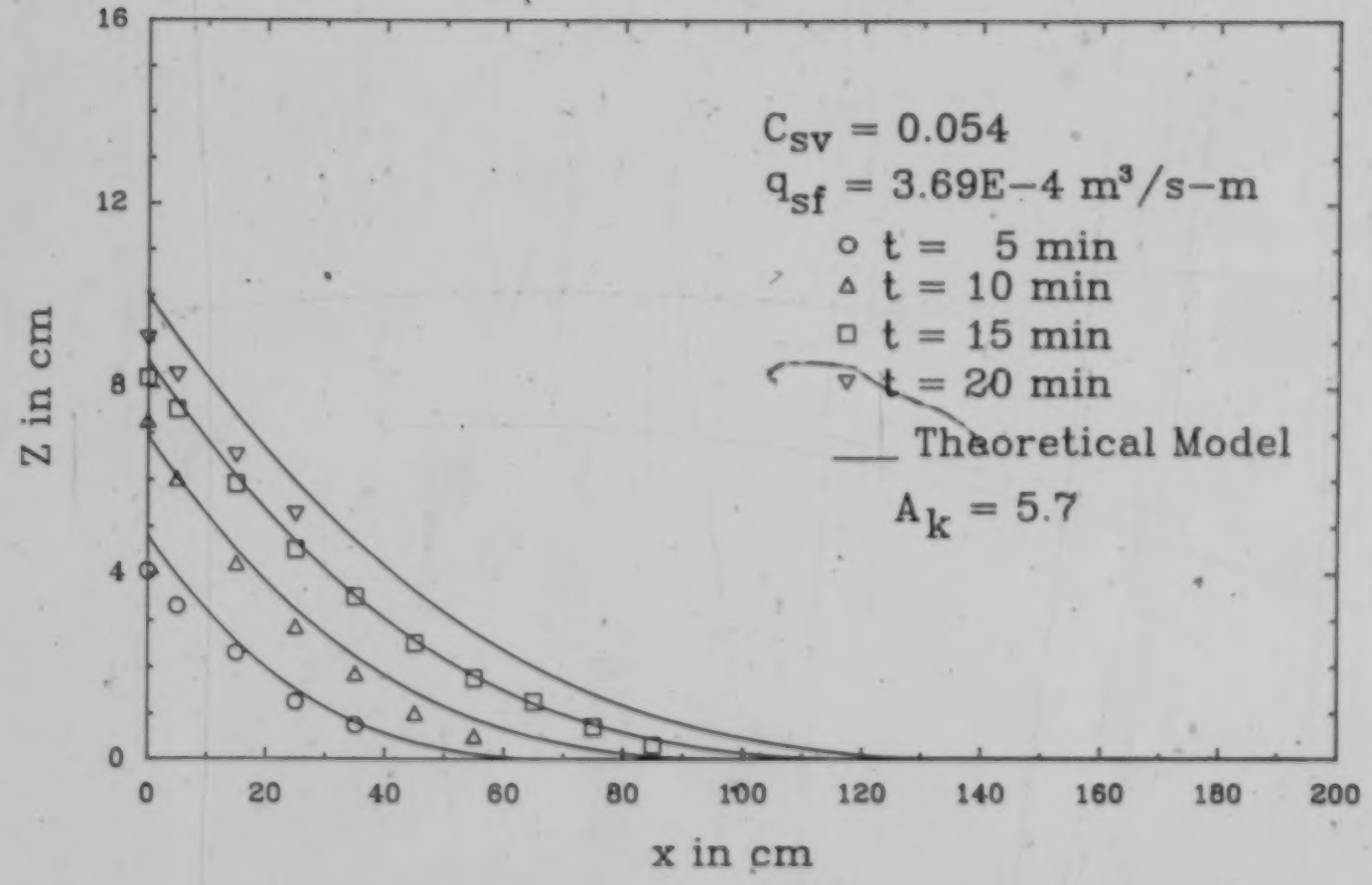

Fig. 6.3a Beach Profiles of Test B1

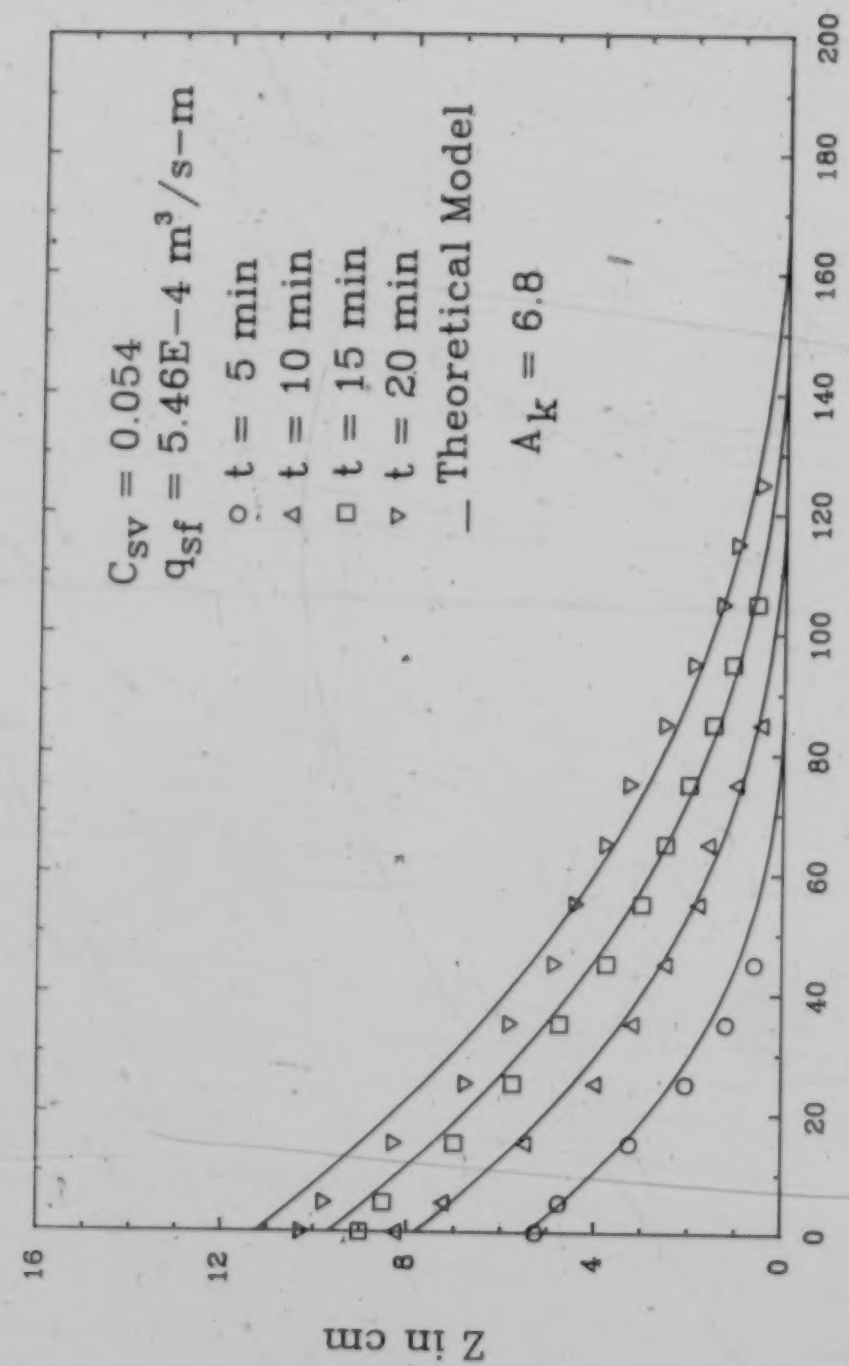

Fig. 6.3b Beach Profiles of Test B2

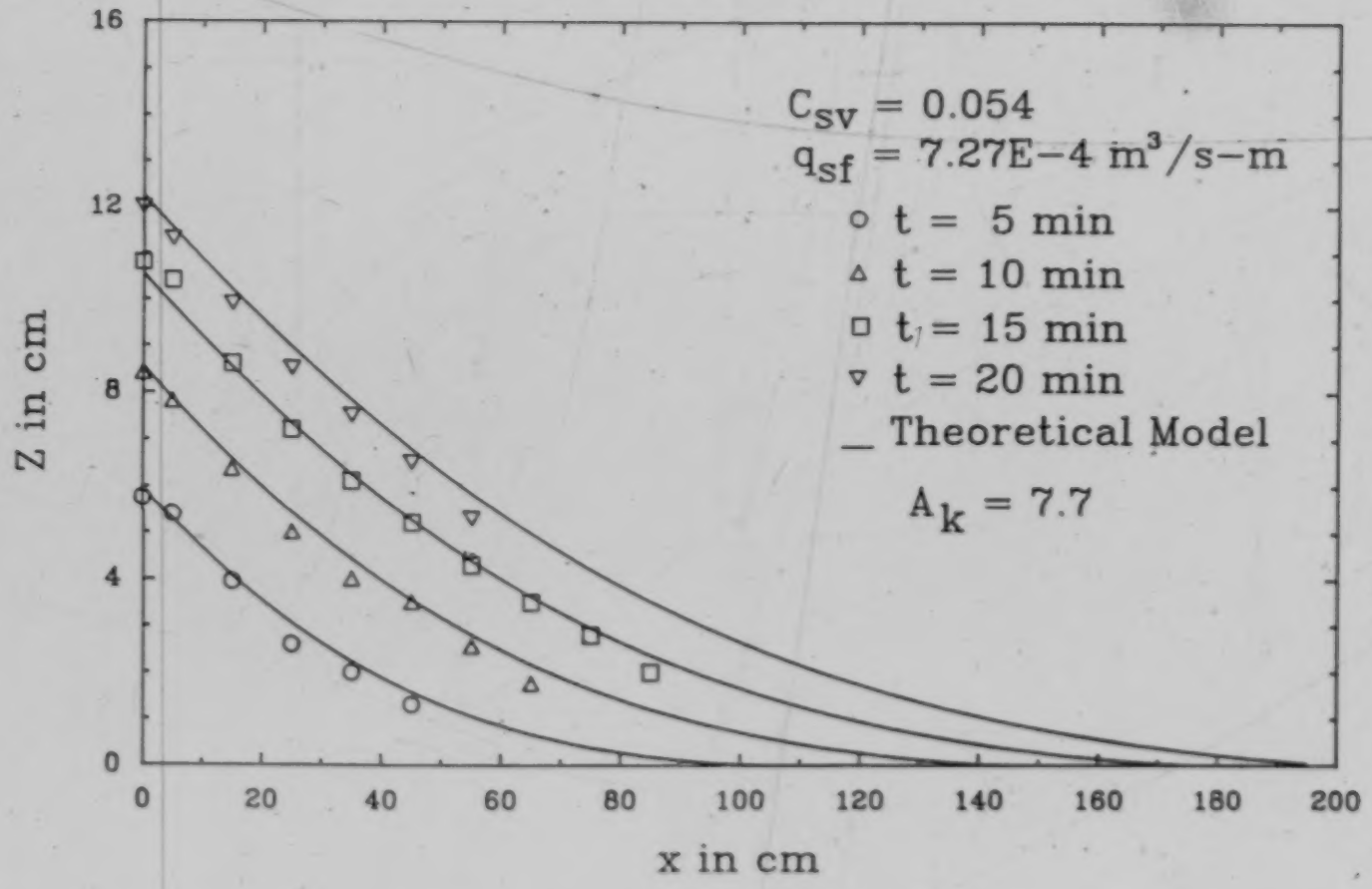

Fig. 6.3c Beach Profiles of Test B3

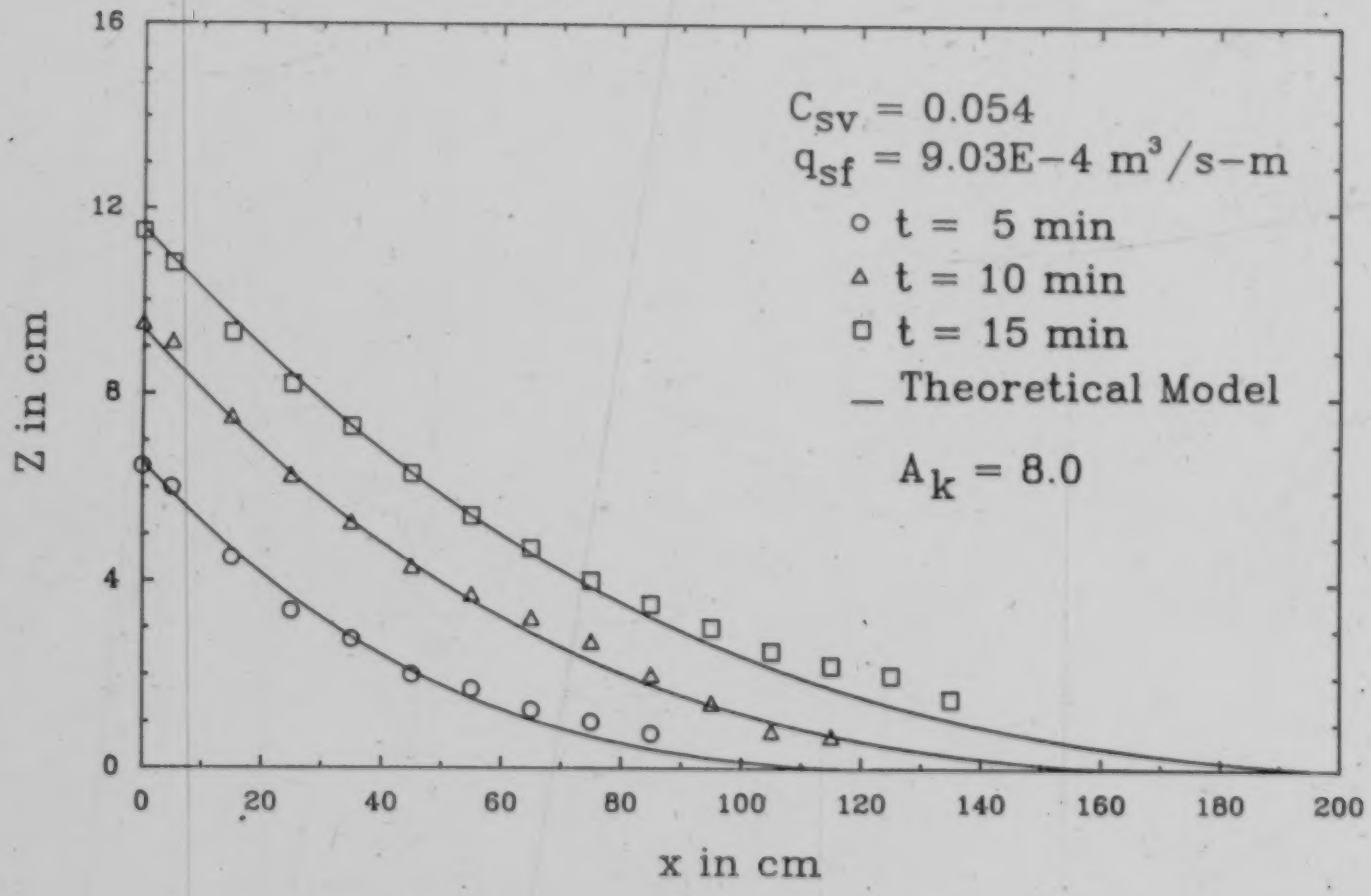

Fig. 6.3d Beach Profiles of Test B4

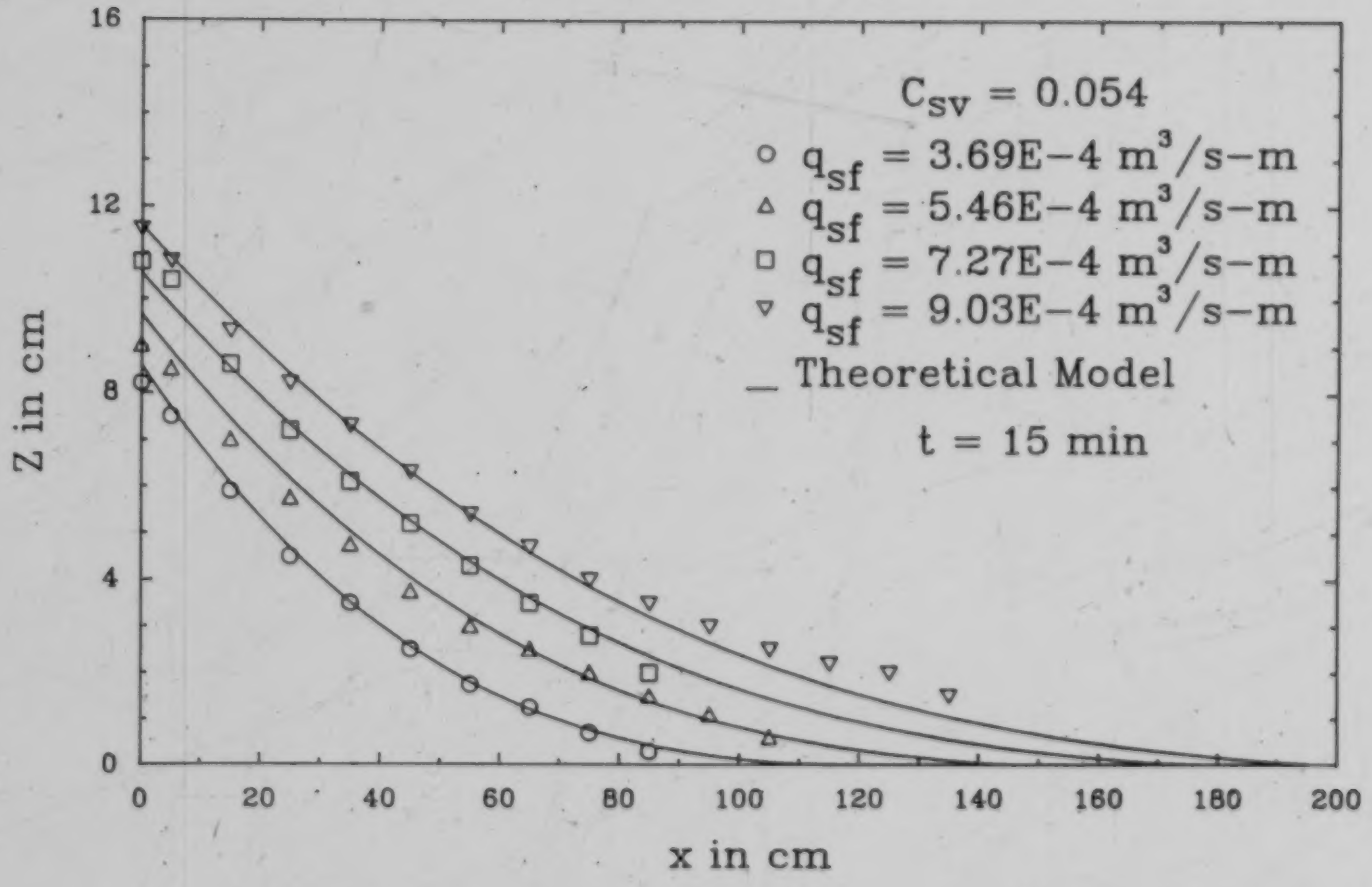

Fig. 6.4 Effect of Total Slurry Discharge on Beach Profiles

profile does not change significantly with the increase of the total slurry discharge.

In summary, with the modified Meyer–Peter and Muller equation as the sediment transport relation, the nonlinear parabolic model developed in this study along with the numerical scheme employed can predict the beach profiles very satisfactorily.

6.1.2 Dimensionless Forms

It is advantageous to present the transient beach profiles in dimensionless forms to make them more general and useful. In this section, two completely different approaches are employed to nondimensionalize the beach profiles to meet different needs. The first method is often used when dealing with aggradation problems in river flow while the second one is used more frequently in predicting the shape of the beach in tailings disposal.

6.1.2.1 Approach One

Following Soni et al. (1980), the depth of deposition, Z, is made dimensionless by Z_0, the maximum depth of deposition at $x = 0$, while the variable time and distance can be combined with the aggradation coefficient, K, to form a nondimensional group:

$$\eta = \frac{x}{2\sqrt{Kt}} \tag{6.2}$$

It needs to be pointed out that in Eq. 6.2, K is a variable depending on, among other things, the slope of the beach. To make plotting practical, at a specified time the average slope of the beach is employed to calculate K used in Eq. 6.2. The

dimensionless beach profiles for each of the group A and B tests obtained by this method are presented in Figs. 6.5 and 6.6, respectively. To have an overall perspective, for the whole group A tests the computed and experimental beach profiles in the dimensionless form are compared in Fig. 6.7 while those for group B tests are given in Fig. 6.8. From Figs. 6.5a to 6.5d, it can be seen that for each of the group A tests, both the experimental beach profiles and the numerically computed ones tend to form a single curve when plotted in the dimensionless form. Fig. 6.5a of test A1 shows some scatter, but the agreement of the experimental data with the numerical results is still fairly good. For each of the tests A2 to A4, the curve from experimental data almost coincides with that from numerical results. From Figs. 6.6a to 6.6d, one can see once again that the data from group B tests are more scattered than those from group A tests, but the agreement between the experimental data and the numerical prediction is still very satisfactory. Figs. 6.7 and 6.8 show that for either group A or B tests, the experimental data closely encompass the single master beach profile from numerically computed results.

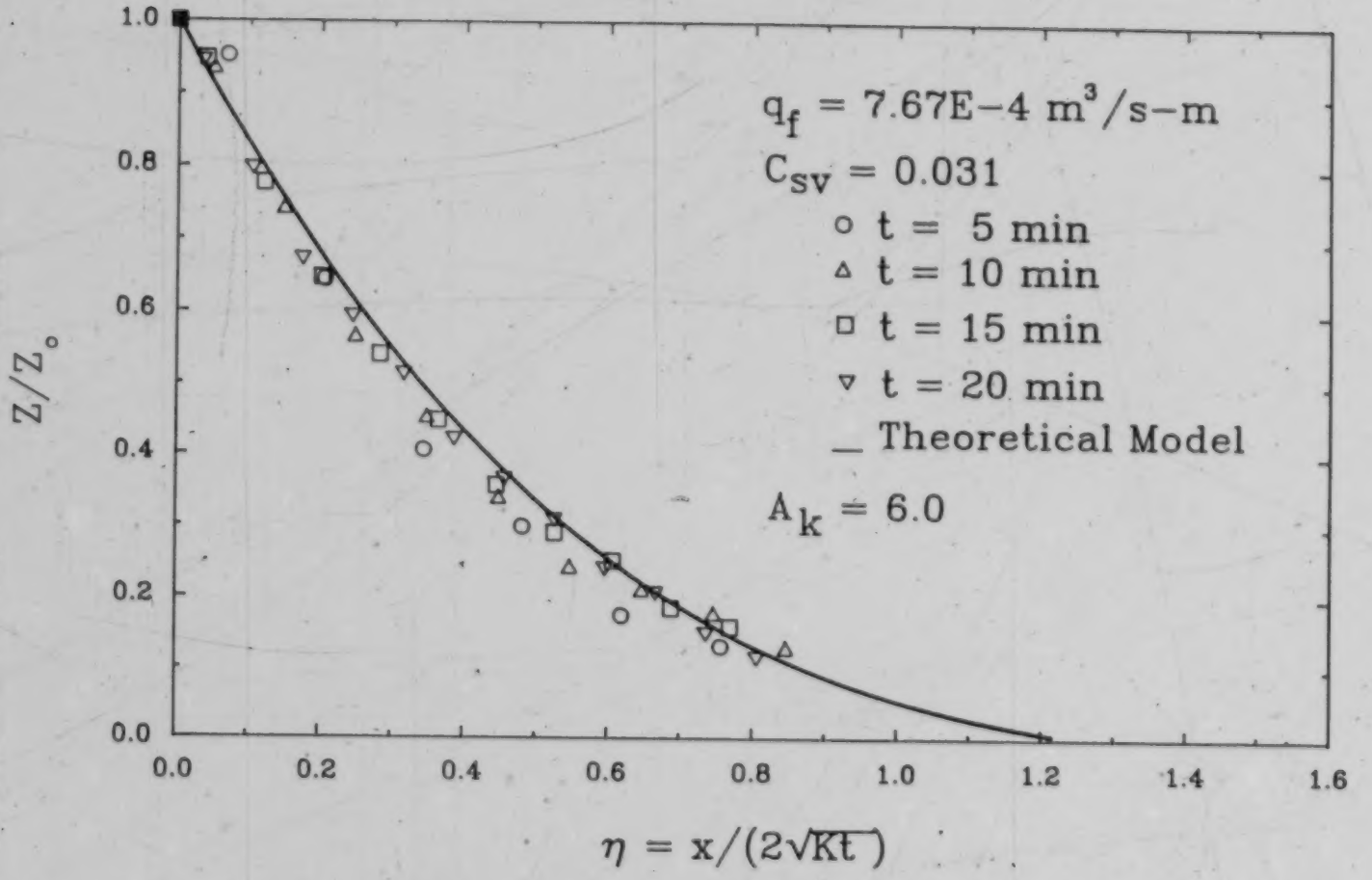

Fig. 6.5a Dimensionless Beach Profiles of Test A1

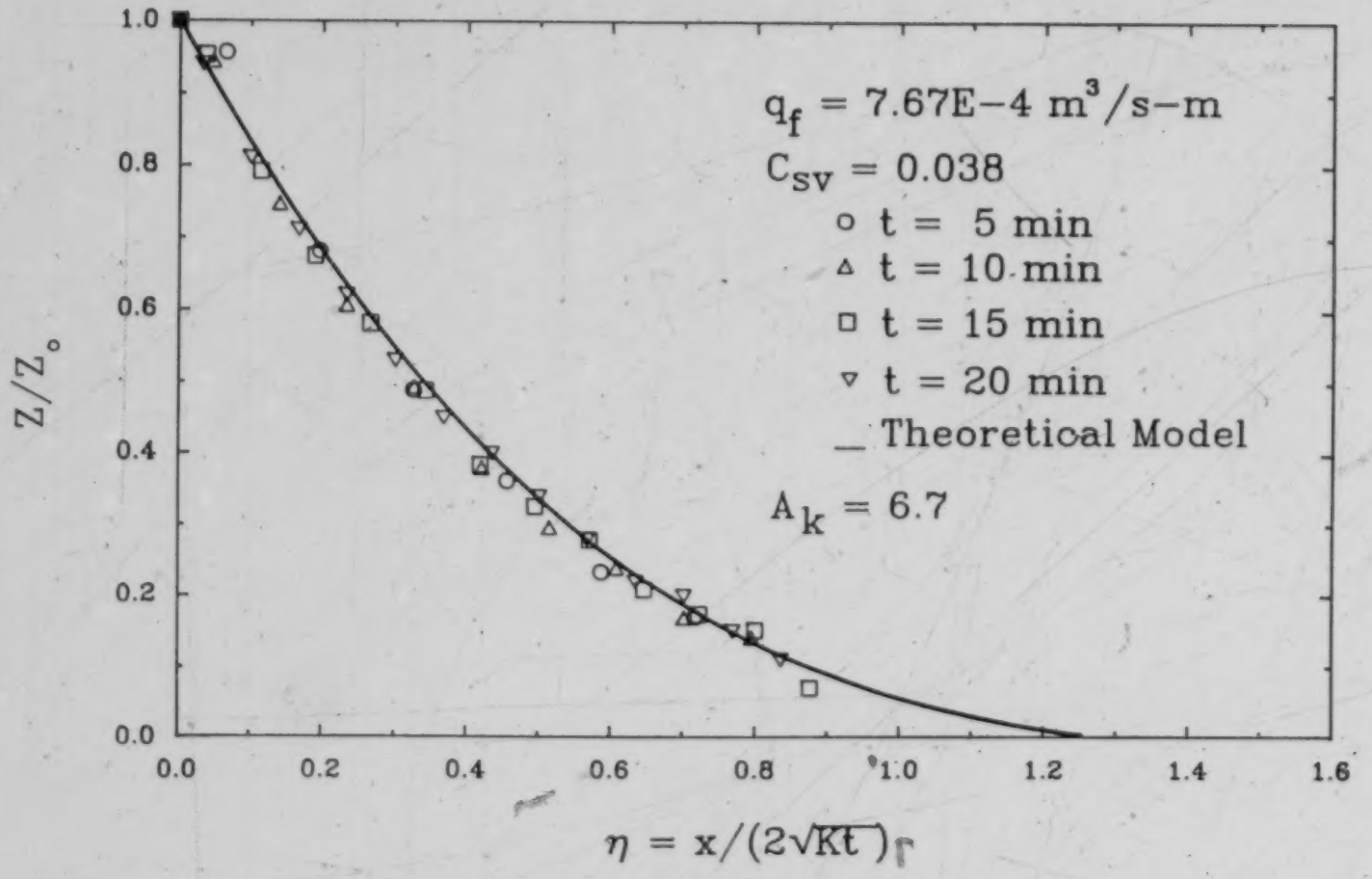

Fig. 6.5b Dimensionless Beach Profiles of Test A2

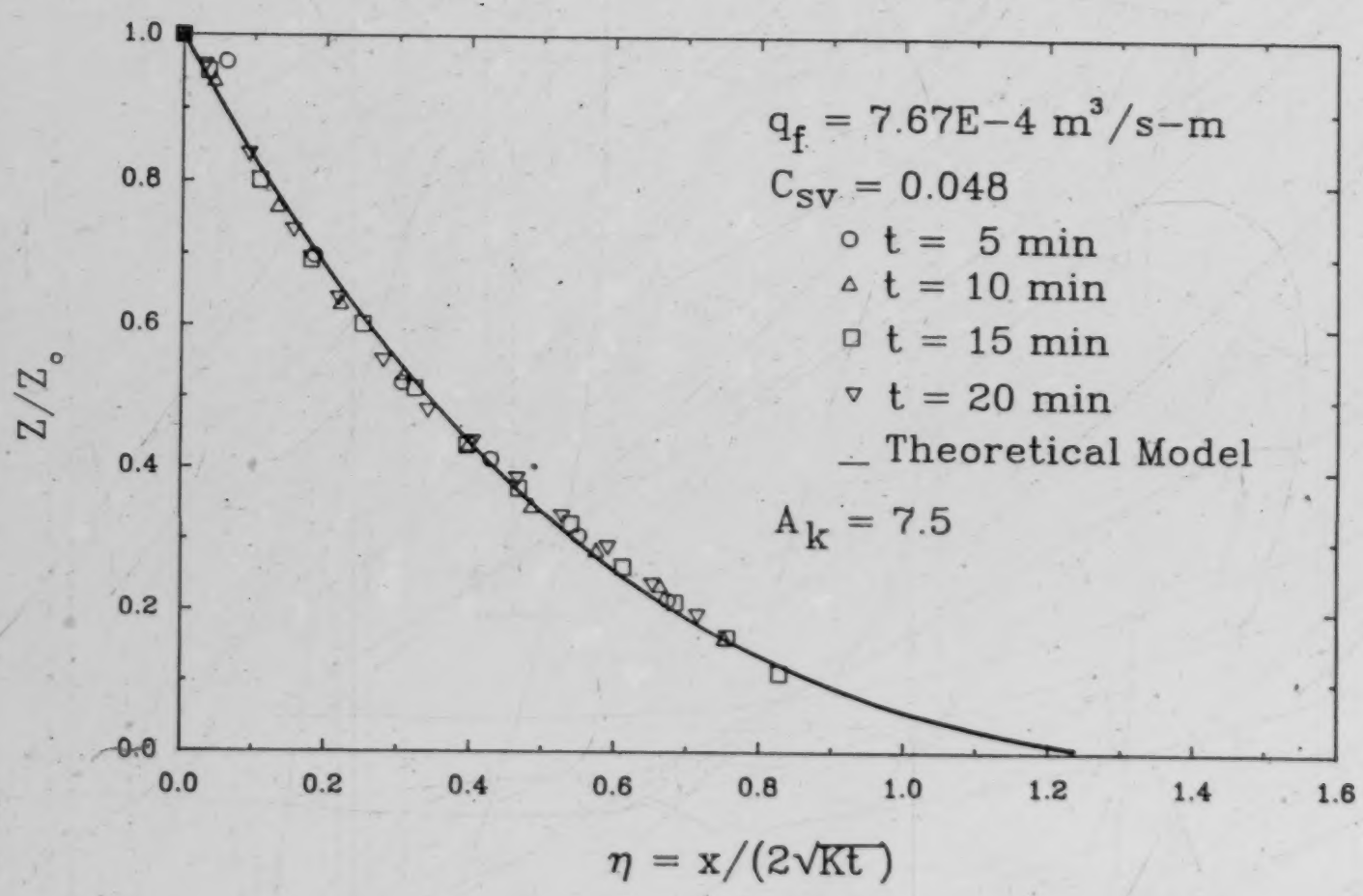

Fig. 6.5c Dimensionless Beach Profiles of Test A3

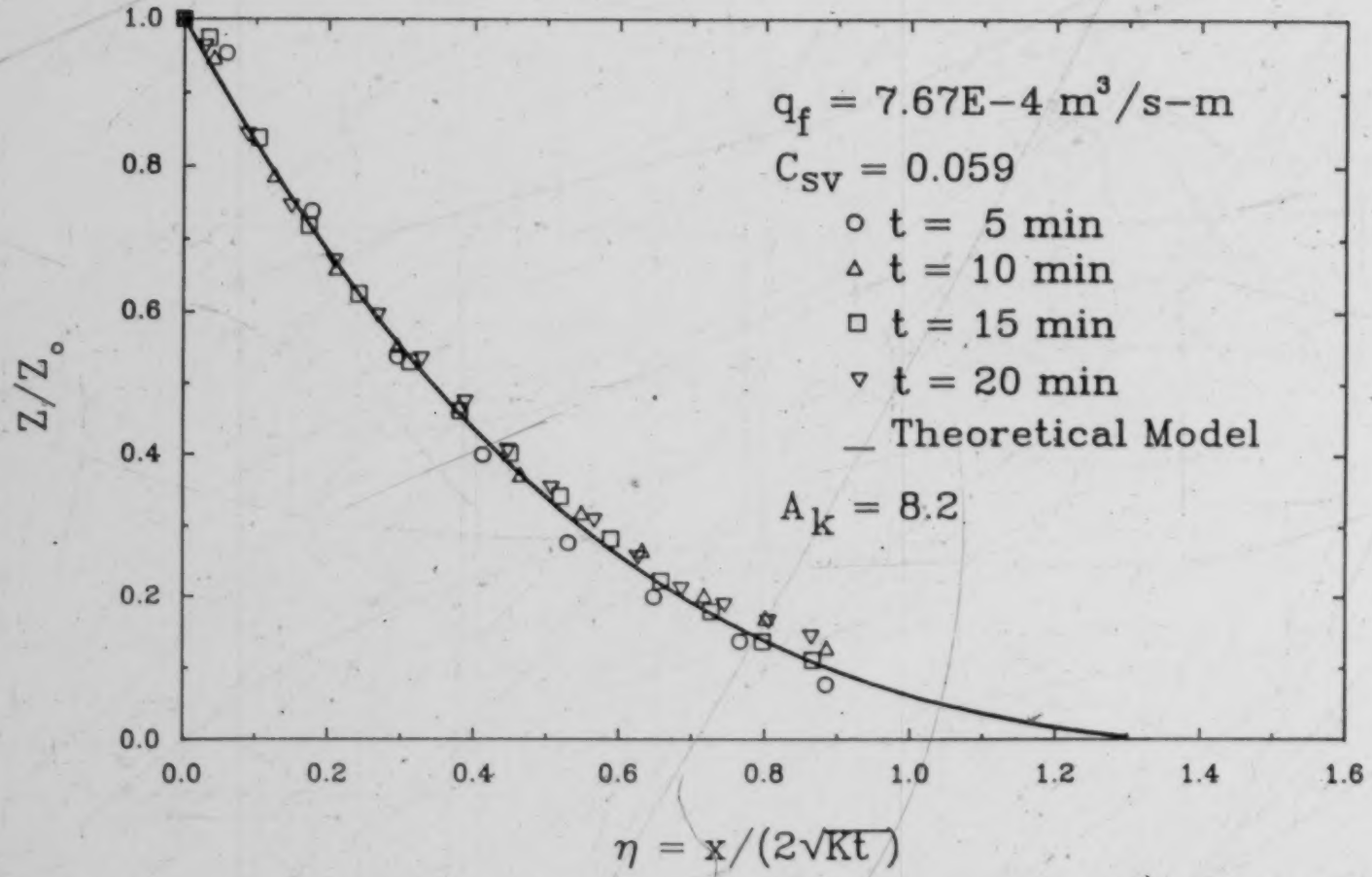

Fig. 6.5d Dimensionless Beach Profiles of Test A4

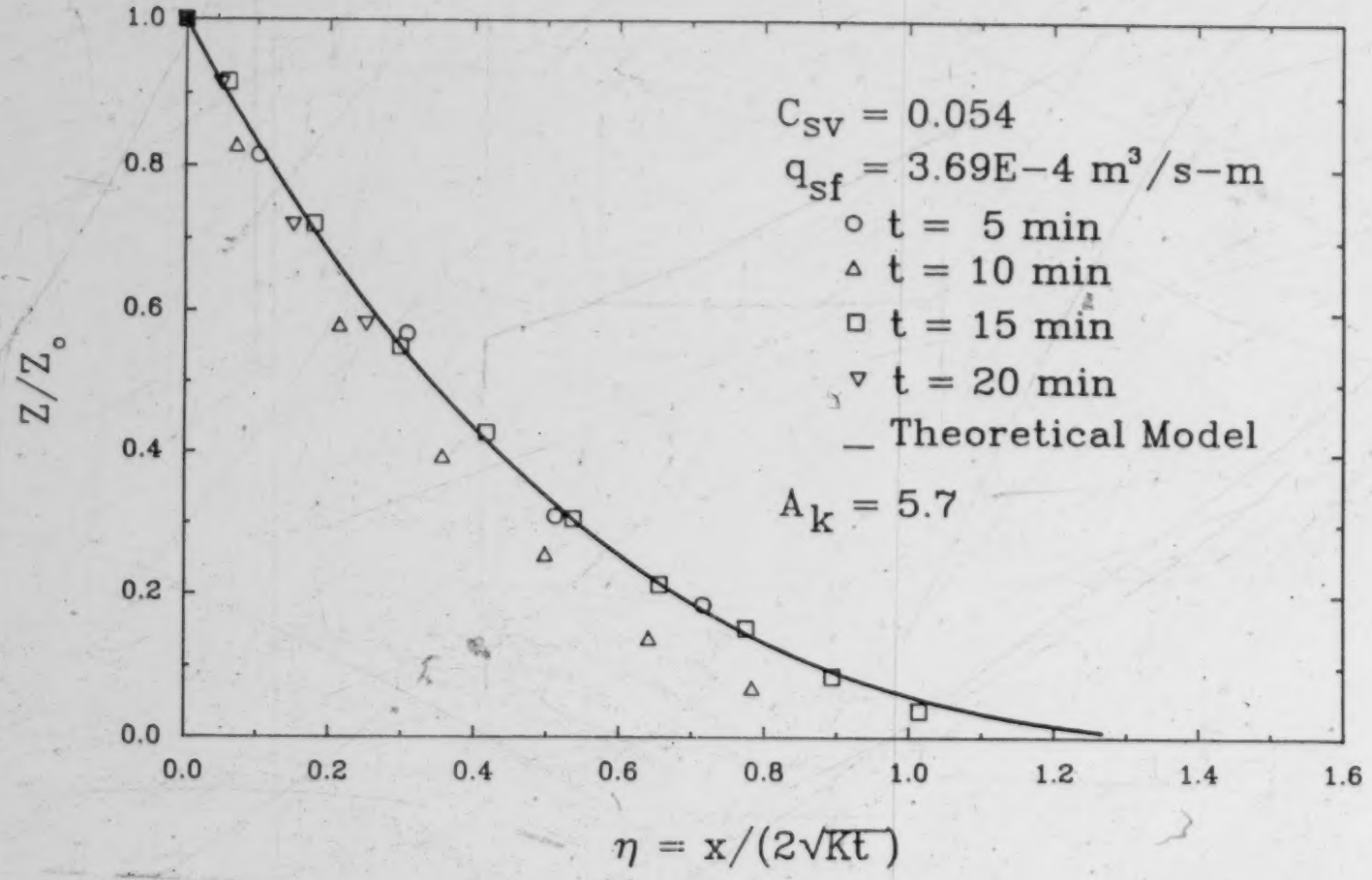

Fig. 6.6a Dimensionless Beach Profiles of Test B1

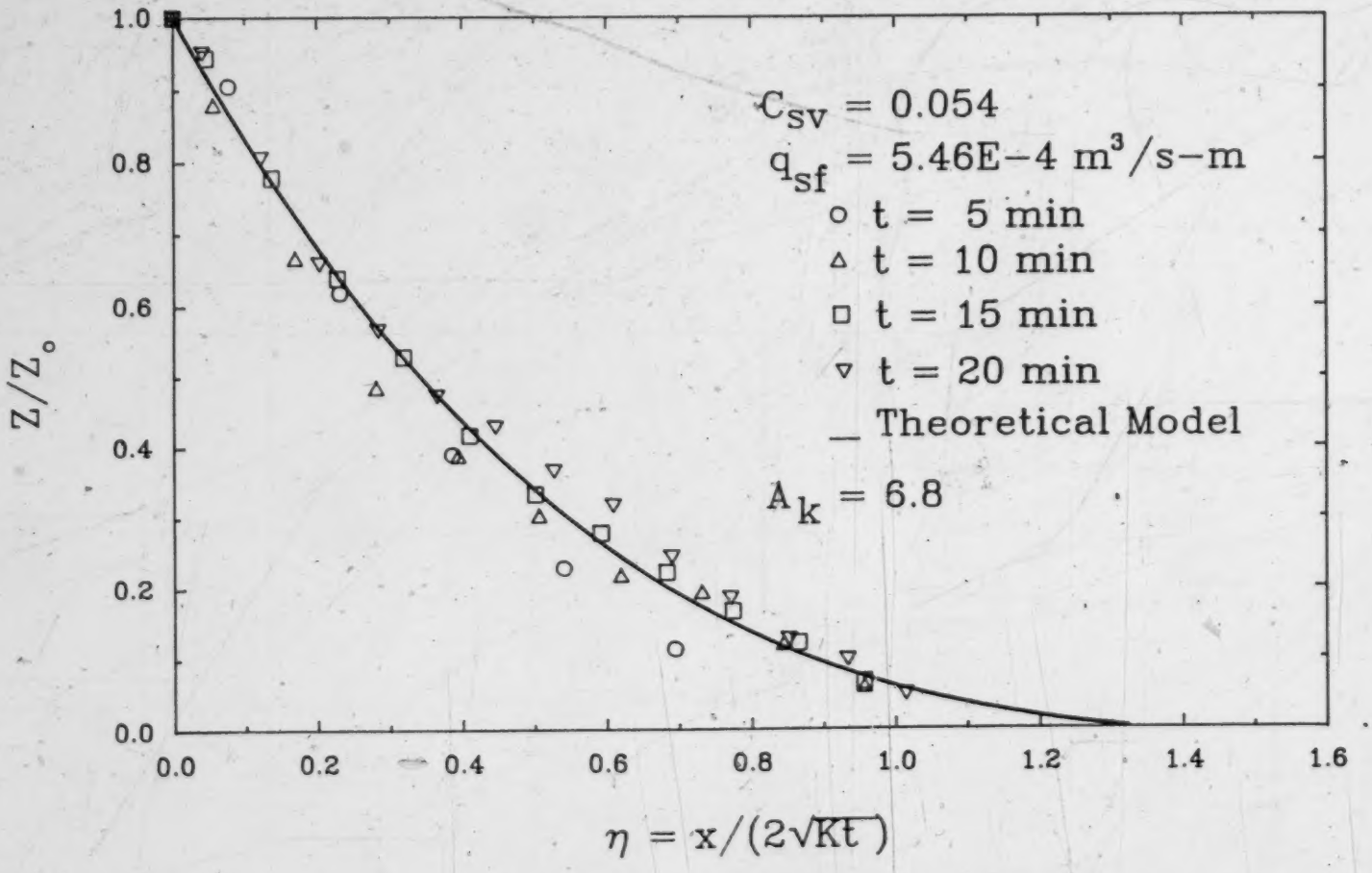

Fig. 6.6b Dimensionless Beach Profiles of Test B2

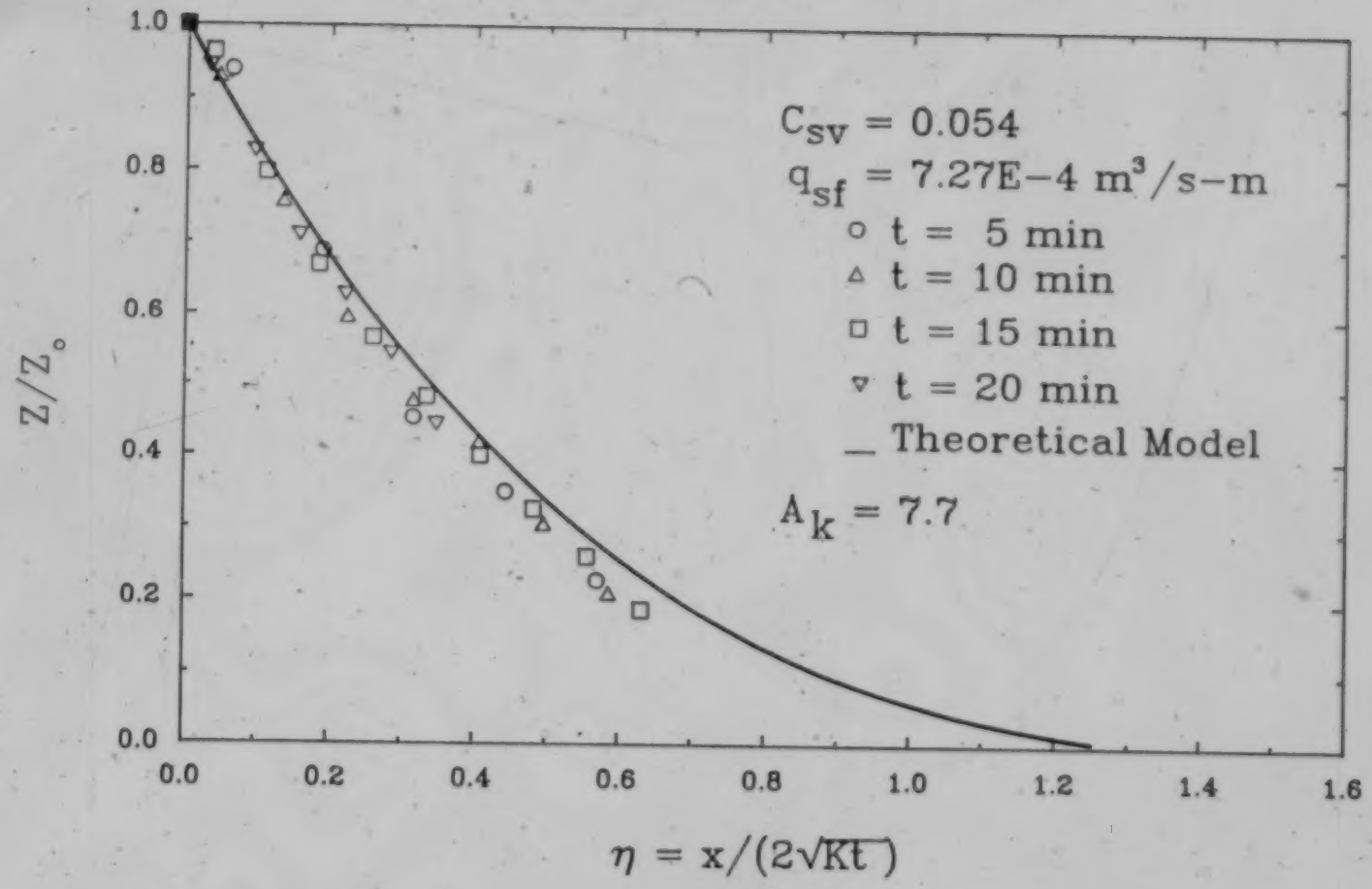

Fig. 6.6c Dimensionless Beach Profiles of Test B3

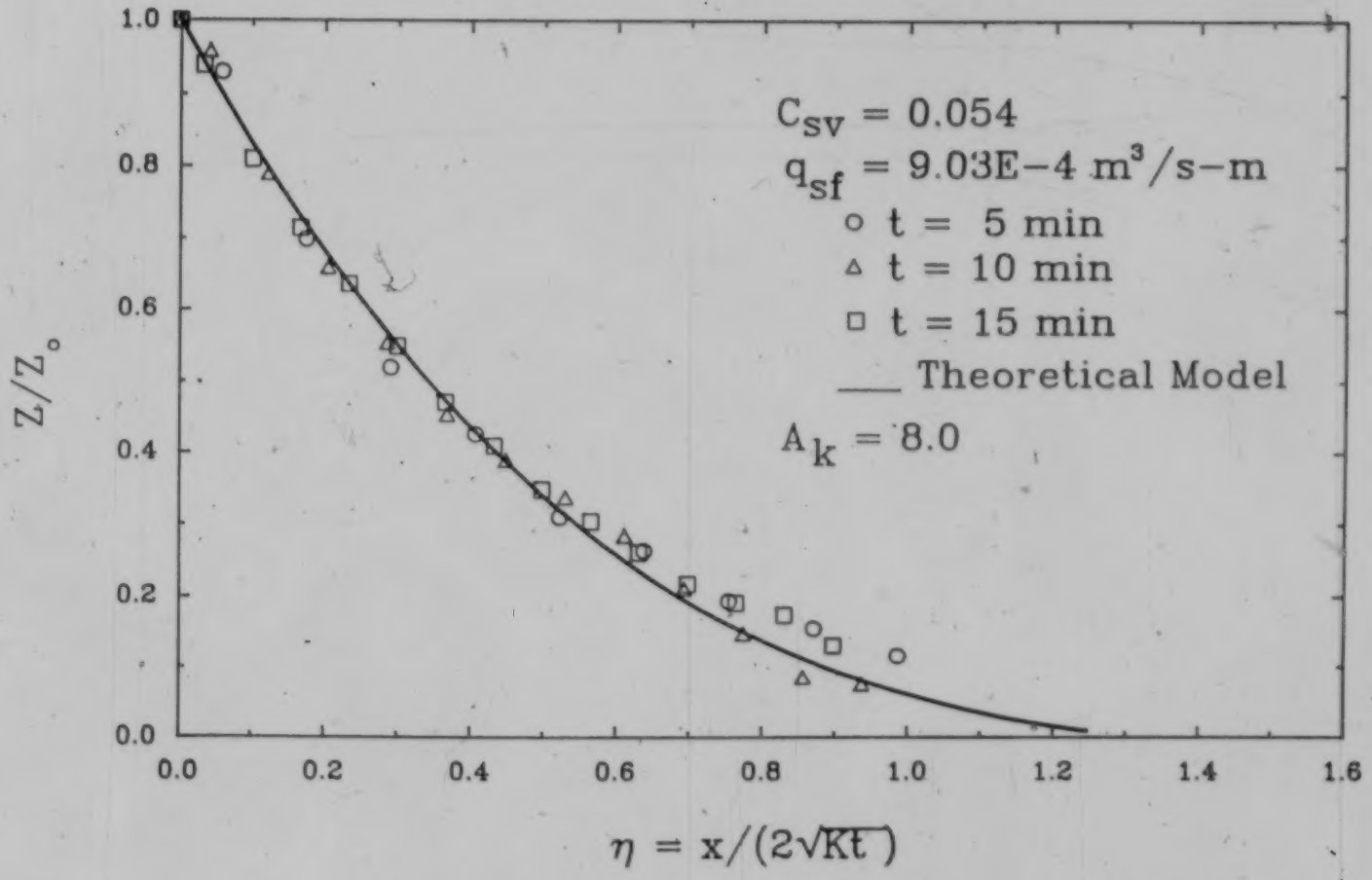

Fig. 6.6d Dimensionless Beach Profiles of Test B4

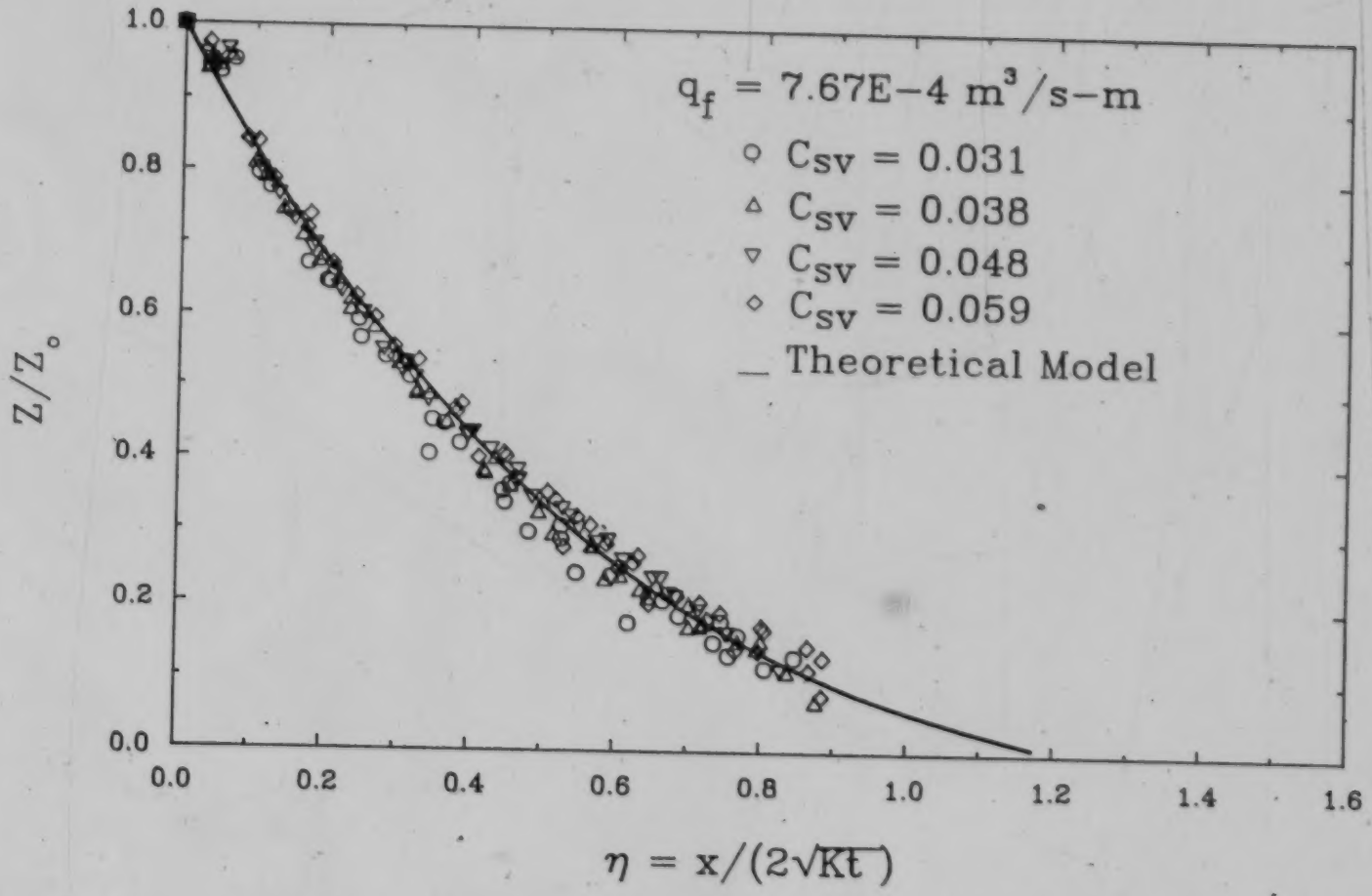

Fig. 6.7 Dimensionless Beach Profiles for All Group A Tests

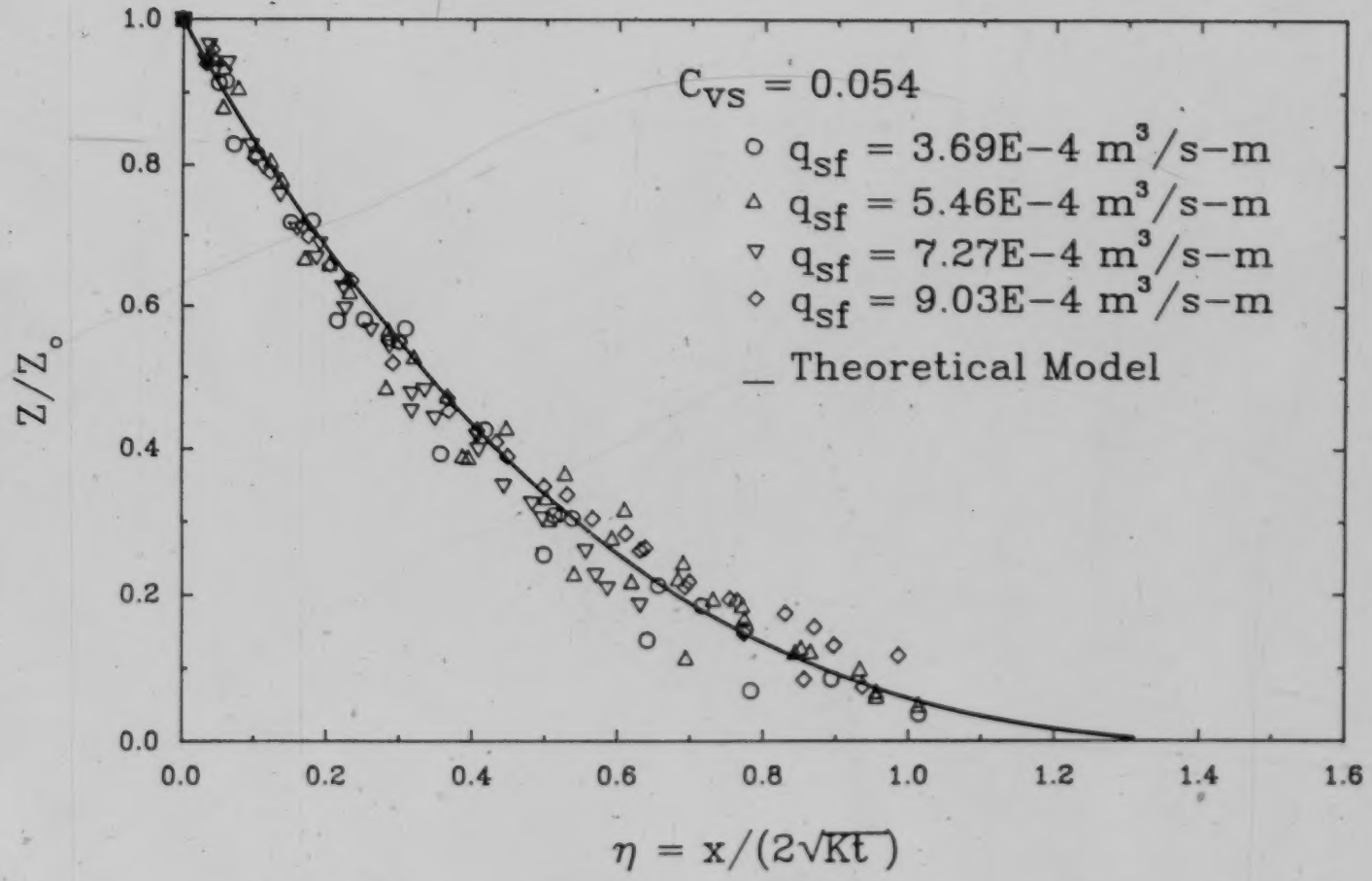

Fig. 6.8 Dimensionless Beach Profiles for All Group B Tests

6.1.2.2 Approach Two

The second method to nondimensionalize the beach profiles was introduced by Melent'ev et al. (1973). With this method, the depth of deposition, Z, is divided by Z_0 to form a dimensionless group (same as in the first method) while x, the horizontal distance along the beach, is made nondimensional by L, the length of the beach. In so doing, one notices that the time is not included explicitly in the dimensionless groups. However, since both Z_0 and L are time dependent, the influence of time can be felt implicitly. Making use of the above nondimensionalization, the following power expression is used by many investigators to model the dimensionless beach profiles (Melent'ev et al., 1973; Blight and Bentel, 1983; Blight et al., 1985; Smith and Nelson, 1986):

$$\frac{Z}{Z_0} = \left[1 - \frac{x}{L}\right]^m \tag{6.3}$$

where m is an exponent which is characteristic of the tailings material. This equation is important from an engineering point of view since one only needs to measure Z_0 and L to predict the shape of the beach profile.

In this study, when all the experimental data for the beach profiles were fitted, using the least square method, it was found that m = 2.16 which is within the range from 1.19 to 2.24 reported by Smith and Nelson (1986).

Computed from Eq. 6.3 with m = 2.16, the typical dimensionless beach profiles for one of group A tests are presented in Fig. 6.9, while the counterparts for group B tests are seen in Fig. 6.10. From Fig. 6.9 one can see that the power law prediction for one of group A tests is excellent. Fig. 6.10 again shows more scatter for one of group B tests but the prediction is acceptable. Fig. 6.11 shows all the experimental data and the curve generated from Eq. 6.3 with m = 2.16. From

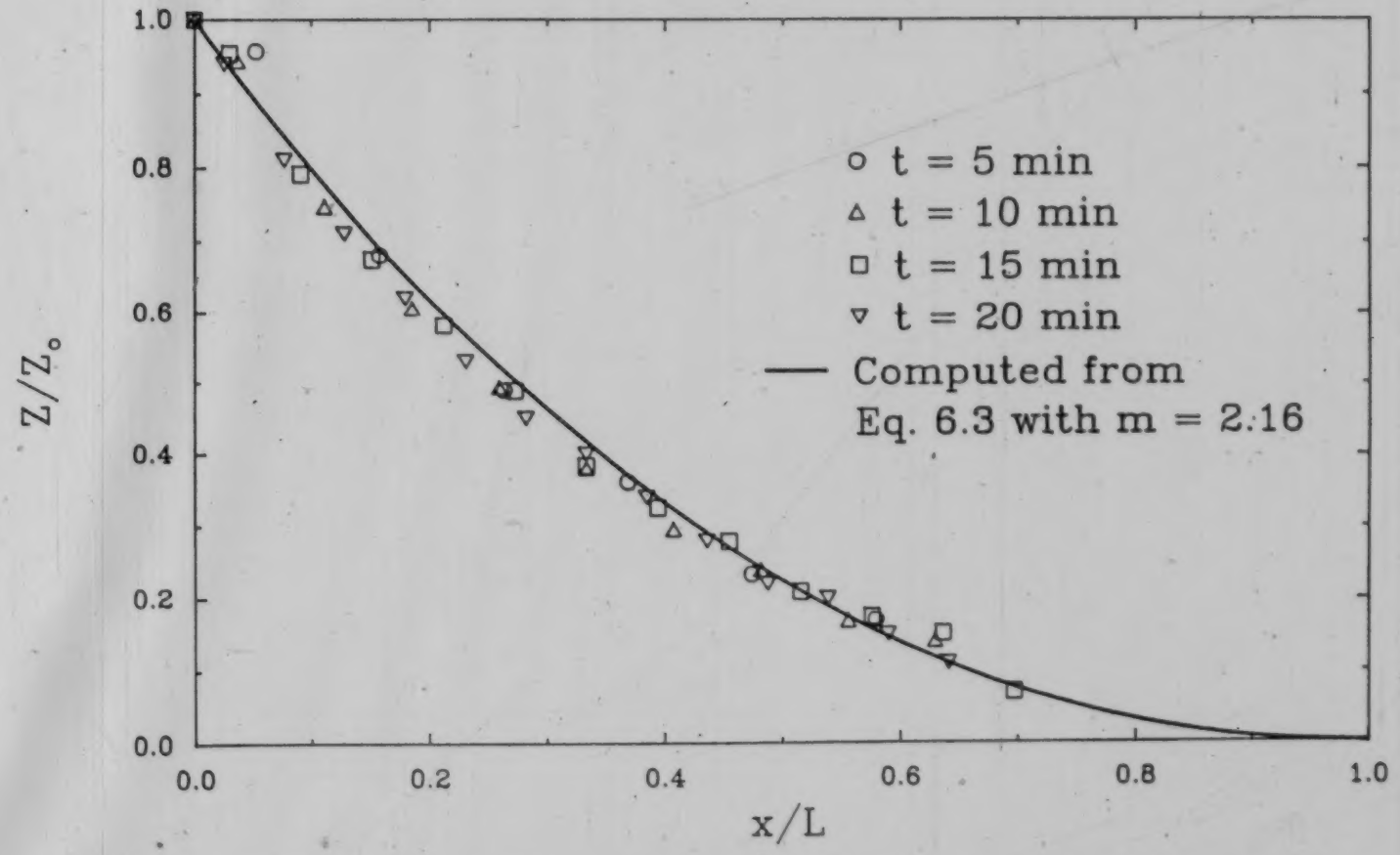

Fig. 6.9 Typical Dimensionless Beach Profiles for Group A Tests Modeled by Power Expression

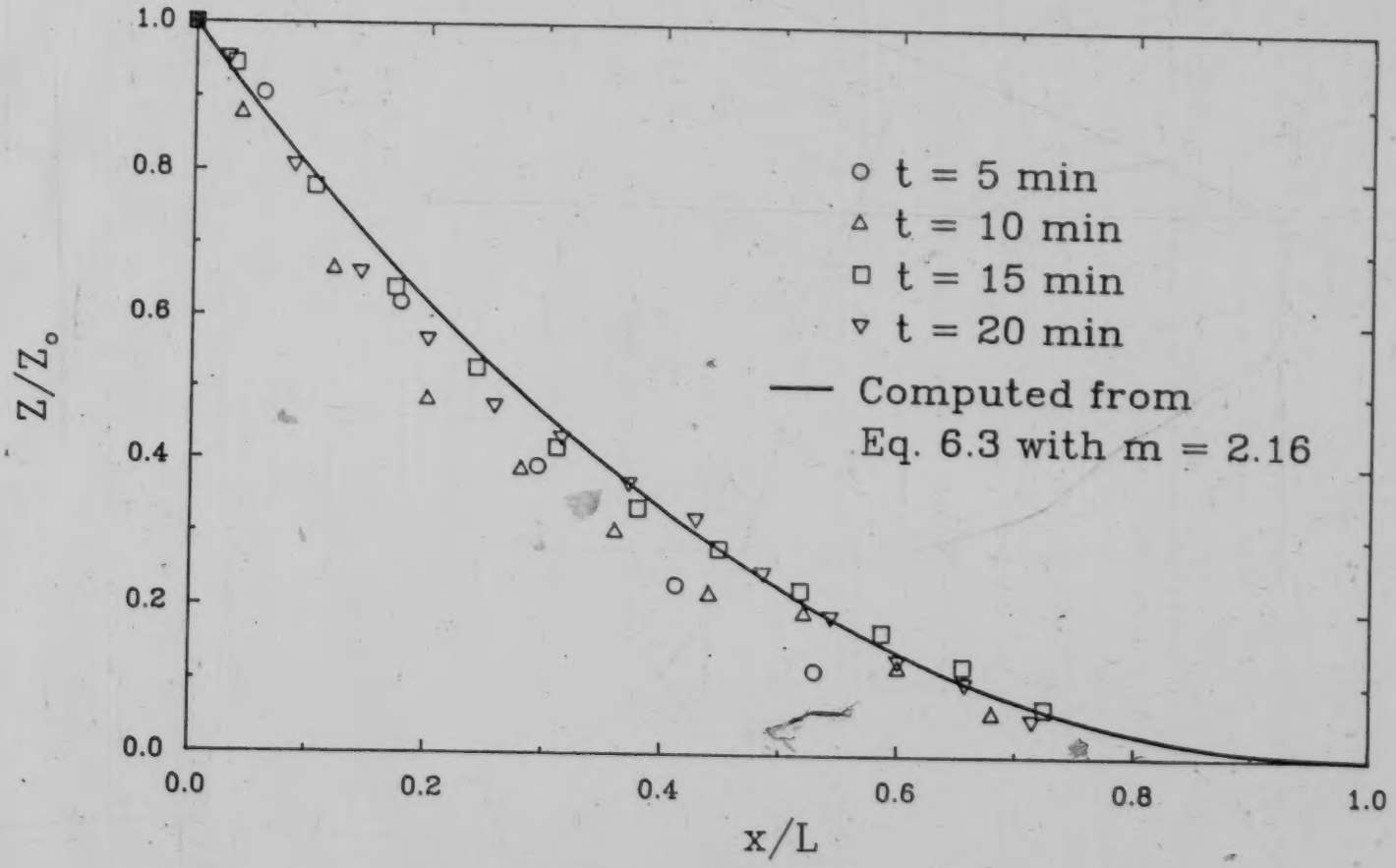

Fig. 6.10 Typical Dimensionless Beach Profiles for Group B Tests Modeled by Power Expression

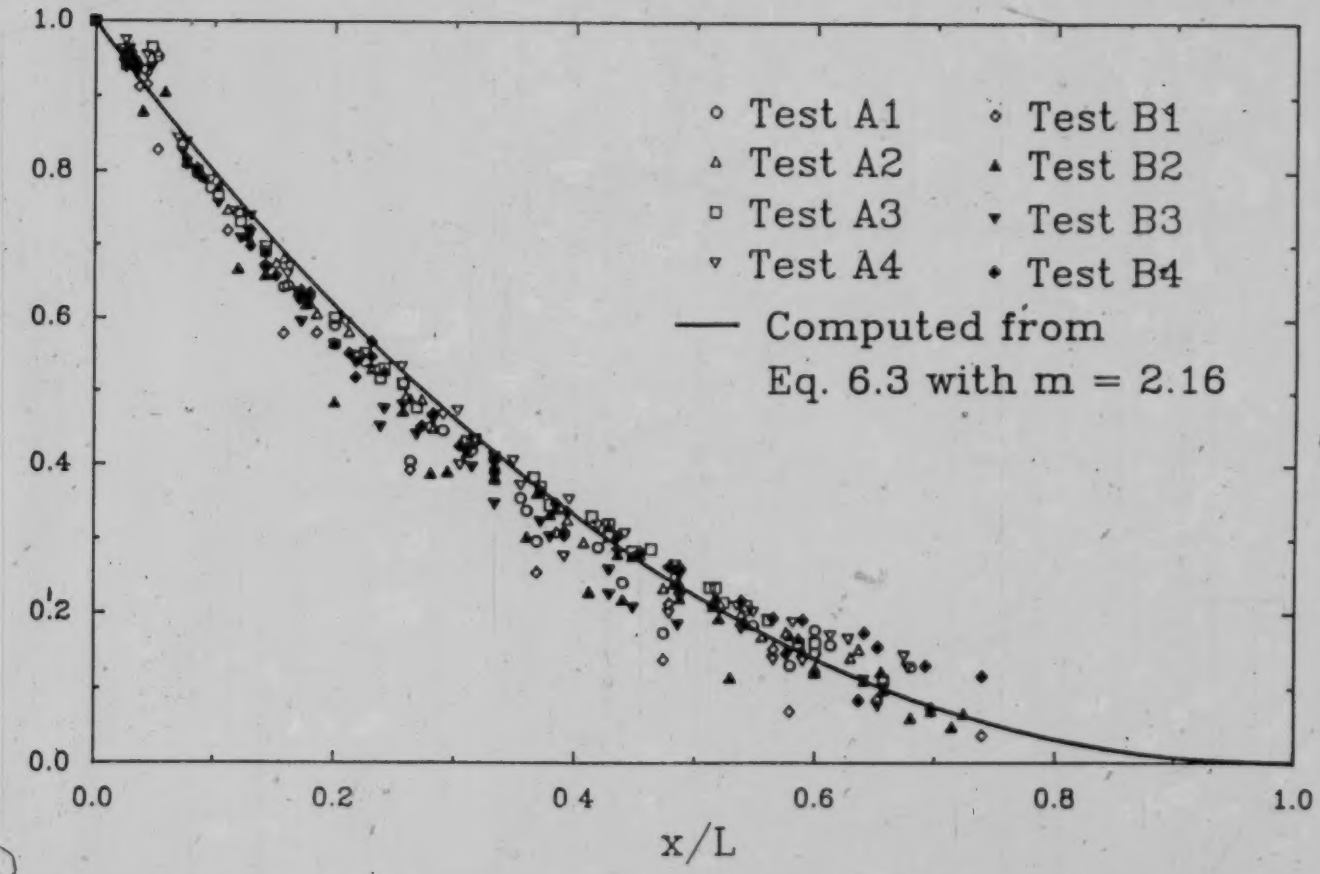

Fig. 6.11 Comparison of All the Beach Profile Data with the Curve Fitted by the Power Expression

Fig. 6.11, one observes that generally the power expression overestimates the depth of deposition at small distance from the feed point and underestimates the depth at large distance. However, the agreement between the experimental data and the prediction by the power expression of Eq. 6.3 is still quite satisfactory.

In summary, the two methods used to nondimensionalize the beach profiles are both workable, with the first one resulting in better agreement. From an engineering point of view, the second method is easier to use as long as the length of the beach and the maximum depth of deposition are available.

6.2 Maximum Depth of Deposition at x = 0

The maximum depth of deposition at x = 0 is plotted against time. The plots for group A and B tests are shown in Figs. 6.12 and 6.13, respectively. Fig. 6.12 shows the effect of feed sediment concentration on the maximum depth of deposition at different time. It is seen that at constant t, as the feed sediment concentration increases, the maximum depth increases. At constant feed sediment concentration, as time increases, the maximum depth increases, but the rate of increase slows down with time. From Fig. 6.13, one observes that at the same feed sediment concentration and constant time, when the total slurry discharge increases, the maximum depth of deposition also increases. For the same total slurry discharge, the maximum depth of deposition increases with time, but the rate of increase slows down with time. Comparing Fig. 6.12 with Fig. 6.13, it is seen that the feed sediment concentration has much more effect on the maximum depth of deposition than the total slurry discharge.

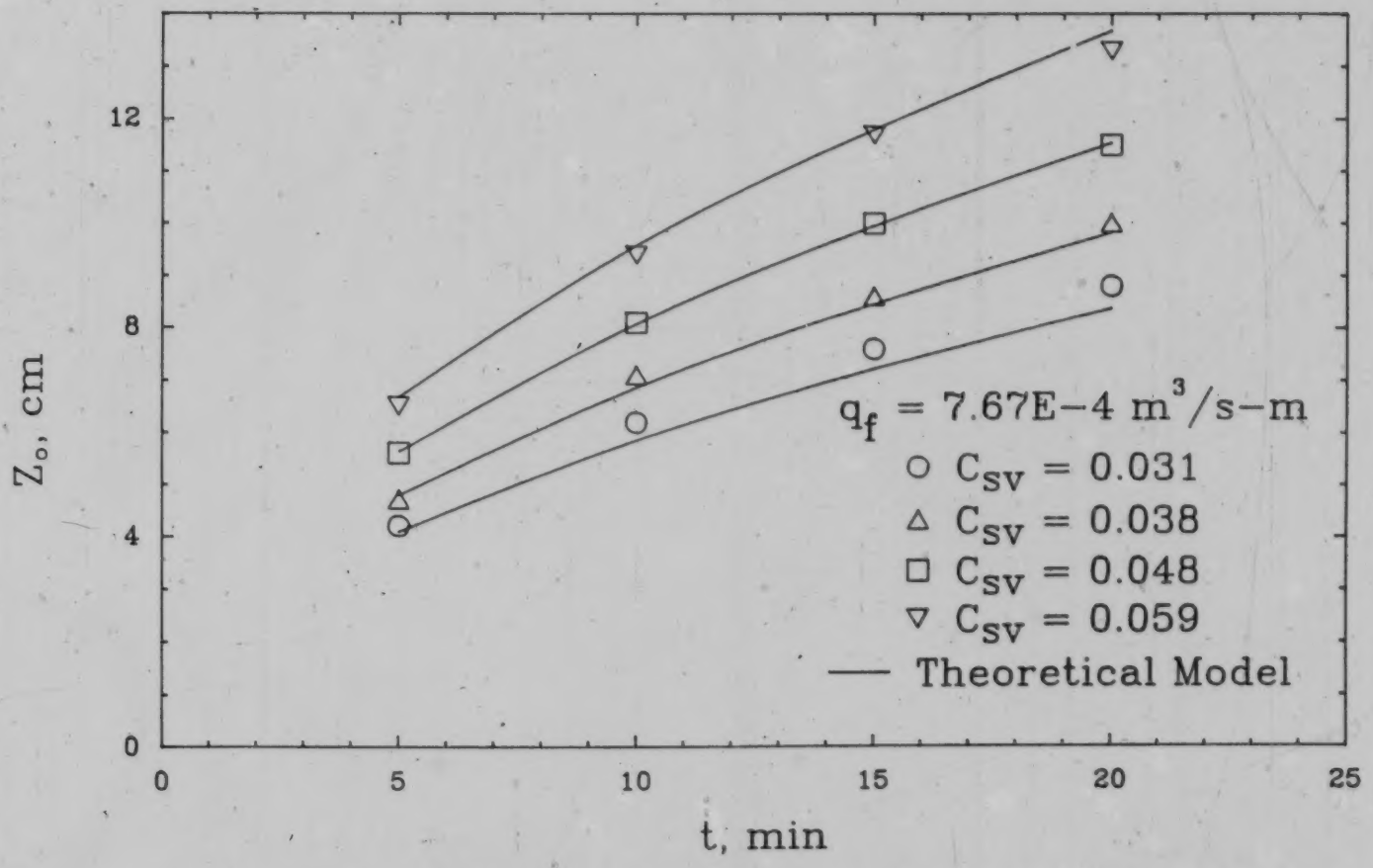

Fig. 6.12 Effect of Feed Sediment Concentration on the Maximum Depth of Deposition

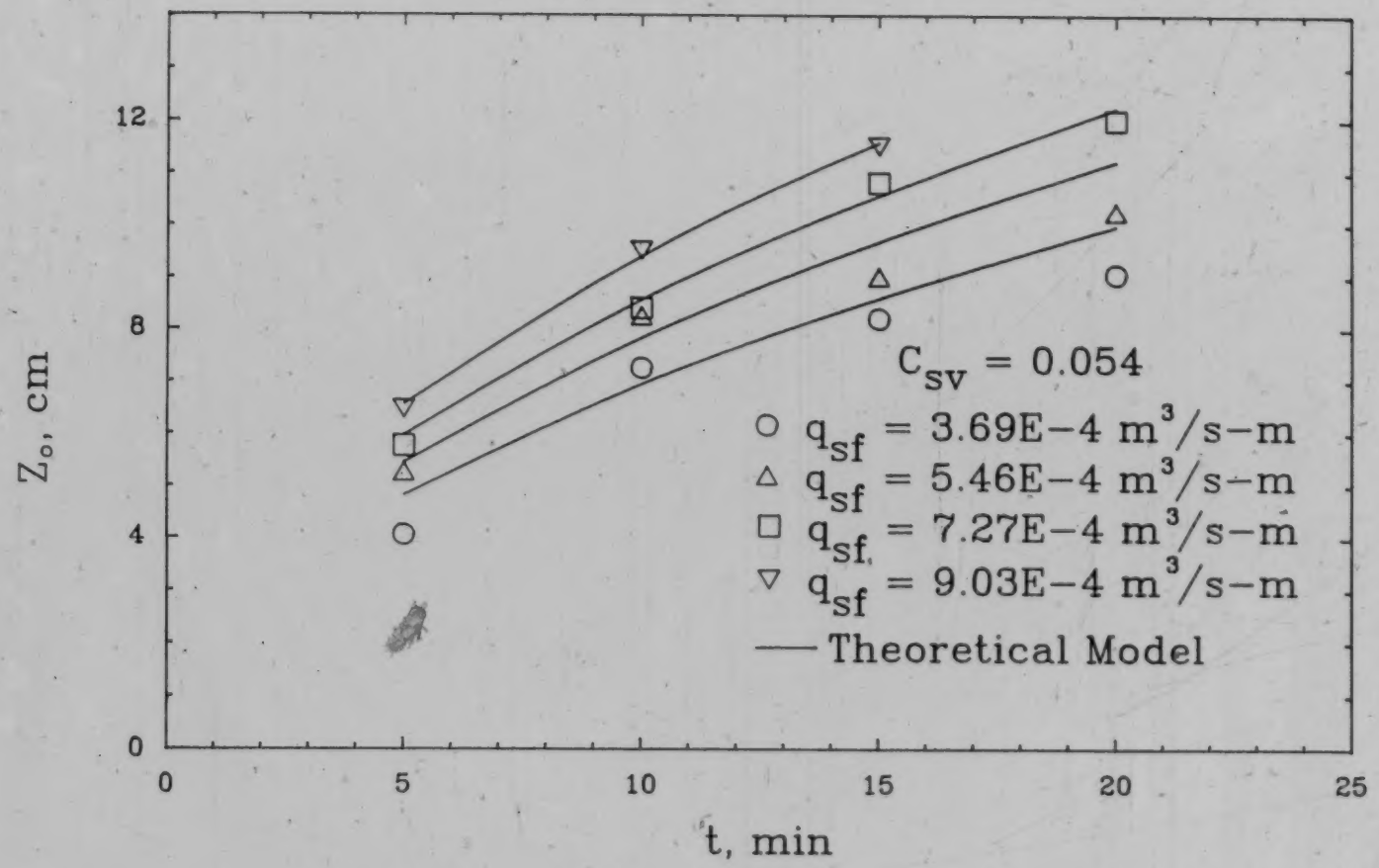

Fig. 6.13 Effect of Total Feed Slurry Discharge on the Maximum Depth of Deposition

7. CONCLUSIONS

1. The transient beach profiles in tailings disposal were simulated using an experimental flume. The experimental beach profiles were compared with the numerical results generated by a nonlinear parabolic model developed in this study. The agreement between the experimental profiles and the numerically generated profiles is excellent.
2. In developing the nonlinear parabolic model, Meyer–Peter and Muller equation was employed as the sediment transport equation. It was found out that in order to predict the beach profiles more accurately, the original constant coefficient of the equation must be replaced by a variable which is slightly dependent on the feed sediment discharge.
3. Under the same water discharge and a given time, when the feed sediment concentration is increased, both the slope of the beach and the maximum depth of deposition increase. Under the same feed sediment concentration and a given time, as the total slurry discharge increases, the maximum depth of deposition increases, but the slope of the beach does not change significantly for the same location.
4. Two approaches to nondimensionalize the beach profiles are employed in this study. The first approach includes both time and distance in the dimensionless group and shows very good agreement between the experimental data and the numerically computed results. The second approach using a power expression can predict the beach profiles with reasonable accuracy as long as the maximum depth of deposition and the length of the beach are available. The exponent of the power expression fitted from the experimental data in this study is 2.16, which is consistent with published results.

8. RECOMMENDATIONS

1. In tailings disposal, the concentration of slurry can be as high as 50 to 60 percent by weight. Owing to various restrictions, the sediment concentrations tested in this study were from 7.9 to 14.1 weight per cent. Therefore, higher concentrations are to be tested.
2. In this study one median sediment size was tested. If the effect of the sediment size on the beach profile is to be investigated, more experiments with different sediment sizes should be conducted.
3. In tailings disposal, it is often desirable to know the fraction and size distribution of the solids in the sludge. Hence some experiments may be arranged with wider range of sediment size distributions.
4. Commercial sand was used in this study to develop the model and test the numerical scheme. The methodology employed in this study can also be used to model the real situation in tailings disposal when the real tailings are used in the experiments.

REFERENCES

Anonymous, 1971. "Sediment Transport Mechanics, H. Sediment Discharge Formulas", Task committee for Preparation of Sediment Manual, *Journal of Hydraulic Division*, Am. Soc. Civ. Eng., Proc. Pap. 8076, Vol. 97, No. HY4, pp. 523–567.

Bhamidipathy, S., and Shen, H. W., 1971. "Laboratory Study of Degradation and Aggradation", *Journal of the Waterways, Harbors and Coastal Engineering Division*, ASCE, Vol. 97, No. WW4, pp. 615–630.

Blight, G. E., and Bentel, G. M., 1983. "The Behavior of Mine Tailings During Hydraulic Deposition", *Journal of the South African Institute of Mining and Metallurgy*, Vol. 83, pp. 73–86.

Blight, G. E.,Thomson, R. R., and Vorster, K., 1985. "Profiles of Hydraulic–Fill Tailings Beaches, and Seepage Through Hydraulically Sorted Tailings",*Journal of the South African Institute of Mining and Metallurgy*, Vol. 85, No. 5, pp. 157–161.

Brawner, C. O., and Campbell, D. B., 1973. "The Tailing Structure and Its Characteristics – a Soils Engineer's Viewpoint", *Proceedings of the First International Tailing Symposium*, Aplin, C.L., and Argall, G.O. (eds.),Miller Freeman, San Francisco, pp. 59–101.

Garde, R. J., and Ranga Raju, K. G., 1985, "Bed Level Variation in Alluvial Streams", *Mechanics of Sediment Transportation and Alluvial Stream Problems*, 2nd ed., Wiley Eastern Ltd., New Delhi. pp. 12–55, 362–433.

Garde, R. J., Ranga Raju, K. G., and Mehta, P. J., 1981. "Bed Level Variation in Aggrading Alluvial Streams", *19th Congress*, IAHR, Vol. 2, Paper 4, Subject A, pp. 247–253.

Gerald, C. F., and Wheatley, P. O., 1984, *Applied Numerical Analysis*, Addison – Weslley, Massachusetts, pp. 474–476.

Gill, M. A., 1983. "Diffusion Model for Aggrading Channels", *Journal of Hydraulic Research*, Vol. 21, No. 5, pp. 355–367.

Gill, M. A., 1987. "Nonlinear Solution of Aggradation and Degradation in Channels", *Journal of Hydraulic Research*, Vol. 25, No. 5, pp. 537–547.

Gill, M. A., 1988. "Hyperbolic Model for Aggrading Channels", *Journal of Engineering Mechanics*, Vol. 114, No. 7, pp. 1245–1255.

Jaramillo, W. F., and Jain, S. C., 1983. "Characteristic Parameters of Nonequilibrium Processes in Alluvial Channels of Finite Length", *Water Resources Research*, Vol. 19, No. 4, pp. 952–958.

Jaramillo, W. F., and Jain, S. C., 1984. "Aggradation and Degradation of Alluvial–Channel Beds", *Journal of Hydraulic Engineering*, ASCE, Vol. 110, No. 8, pp. 1072–1085.

Jain, S. C., 1980. Discussion of "Aggradation in Streams Due to Overloading", by Soni et al, *Journal of the Hydraulics Division*, ASCE, Vol. 106, No. HY11, pp. 1955–1958.

Jain, S. C., 1981. "River Bed Aggradation Due to Overloading", *Journal of the Hydraulics Division*, ASCE, Vol. 107, No. HY1, pp. 120–124.

Mehta, P. J., Garde, R. J., and Ranga Raju, K.G., 1983. "Transient Bed Profiles in Aggrading Streams", *Proceedings of the Second International Symposium on River Sedimentation*, Nanjing, China, pp. 149–161.

Melent'ev, V. A., Kolpashnikov, N. P., and Volnin, B. A., 1973. "Hydraulic Fill Structures", *Energy*, Moscow, translated by B. Nowak (University Witwatersand), edited by D. van Zyl.

Mittal, H. K., and Hardy, R. M., 1977. "Geotechnical Aspects of a Tar Sand Tailings Dyke", *Proceedings of the Conference on Geotechnical Practice for Disposal of Solid Waste Materials,* ASCE, Ann Arbor, Michigan, pp. 327–347.

Mittal, H. K., 1981. "Tailings Disposal Concepts in Oil Sands Open Pit Mining", *Design and Construction of Tailings Dams,* Wilson, D. (ed.), Colorado School of Mines, Colorado, pp. 206–229.

Nyren, R. H., Haakonson, K. A., and Mittal, H. K., 1979. "Disposal of Tar Sand Tailings at Syncrude Canada Ltd.", *Proceedings of the second Tailing Symposium,* Argall, G. O. (ed.), Miller Freeman, San Francisco, pp. 54–74.

Park, I., and Jain, S. C., 1986. "River–Bed Profiles with Imposed Sediment Load", *Journal of Hydraulic Engineering,* ASCE, Vol. 112, No. 4, pp. 267–280.

Ranga Raju, K. G., 1981. *Flow through Open Channels,* Tata McGraw–Hill, New Delhi, pp. 36–37.

Ribberink, J. S., and Vander Sande, J. T. M., 1985. "Aggradation in Rivers Due to Overloading – Analytical Approaches", *Journal of Hydraulic Research,* Vol. 23, No. 3, pp. 273–283.

Robinsky, E. I., 1975. "Thickened Discharge – a New Approach to Tailings Disposal", *CIM Bulletin,* Vol. 68, No. 764, pp. 47–53.

Robinsky, E. I., 1979. "Tailing Disposal by the Thickened Discharge Method for Improved Economy and Environmental Control", *Proceedings of the second International Tailing Symposium,* Argall, G.O. (ed.), Miller Freeman, San Francisco, pp. 75–95.

Smith, G. M. and Nelson, J. D., 1986. "Profile Prediction of Hydraulically Deposited Tailings", *Transactions of Society of Mining Engineers,* Vol. 280, pp. 2024–2027.

Soni, J. P., Garde, R. J., and Ranga Raju, K. G., 1977a. "Aggradation in Alluvial Channels Due to Increase in Sediment Load", *17th Congress*, IAHR, Vol. 1, Paper A20, pp. 151–155.

Soni, J. P., Garde, R. J., and Ranga Raju, K. G., 1977b. "Nonuniform Flow in Aggrading Channels", *Journal of the Waterway, Port, Coastal and Ocean Division*, ASCE, Vol. 103, No. WW3, pp. 321–333.

Soni, J. P., Garde, R. J., and Ranga Raju, K. G., 1980. "Aggradation in Streams Due to Overloading", *Journal of the Hydraulics Division*, ASCE, Vol. 106, No. HY1, pp. 117–132.

Soni, J. P., 1981a. "Laboratory Study of Aggradation in Alluvial Channels", *Journal of Hydrology*, Vol. 49, pp. 87–106.

Soni, J. P., 1981b. "An Error Function Solution of Sediment Transport in Aggrading Channels", *Journal of Hydrology*, Vol. 49, 107–119.

Soni, J. P., 1981c. "Unsteady Sediment Transport Law and Prediction of Aggradation Parameters", *Water Resources Research*, Vol. 17, No. 1, pp. 33–40.

Vries, M. de, 1959. "Transients in Bed Load Transport (Basic Considerations)", *Report R3*, Waterloopkunding Laboratoriumm, Delft.

Vries, M. de, 1965. "Considerations About Non–Steady Bed–Load Transport in Open Channels", *11th Congress*, IAHR, Vol. 3, Paper No. 3.8.

Vries, M. de, 1969. "Solving River Problems by Hydraulic and Mathematical Models", Delft Hydraulic Laboratory, Publication 76–II.

Vries, M. de, 1973. "River–Bed Variations – Aggradation and Degradation", Delft Hydraulic Laboratory, Publication No. 107.

Wang, K., Zhu, Q., and Zhang, Z., 1983. "On the Problem of the Equilibrium Longitudinal Profile of the River", *Proceedings of the Second International Symposium on River Sedimentation*, Nanjing, China, pp 620–627 (in Chinese).

Wiberg, P. L. and Smith, J. D., 1989. "Model for Calculating Bed Load Transport of Sediment", *Journal of Hydraulic Engineering*, Vol. 115, No. 1, pp. 101–123.

Yalin, M. S., 1977. *Mechanics of Sediment Transport*, 2nd ed., Pergamon Press, Oxford.

Zhang, H., and Kahawita, R. 1987. Discussion of "Aggradation and Degradation of Alluvial – Channel Beds", Jaramillo, W.F., and Jain, S.C., *Journal of Hydraulic Engineering*, ASCE, Vol. 113, No. 2, pp. 272–273.

Zhang, H., and Kahawita, R.,1987. "Nonlinear Model for Aggradation in Alluvial Channels", *Journal of Hydraulic Engineering*, ASCE, Vol. 113, No. 3, pp. 353–369.

Zhang, H., and Kahawita, R., 1988. "Nonlinear Hyperbolic System and Its Solutions for Aggradated Channels", *Journal of Hydraulic Research*, Vol. 26, No. 3, pp. 323–342.

APPENDIX A

Fortran Program for Beach Profile Generation

```
************************************************************
*                                                          *
* This program is designed to compute the beach profiles   *
* for tailings disposal using a nonlinear parabolic model. *
*                                                          *
* The input variables are:                                 *
*                                                          *
*   NDATA  = Number of data sets for computation           *
*   S0     = Dimensionless initial beach slope             *
*   QF     = Water discharge per unit width                *
*   QST    = Total sediment discharge per unit width       *
*   DX     = x increment                                   *
*   DT     = t increment                                   *
*   M      = Number of grid points in x direction          *
*   TPRINT = Time interval for printing the results        *
*   TMAX   = Upper limit of time for computation           *
*   AK     = Coefficient of Meyer-Peter Muller equation    *
*                                                          *
* Parameters entered from BLOCK DATA subprogram            *
*                                                          *
*   BETA   = solid volume / total volume in bed,           *
*            β = 1 - bed porosity                          *
*   G      = Gravitational acceleration                    *
*   RKS    = sand roughness, D50                           *
*   RHOF   = Density of water                              *
*   RHOS   = Density of sand                               *
*   YCR    = Critical mobility number                      *
*                                                          *
************************************************************
*                                                          *
      REAL Z0(100),Z1(100),Z(100),X(100)
      COMMON /COM1/ S0,Z0,DX,DT,QF,QST,M,AK
      COMMON /COM2/ Z1,Z,IEND
      COMMON /COM3/ BETA,G,RKS,RHOF,RHOS,YCR
      OPEN(UNIT=7,FILE='FLUME1.DAT')
      OPEN(UNIT=8,FILE='FLUME1.RES')
      READ(7,*) NDATA
      DO 1000 NTT = 1,NDATA
      READ(7,*) S0,QF,QST,DX,DT,M,TPRINT,TMAX,AK
*
      NTMAX = INT(TMAX / DT + 0.1)
      RTL = DX * FLOAT(M-1)
      NP = INT(TPRINT / DT + 0.1)
      DO 10 I = 1,M
        X(I) = FLOAT(I-1)*DX
        Z0(I) = S0 * (RTL-X(I))
        Z(I) = Z0(I)
 10   CONTINUE
      WRITE(8,5) S0,QF,QST,DX,DT,M,TMAX,AK
 5    FORMAT(/T5,'S0=',F7.5,1X,'QF=',E10.3,
```

```
     &     1X,'QST=',E10.3/T5,'DX=',F6.3,1X,'DT=',F4.2,1X,
     &     'M=',I4,1X,'TMAX=',F7.0,1X,'AK=',F6.2)
*
      DO 100 NT = 1,NTMAX
        CALL ZSUB
        T = NT * DT /60.0
        IF(NT/NP*NP .EQ. NT) THEN
          WRITE(8,15) T
 15       FORMAT(/T5,'T = ',F4.1,' minutes.',/
     &          T6,'X(cm)',T15,'Z(cm)'/)
          DO 20 I = 1,3,2
                XI = FLOAT(I-1)*2.5
                ZI = (Z(I)-Z0(I))*100.0
            WRITE(8,25) XI,ZI
 25         FORMAT(T4,F6.1,F10.3,1X)
 20       CONTINUE
          DO 30 I = 7,M,4
                XI = FLOAT(I-1)*2.5
                ZI = (Z(I)-Z0(I))*100.0
            WRITE(8,25) XI,ZI
 30       CONTINUE
        END IF
 100  CONTINUE
 1000 CONTINUE
      STOP
      END
*
*  ------------------------------------------------------------
*
      SUBROUTINE ZSUB
      REAL Z0(100),Z1(100),Z2(100)
      COMMON /COM1/ S0,Z0,DX,DT,QF,QST,M,AK
      COMMON /COM2/ Z1,Z2,IEND
      COMMON /COM3/ BETA,G,RKS,RHOF,RHOS,YCR
      RHOR = (RHOS-RHOF)/RHOF
      CONST1 = 0.284*G**(-0.3)*RKS**0.1*QF**0.6
      CONST2 = YCR*RHOR*RKS
*
      DO 10 I = 1,M
        Z1(I) = Z2(I)
 10   CONTINUE
*
      DO 20 I = 1,M
        IF( Z1(I) - Z0(I) .LT. RKS ) THEN
          IEND = I
          GO TO 30
        END IF
        IEND = I
 20   CONTINUE
*
 30   DZZ = Z2(1) - Z0(1)
      IF ( DZZ .LE. 0.029 ) THEN
        DX0 = 0.05/0.029*DZZ
      ELSE
```

```
        DX0 = 0.05
      END IF
*
      XX = FLOAT(IEND-1)*DX
*
      IF (IEND .EQ. 1) THEN
        QS1 = QST
      ELSE
        QS1 = XX/(XX+DX0)*QST
      END IF
*
      S2 = (Z1(1)-Z1(3))/2./DX
      S3 = (Z1(2)-Z1(4))/2./DX
      TEST2 = CONST1*S2**0.7 - CONST2
      TEST3 = CONST1*S3**0.7 - CONST2
      IF (S2 - S0 .LE. 1.0E-5 .OR. TEST2 .LE. 0.0) THEN
        Q2 = 0.0
        Q3 = 0.0
      ELSE IF(S3-S0 .LE. 1.0E-5 .OR. TEST3 .LE. 0.0) THEN
        Q2 = AK*G**0.5/RHOR*TEST2**1.5
        Q3 = 0.0
      ELSE
        Q2 = AK*G**0.5/RHOR*TEST2**1.5
        Q3 = AK*G**0.5/RHOR*TEST3**1.5
      END IF
*
*  ------------------------------------------------------
*
      Z2(1) = Z1(1)+DT/BETA/2./DX*(3.0*QS1-4.*Q2+Q3)
      DO 40 I = 2,IEND
        IF (I .LT. M) THEN
          Z2(I) = Z1(I)+RKZ(I)*DT/DX/DX
     &             *(Z1(I+1)-2.*Z1(I)+Z1(I-1))
        ELSE
          Z2(I) = Z1(I)+RKZ(I)*DT/DX/DX
     &         *(-Z1(I-3)+4.*Z1(I-2)-5.0*Z1(I-1)+2.0*Z1(I))
        END IF
 40   CONTINUE
      DO 50 I = IEND + 1 ,M
        Z2(I) = Z1(I)
 50   CONTINUE
      RETURN
      END
*
*  ------------------------------------------------------
*
      REAL FUNCTION RKZ(I)
      REAL Z0(100),Z1(100),Z2(100)
      COMMON /COM1/ S0,Z0,DX,DT,QF,QST,M,AK
      COMMON /COM2/ Z1,Z2,IEND
      COMMON /COM3/ BETA,G,RKS,RHOF,RHOS,YCR
      RHOR = (RHOS-RHOF)/RHOF
      CONST1 = 0.284*G**(-0.3)*RKS**0.1*QF**0.6
      CONST2 = YCR*RHOR*RKS
```

```
*
*    ------------------------------------------------------
*
      IF (I .LT. M) THEN
        S = (Z1(I-1) - Z1(I+1))/2./DX
      ELSE
        S = (-Z1(I-2)+4.*Z1(I-1)-3.*Z1(I))/2./DX
      END IF
*
*    ------------------------------------------------------
*
      IF(S.LE.0.0) STOP 111
      TEST = CONST1*S**0.7 - CONST2
      IF (TEST .LE. 0.0) THEN
        RKZ = 0.0
      ELSE
      RKZ = 0.298*G**0.2*AK*RKS**.1*QF**.6
     &      /BETA/RHOR*S**(-.3)*TEST**0.5
      END IF
*
      RETURN
      END
*
*   ------------------------------------------------------
*
      BLOCK DATA
      COMMON /COM3/ BETA,G,RKS,RHOF,RHOS,YCR
      DATA BETA,G,RKS /0.57,9.81,2.67E-4/
      DATA RHOF,RHOS,YCR /1000.,2650.,0.047/
      END
```

Note: Typical input for modeling Test A1

```
NDATA  = 1
S0     = 5.43E-3
QF     = 7.67E-4
QST    = 2.47E-5
DX     = 25.0E-3
DT     = 0.50
M      = 81
TPRINT = 300
TMAX   = 1200
AK     = 6.0
```

APPENDIX B

NUMERICAL RESULTS FOR TESTS A AND B

Table B.1 Numerical Results Modeling Test A1, $A_k = 6.0$

$q_f = 7.67 \times 10^{-4} m^3/s\text{–}m$, $q_{stot} = 2.47 \times 10^{-5} m^3/s\text{–}m$, $S_0 = 0.00543$

x (cm)	Z,cm t=5 min	Z,cm t=10 min	Z,cm t=15 min	Z,cm t=20 min
0	4.090	5.860	7.227	8.383
5	3.584	5.340	6.702	7.853
15	2.691	4.387	5.721	6.856
25	1.954	3.548	4.834	5.940
35	1.363	2.819	4.039	5.105
45	0.903	2.194	3.333	4.349
55	0.557	1.668	2.713	3.668
65	0.307	1.232	2.173	3.061
75	0.135	0.877	1.708	2.523
85	0.022	0.593	1.313	2.051
95	0.000	0.371	0.981	1.640
105	0.000	0.201	0.706	1.286
115	0.000	0.075	0.481	0.983
125	0.000	0.000	0.300	0.727
135	0.000	0.000	0.156	0.512
145	0.000	0.000	0.046	0.335
155	0.000	0.000	0.000	0.190
165	0.000	0.000	0.000	0.074
175	0.000	0.000	0.000	0.000

Table B.2 Numerical Results Modeling Test A2, $A_k = 6.7$

$q_f = 7.67 \times 10^{-4} m^3/s–m$, $q_{stot} = 3.07 \times 10^{-5} m^3/s–m$, $S_0 = 0.00543$

x (cm)	Z,cm t=5 min	Z,cm t=10 min	Z,cm t=15 min	Z,cm t=20 min
0	4.792	6.871	8.473	9.827
5	4.232	6.296	7.893	9.243
15	3.237	5.238	6.806	8.139
25	2.406	4.299	5.817	7.119
35	1.728	3.474	4.923	6.184
45	1.190	2.761	4.124	5.331
55	0.776	2.151	3.414	4.558
65	0.469	1.638	2.789	3.862
75	0.248	1.212	2.245	3.240
85	0.096	0.865	1.776	2.687
95	0.000	0.587	1.376	2.201
105	0.000	0.369	1.038	1.776
115	0.000	0.201	0.757	1.407
125	0.000	0.076	0.525	1.091
135	0.000	0.000	0.337	0.821
145	0.000	0.000	0.187	0.594
155	0.000	0.000	0.070	0.405
165	0.000	0.000	0.000	0.248
175	0.000	0.000	0.000	0.121
185	0.000	0.000	0.000	0.022
195	0.000	0.000	0.000	0.000

Table B.3 Numerical Results Modeling Test A3, $A_k = 7.5$

$q_f = 7.67 \times 10^{-4} m^3/s\text{–}m$, $q_{stot} = 3.83 \times 10^{-5} m^3/s\text{–}m$, $S_0 = 0.00543$

x (cm)	Z,cm t=5 min	Z,cm t=10 min	Z,cm t=15 min	Z,cm t=20 min
0	5.633	8.077	9.959	11.549
5	5.012	7.441	9.318	10.904
15	3.902	6.265	8.111	9.679
25	2.963	5.213	7.007	8.543
35	2.186	4.281	6.003	7.495
45	1.558	3.465	5.096	6.533
55	1.064	2.760	4.285	5.655
65	0.686	2.157	3.563	4.857
75	0.407	1.649	2.928	4.138
85	0.207	1.228	2.372	3.494
95	0.070	0.883	1.892	2.920
105	0.000	0.605	1.480	2.412
115	0.000	0.386	1.131	1.966
125	0.000	0.216	0.838	1.578
135	0.000	0.084	0.595	1.242
145	0.000	0.000	0.397	0.954
155	0.000	0.000	0.236	0.710
165	0.000	0.000	0.108	0.503
175	0.000	0.000	0.000	0.331
185	0.000	0.000	0.000	0.186
195	0.000	0.000	0.000	0.060

Table B.4 Numerical Results Modeling Test A4, $A_k = 8.2$

$q_f = 7.67 \times 10^{-4} m^3/s-m$, $q_{stot} = 4.77 \times 10^{-5} m^3/s-m$, $S_0 = 0.00543$

x (cm)	Z,cm t=5 min	Z,cm t=10 min	Z,cm t=15 min	Z,cm t=20 min
0	6.679	9.578	11.809	13.686
5	5.979	8.861	11.086	12.960
15	4.718	7.530	9.722	11.579
25	3.642	6.332	8.468	10.292
35	2.742	5.263	7.322	9.099
45	2.005	4.321	6.281	7.999
55	1.415	3.498	5.342	6.988
65	0.955	2.788	4.502	6.066
75	0.606	2.182	3.755	5.228
85	0.350	1.672	3.097	4.471
95	0.168	1.248	2.521	3.792
105	0.046	0.901	2.022	3.186
115	0.000	0.622	1.594	2.648
125	0.000	0.400	1.229	2.173
135	0.000	0.227	0.922	1.756
145	0.000	0.096	0.666	1.391
155	0.000	0.000	0.455	1.073
165	0.000	0.000	0.284	0.795
175	0.000	0.000	0.146	0.549
185	0.000	0.000	0.039	0.329
195	0.000	0.000	0.000	0.126

Table B.5 Numerical Results Modeling Test B1, $A_k = 5.7$

$q_f = 3.49 \times 10^{-4} m^3/s\text{–}m$, $q_{stot} = 1.99 \times 10^{-5} m^3/s\text{–}m$, $S_0 = 0.00543$

x (cm)	Z,cm t=5 min	Z,cm t=10 min	Z,cm t=15 min	Z,cm t=20 min
0	4.810	6.939	8.586	9.979
5	3.956	6.054	7.687	9.071
15	2.550	4.502	6.067	7.410
25	1.517	3.230	4.681	5.953
35	0.810	2.220	3.518	4.695
45	0.364	1.447	2.565	3.625
55	0.112	0.877	1.801	2.731
65	0.000	0.478	1.206	1.997
75	0.000	0.214	0.757	1.408
85	0.000	0.054	0.430	0.946
95	0.000	0.000	0.204	0.593
105	0.000	0.000	0.056	0.332
115	0.000	0.000	0.000	0.148
125	0.000	0.000	0.000	0.025
135	0.000	0.000	0.000	0.000

Table B.6 Numerical Results Modeling Test B2, $A_k = 6.8$

$q_f = 5.17 \times 10^{-4} m^3/s-m$, $q_{stot} = 2.94 \times 10^{-5} m^3/s-m$, $S_0 = 0.00543$

x (cm)	Z,cm t=5 min	Z,cm t=10 min	Z,cm t=15 min	Z,cm t=20 min
0	5.444	7.828	9.667	11.221
5	4.697	7.060	8.889	10.437
15	3.403	5.667	7.451	8.971
25	2.365	4.462	6.168	7.641
35	1.563	3.437	5.036	6.443
45	0.968	2.581	4.049	5.374
55	0.547	1.882	3.200	4.430
65	0.266	1.323	2.480	3.602
75	0.090	0.887	1.887	2.885
85	0.000	0.556	1.381	2.271
95	0.000	0.313	0.980	1.751
105	0.000	0.141	0.662	1.316
115	0.000	0.024	0.414	0.958
125	0.000	0.000	0.227	0.667
135	0.000	0.000	0.089	0.434
145	0.000	0.000	0.000	0.253
155	0.000	0.000	0.000	0.113
165	0.000	0.000	0.000	0.008
175	0.000	0.000	0.000	0.000

Table B.7 Numerical Results Modeling Test B3, $A_k = 7.7$

$q_f = 6.88 \times 10^{-4} m^3/s-m$, $q_{stot} = 3.91 \times 10^{-5} m^3/s-m$, $S_0 = 0.00543$

x (cm)	Z,cm t=5 min	Z,cm t=10 min	Z,cm t=15 min	Z,cm t=20 min
0	5.962	8.555	10.552	12.239
5	5.284	7.860	9.850	11.532
15	4.075	6.576	8.532	10.194
25	3.059	5.433	7.330	8.956
35	2.226	4.426	6.241	7.818
45	1.561	3.550	5.263	6.776
55	1.045	2.798	4.392	5.830
65	0.657	2.161	3.622	4.975
75	0.375	1.629	2.948	4.208
85	0.179	1.193	2.364	3.525
95	0.049	0.841	1.863	2.920
105	0.000	0.561	1.438	2.388
115	0.000	0.344	1.081	1.925
125	0.000	0.180	0.785	1.526
135	0.000	0.055	0.543	1.183
145	0.000	0.000	0.348	0.893
155	0.000	0.000	0.193	0.649
165	0.000	0.000	0.073	0.446
175	0.000	0.000	0.000	0.280
185	0.000	0.000	0.000	0.144
195	0.000	0.000	0.000	0.048

Table B.8 Numerical Results Modeling Test B4, $A_k = 8.0$

$q_f = 8.54 \times 10^{-4} m^3/s-m$, $q_{stot} = 4.86 \times 10^{-5} m^3/s-m$, $S_0 = 0.00543$

x (cm)	Z,cm t=5 min	Z,cm t=10 min	Z,cm t=15 min	Z,cm t=20 min
0	6.549	9.387	11.573	
5	5.885	8.710	10.888	
15	4.687	7.446	9.595	
25	3.657	6.304	8.402	
35	2.788	5.280	7.307	
45	2.069	4.372	6.309	
55	1.488	3.574	5.404	
65	1.028	2.881	4.590	
75	0.673	2.284	3.862	
85	0.407	1.776	3.217	
95	0.213	1.350	2.648	
105	0.077	0.997	2.150	
115	0.000	0.708	1.720	
125	0.000	0.475	1.349	
135	0.000	0.291	1.034	
145	0.000	0.146	0.768	
155	0.000	0.036	0.546	
165	0.000	0.000	0.362	
175	0.000	0.000	0.212	
185	0.000	0.000	0.091	
195	0.000	0.000	0.000	